To the Graduate Council:

I am submitting herewith a dissertation written by Michael Boyd McGinnis entitled "The Use of *B*-Haloboranes in Solution and on Alumina in Organic Chemistry." I have examined the final copy of this dissertation for form and content and recommend that it be accepted in partial fulfillment of the requirements for the degree of Doctor of Philosophy, with a major in Chemistry.

Richard M. Pagni, Major Professor

We have read this dissertation
and recommend its acceptance:

Accepted for the Council:

Associate Vice Chancellor and
Dean of The Graduate School

THE USE OF *B*-HALOBORANES IN SOLUTION AND ON ALUMINA IN ORGANIC CHEMISTRY

A Dissertation

Presented for the

Doctor of Philosophy

Degree

The University of Tennessee, Knoxville

Michael Boyd McGinnis

May 1997

DEDICATION

This dissertation is dedicated to my family. In special recognition of their love, support, and strength, I dedicate this dissertation to my grandmother, Charlotte McGinnis, my mother, Phyllis McGinnis, and my wife, Maryann McGinnis.

ACKNOWLEDGMENTS

I would like to express my deepest appreciation and thanks to Dr. Richard M. Pagni and Dr. George W. Kabalka for their guidance and financial support. I feel privileged to have worked in their laboratory and had the opportunity to present our research at regional and national scientific meetings.

The Department of Chemistry, National Science Foundation, Science Alliance, and the United States Department of Energy deserve recognition for their generous financial support of my research at the University of Tennessee, Knoxville.

Special thanks must be given to Dr. Jim Green. Without the interesting discussions and crazy ideas, my graduate career would have been much less enjoyable.

To my lab mates for their friendship and help throughout my graduate career. Also, special thanks to Dr. Chuck Anderson for his help in obtaining 400 MHz NMR spectra and Dr. Anna Edwards for her help in obtaining FT-IR spectra. The University of Tennessee staff, especially Bill Gurley and Pat McDaniel, whose accomplishments are rarely recognized, are thanked for their support.

Most importantly, I thank my wife, Maryann, for her love, support, friendship, and patience.

ABSTRACT

A series of boronated aluminas were prepared by the reaction of BX_3 (X = F, Cl, Br) with alumina or by a two step synthesis involving the reaction of $BH_3 \cdot Me_2S$ with alumina and then with I_2. The modified aluminas, BX_n/Al_2O_3, were found to have n = 3 (F), n = 1.5 (Cl), n = 1 (Br) and n = 1 (I). The acidity of the solids (indicator dyes) were large and decreased in the order: I~Br>Cl>F. Isomerizations of several dienes, including dimethyl maleate to dimethyl fumarate, were completed within minutes with the iodo- and bromoboronated aluminas. The solids catalyzed the Diels-Alder reactions of methyl acrylate with cyclopentadiene, isoprene with methyl acrylate, and dimethyl maleate with cyclopentadiene, all of which occurred in high yield and with high selectivity. The regioselectivity of the isoprene/methyl acrylate reaction in fact is higher than seen previously. The results of the heterogeneous reactions were compared to those catalyzed by *B*-bromo- and *B*-chlorocatecholborane, which serve as models for the boronated aluminas.

To compare the acidity with the boronated aluminas, *(E)*-2-butenal was complexed with *B*-bromo- and *B*-chlorocatecholborane in CD_2Cl_2 at -20°C. The proton and carbon NMR chemical shifts of the aldehyde showed two species that unexpectedly moved upfield which indicated pi-complexed s-cis and s-trans conformations. The hypothesis was confirmed with COSY, HETCOR, NOESY, and ROESY 2D NMR experiments. The *s-cis* and *s-trans* conformations of the aldehyde exist in equal amounts which interconvert (EXSY 2D NMR). Infrared spectrum of the complexes validated the existence of the carbonyl vibration.

Reaction of the complexes with cyclopentadiene afforded the Diels-Alder endo and exo adducts cleanly. Quenching the complex with water generated catechol, boric acid, *(E)*-2-butenal, and 3-bromobutanal, as expected.

TABLE OF CONTENTS

PART 1

Reactions Catalyzed by Highly Acidic Boronated Aluminas **1**

A. Introduction 2

B. Results and Discussion 17

C. Conclusions 47

D. Experimental 47

E. Materials 54

List of References 57

PART 2

The *s-cis* and *s-trans* Pi-Complexes of *(E)*-2-Butenal and *B*-Bromocatecholborane **61**

A. Introduction 62

B. Results and Discussion 68

C. Conclusion 120

D. Experimental 121

E. Materials 125

List of References 128

APPENDIX: Supplemental NMR Spectra **131**

Vita **152**

LIST OF TABLES

Table	Description	Page
1-1	Advantages and Disadvantages of Inorganic Solids	3
1-2	IR Frequencies of Alumina Hydroxyls	9
1-3	Results of Methyl Acylate and Cyclopentadiene Cycloaddition	14
1-4	Results Lewis Acid Incorporated Alumina and Silica Gel Catalyzed Methyl Acrylate and Cyclopentadiene Reaction	16
1-5	Weight Increase of Adding Boron Tribromide to Alumina: Comparison of Experimental with Theoretical Predictions	24
1-6	Summary of BX_n/Al_2O_3 Characteristics	29
1-7	Isomerization of DMM to DMF with Boronated Solids	30
1-8	Neat Reactions of MA and CP with Boronated Solids	35
1-9	Reactions of MA and CP with Boronated Solids	36
1-10	Time Dependent Reactions of MA and CP with BBr/Al_2O_3	37
1-11	Stoichiometric Changes in the Reaction of MA and CP with BBr/Al_2O_3	40
1-12	Reactions of DMM and CP with Boronated Solids	41
1-13	Reactions of MA and IP with Boronated Solids	44
1-14	Homogeneous versus Heterogeneous Diels-Alder Reactions	46
2-1	Proton Chemical Shifts of Crotonaldehyde on Complexation with Lewis Acids at -20°C	67
2-2	Proton Chemical Shifts of Crotonaldehyde and *B*-halocatecholborane Complexes at -20°C	74
2-3	Coupling Constants of Crotonaldehyde and *B*-halocatecholborane Complexes at -20°C	75

2-4	Carbon-13 Chemical Shifts of Crotonaldehyde and *B*-Halocatecholborane Complexes at -20°C in CD_2Cl_2	81
2-5	*B*-Bromocatecholborane Catalyzed D-A Reaction of CA and CP at Various Temperatures	98
2-6	Proton Chemical Shifts of Mesityl Oxide and BCB	101
2-7	Carbon-13 Chemical Shifts of Mesityl Oxide and BCB	102
2-8	Proton Chemical Shifts of Methyl 3,3-Dimethyl Acrylate and BCB	104
2-9	Proton Chemical Shifts of Methyl Crotonate and BCB	104
2-10	Proton Chemical Shifts of Methyl Acrylate and BCB	105
2-11	Carbon-13 Chemical Shifts of Methyl Acrylate and BCB	105
2-12	Proton Chemical Shifts of Acrylonitrile and BCB	106
2-13	Carbon-13 Chemical Shifts of Acrylonitrile and BCB	106
2-14	Proton Chemical Shifts of Butyraldehyde (butanal) and BCB	107
2-15	Proton Chemical Shifts of CA with Model Compounds of BCB at -20°C in CD_2Cl_2	116
2-16	Carbon-13 Chemical Shifts of CA with Model Compounds of BCB at -20°C in CD_2Cl_2	117
2-17	NMR Chemical Shifts of *B*-Methoxycatecholborane	119

LIST OF FIGURES

Figure	Description	Page
1-1	General Diels-Alder Reaction	1
1-2	Formation of the Transition Aluminas	6
1-3	Layering of Alumina	6
1-4	The Knözinger and Ratnasamy Layers of gamma-Alumina	7
1-5	Hydroxyl Types on the A- and B-layers of gamma-Alumina	8
1-6	Activation and Dehydration of γ-alumina	9
1-7	Iodinations using Alumina	11
1-8	Reactions Catalyzed by Alumina	12
1-9	Activation of Alumina to 400°C	13
1-10	Cycloaddition of Methyl Acrylate and Cyclopentadiene	14
1-11	Boron Trihalides Acidity and Hydrolysis Character	18
1-12	Chemisorption of BX_3 onto Alumina	18
1-13	Reaction of BF_3 and Alumina	19
1-14	Reaction of BCl_3 and Alumina	20
1-15	Reaction of BBr_3 and Alumina	21
1-16	Boron-11 SSNMR of BBr/Al_2O_3 After the Addition of Pyridine	22
1-17	Weight Increase of Adding Boron Tribromide to Alumina: Comparison of Experimental with Theoretical Predictions	24
1-18	FT-IR Spectrum of Alumina	25
1-19	FT-IR Spectrum of BBr/Al_2O_3	26
1-20	Addition of BI to Alumina	28
1-21	Isomerization of DMM to DMF by BX_n/Al_2O_3	31

1-22	Lewis Acid Effect on a Dienophile	33
1-23	Lewis Acid-Catalyzed Diels-Alder Transition States	33
1-24	Diels-Alder Reactions	34
1-25	IP and MA Reaction Transition States	43
1-26	*B*-Halocatecholboranes	46
2-1	Favorable Orbital Overlap for Acrolein and Butadiene	62
2-2	Frontier Orbital Interactions of a Dienophile and a Diene in the Diels-Alder Reaction	63
2-3	Conformations of Acrolein - Lewis Acid Complexes	65
2-4	Reaction of a Lewis Acid with Crotonaldehyde	67
2-5	Proton NMR Spectrum of CA:BCB complex at -20°C in CD_2Cl_2	69
2-6	Expanded Vinylic Region of Proton NMR Spectrum of CA:BCB complex at -20°C in CD_2Cl_2	70
2-7	Proton NMR Spectrum of CA at -20°C in CD_2Cl_2	71
2-8	Proton NMR Spectrum of BCB at -20°C in CD_2Cl_2	72
2-9	Reaction of *B*-Bromocatecholborane with Crotonaldehyde	73
2-10	^1H-^1H COSY Spectrum of CA:BCB Complex at -50°C in CD_2Cl_2	76
2-11	Carbon-13 NMR Spectrum of CA:BCB Complex at -20°C in CD_2Cl_2	78
2-12	Carbon-13 NMR Spectrum of CA at -20°C in CD_2Cl_2	79
2-13	Carbon-13 NMR Spectrum of BCB at -20°C in CD_2Cl_2	80
2-14	Boron-11 NMR Spectrum: Titration of BCB with CA at -20°C in CD_2Cl_2	82
2-15	^1H-^{13}C HETCOR Spectrum of CA:BCB Complex at -50°C in CD_2Cl_2	84

2-16	^1H-^1H ROESY Spectrum of CA:BCB Complex at -50°C in CD_2Cl_2	86
2-17	EXSY of CA:BCB Complex at -50°C in CD_2Cl_2	87
2-18	The CA:BCB Complex Created by MNDO Theoretical Minimization Using CaCHe Software	89
2-19	The *s-trans* Conformation of the CA:BCB Complex	90
2-20	The *s-cis* Conformation of the CA:BCB Complex	90
2-21	Possible Boron Enolate Products if CA Reacted with BCB	91
2-22	Low Temperature IR Instrument Set-up	92
2-23	IR Spectrum of CA at -17°C in CH_2Cl_2	93
2-24	IR Spectrum of CA:BCB Complex at -17°C in CH_2Cl_2	94
2-25	Expanded Region of IR Spectra of CA, BCB and CA:BCB Complex at -17°C in CH_2Cl_2	95
2-26	The BCB Catalyzed Reaction of CA and CP	97
2-27	Conjugate Bases Complexed with BCB	100
2-28	Complex of Mesityl Oxide and *B*-Bromocatecholborane	101
2-29	Hydrogen Bromide Addition to Conjugated Carbonyls	102
2-30	Proton NMR Spectrum of BTA and BCB at -20°C in CD_2Cl_2	108
2-31	Proton NMR Spectrum of BTA at -20°C in CD_2Cl_2	109
2-32	IR Spectrum of BTA at -17°C in CH_2Cl_2	110
2-33	IR Spectrum of BTA and BCB at -17°C in CH_2Cl_2	111
2-34	Expanded Region of IR Spectra of BCB, BTA, and BTA:BCB at -17°C in CH_2Cl_2	112
2-35	Reaction of Butyraldehyde (butanal) and *B*-Bromocatecholborane	113
2-36	Reactions of Catecholborane with Various Acids	115

A-1	Proton NMR Spectrum of MSO and BCB at -20°C in CD_2Cl_2	131
A-2	Proton NMR Spectrum of MA and BCB at -20°C in CD_2Cl_2	132
A-3	Proton NMR Spectrum of MDA and BCB at -20°C in CD_2Cl_2	133
A-4	Proton NMR Spectrum of MC and BCB at -20°C in CD_2Cl_2	134
A-5	Proton NMR Spectrum of AN and BCB at -20°C in CD_2Cl_2	135
A-6	Proton NMR Spectrum of BZ and BCB at -20°C in CD_2Cl_2	136
A-7	Proton NMR Spectrum of CB at -20°C in CD_2Cl_2	137
A-8	Carbon-13 NMR Spectrum of CB at -20°C in CD_2Cl_2	138
A-9	Proton NMR Spectrum of MeOCB at -20°C in CD_2Cl_2	139
A-10	Carbon-13 NMR Spectrum of MeOCB at -20°C in CD_2Cl_2	140
A-11	Proton NMR Spectrum of MeOCB and CA at -20°C in CD_2Cl_2	141
A-12	Proton NMR Spectrum of TFACB at -20°C in CD_2Cl_2	142
A-13	Carbon-13 NMR Spectrum of TFACB at -20°C in CD_2Cl_2	143
A-14	Proton NMR Spectrum of TFACB and CA at -20°C in CD_2Cl_2	144
A-15	Proton NMR Spectrum of TfCB at -20°C in CD_2Cl_2	145
A-16	Carbon-13 NMR Spectrum of TfCB at -20°C in CD_2Cl_2	146
A-17	Proton NMR Spectrum of TfCB and CA at -20°C in CD_2Cl_2	147
A-18	Proton NMR Spectrum of FCB at -20°C in CD_2Cl_2	148
A-19	Carbon-13 NMR Spectrum of FCB at -20°C in CD_2Cl_2	149
A-20	Proton NMR Spectrum of FCB and CA at -20°C in CD_2Cl_2	150

LIST OF ABBREVIATIONS

1D	one-dimensional
2D	two-dimensional
AN	acrylonitrile
BCB	*B*-bromocatecholborane
BMS	borane-dimethylsulfide complex
BTA	butanal
BX_3	boron trihalides
BZ	benzaldehyde
CA	trans-crotonaldehyde; *(E)*-2-butenal
CB	catecholborane
CCB	*B*-chlorocatecholborane
COSY	correlated spectroscopy
CP	cyclopentadiene
CPMAS	cross polarization magic angle spinning
D-A	Diels-Alder
DMF	dimethyl fumarate
DMM	dimethyl maleate
DMS	dimethyl sulfide
eq	equivalent
ESCA	electron spectroscopy for chemical analysis
EXSY	exchange spectroscopy
FAB-MS	fast atom bombardment mass spectrometry
FCB	*B*-fluorocatecholborane

FT-IR	Fourier transform infrared spectrometer
GC	gas chromatograph; gas chromatography
GC/MS	gas chromatograph with a mass spectrometer
gm, gms	gram, grams
h, hr, hrs	hour, hours
H_0	acidity function
HETCOR	heteronuclear chemical shift correlation spectroscopy
HOMO	highest occupied molecular orbital
HPLC	high performance liquid chromatography
HX	hydrogen halides (HF, HCl, HBr, HI)
Hz	hertz
IP	isoprene
IR	infrared spectra, infrared spectrometer
J, J_{xx}	coupling constant in Hz (where x is the atom designation)
L	liter
L.A., LA	Lewis acid
LUMO	lowest unoccupied molecular orbital
M	molarity (mols/L)
MA	methyl acrylate
MC	methyl crotonate
MDA	methyl-3,3-dimethyl acrylate
MeOCB	*B*-methoxycatecholborane
MeOH	methyl alcohol, methanol
meq	milliequivalent
MHz	megahertz

min	minute
mL	milliliter
mmol, mmols	millimole, millimoles
MO	molecular orbital theory
MSO	mesityl oxide
NMR	nuclear magnetic resonance
NOE	nuclear Overhauser effect
NOESY	nuclear Overhauser and exchange spectroscopy
ppm	parts per million
ref	reference
ROESY	rotating frame Overhauser enhancement spectroscopy
rxn	reaction
sec	second, seconds
SSNMR	solid state nuclear magnetic resonance
TF	trifluoromethanesulfonic acid; triflic acid
TFA	trifluoroacetic acid
TFACB	*B*-trifluoroacetocatecholborane
TfCB	*B*-trifluoromethanesulfonocatecholborane
THF	tetrahydrofuran
TLC	thin layer chromatography
TMS	tetramethylsilane
UV, UV-vis	ultraviolet-visible spectroscopy
μL	microliter

PART 1

Reactions Catalyzed

by

Highly Acidic Boronated Aluminas

A. INTRODUCTION

The Diels-Alder (D-A) reaction is of great importance to the organic chemist. The D-A reaction is a concerted [2 + 4] cycloaddition of an electron deficient 2-electron dienophile and a 4-electron conjugated diene which creates a new six-membered ring (see Figure 1-1).[1] As many as four new stereogenic centers are formed in the reaction. Uncatalyzed D-A reactions often require long reaction times and elevated temperatures and are relatively unselective. Remarkably, added Lewis acids increase the stereoselectivity, regioselectivity,[2] and rate[3] of the D-A reaction. Lewis acids that have been widely used in this reaction include $AlCl_3$, $LiClO_4$, and BF_3.

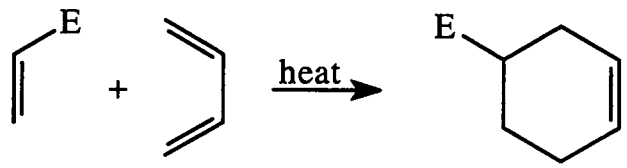


Figure 1-1. General Diels-Alder reaction

Historically, organic reactions were carried out in homogenous environments. This has changed in recent years. For example, polymers[4] and inorganic solids[5] have increasingly been used as catalysts for organic reactions, often giving better yields, increased diastereoselectivity, enhanced enantioselectivity, and superior regioselectivity. The focus of this section of the dissertation is on the effect of inorganic solids, in particular alumina, on the Diels-Alder reaction.

Heterogeneous inorganic solids are increasingly being used as catalysts for the D-A and other organic reactions. Solids, such as alumina,[6,7] clays,[8] zeolites,[9] and silica gel[10] have been used extensively in organic synthesis as mild acids and bases. Surface reactions often yield comparable or better results than their counterpart homogeneous reactions. A review by Smith summarized the advantages and disadvantages that inorganic solids possess for use as catalysts for organic reactions (Table 1-1).[5a] The information in Table 1-1 can be applied to most inorganic, heterogeneous solids, including alumina. Our group[6,7,11] and several others[12] have extensively studied the use of activated and unactivated alumina as a catalyst, reactant, and reagent.

Alumina is a metal oxide matrix containing aluminum and oxygen ions with anhydrous and hydrated forms. Alumina exists in several forms including α, γ, δ, θ, κ, χ, and η. These materials are prepared from Bauxite (natural occurring aluminum ore) via the Bayer process and are commercially available.

α–Alumina (corundum) is naturally occurring and does not function as a catalyst. Its lattice structure is very compact, with most of the aluminum 3^+ ions in the octahedral state and the oxygen 2^- ions in the hexagonal state. These characteristics produce a very strong mechanical strength, good thermal stability, and high density. Although its uses as a catalyst are limited, α–alumina has been used in several industrial applications including abrasives and ceramics.[7]

The remaining forms (γ, δ, θ, κ, χ, η) are classified as the transition aluminas and are prepared by the dehydration and calcination of their hydrated, natural occurring aluminum oxides. Continued dehydration will eventually produce the inert α–alumina species described above (see Figure 1-2).[7]

Table 1-1. Advantages and Disadvantages of Inorganic Solids [5a]

Advantages
• Several 'supported reagents' are commercially available and can be used 'off-the shelf'.
• Reagents can offer a simple procedure and purification; solvent choice can be extended.
• Some of the new methodologies associated with these reagents introduce superior reaction selectivity and control in comparison to homogeneous counterparts.
• 'Solid reagents' are safe and easy to handle; generally non-volatile and odorless.
• They are normally environmentally compatible.
Disadvantages
• The materials are often ill-defined in terms of their physical and chemical properties; it is difficult to quantify surface properties in familiar solution terms (e.g. pK_a).
• Structural composition and properties can vary significantly because there are many commercial suppliers and manufacturers of amorphous inorganic oxides.
• Some procedures for preparing and handling the solids require the use of specialist apparatus (e.g. high temperature furnace, glove box). Their lifetime can be limited.
• Some reagents require a low 'loading' of reactants, resulting in poor efficiency for large scale work. However, these problems can potentially be avoided by doing reactions in a 'column-mode'.

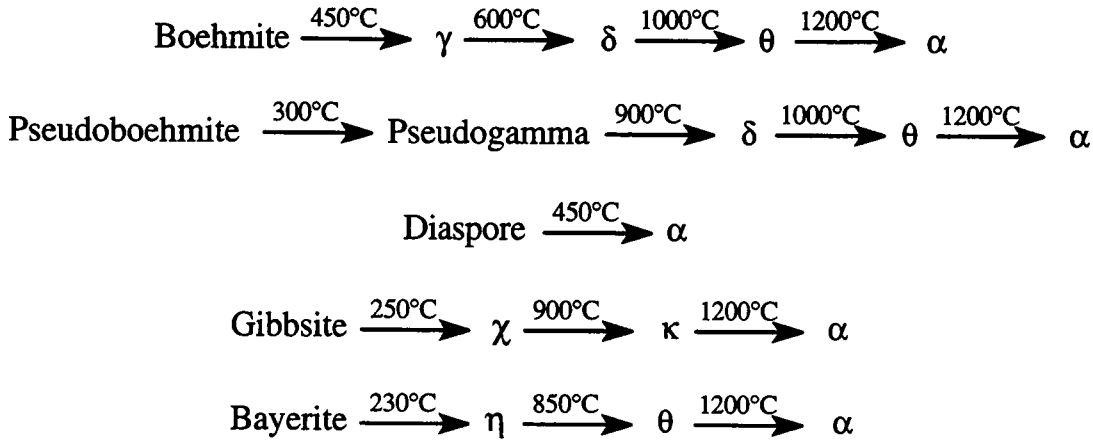


Figure 1-2. Formation of the Transition Aluminas

The transition aluminas, due to their chemical reactivity, make them catalytically important to the organic chemist. Gamma-alumina (γ-Al_2O_3) has been extensively studied by several research groups and is used more frequently than any of the other forms due to its enhanced catalytic activity and high surface area. Both acidic, neutral, and basic γ-alumina can be produced, all of which have a maximum surface area of 200 m^2/g. By heating the solids (activation), more acidic, neutral, or basic sites of the γ-alumina are exposed.

Knözinger and Ratnasamy[13] and Peri[14] have extensively studied the surface structure of alumina and its many forms. Knözinger and Ratnasamy were the first chemists to identify γ-alumina's framework by using the spinel defect model.[13] Their work showed unit cells comprised of 21-1/3 aluminum atoms per 32 oxygen atoms; hence the formula Al_2O_3. The non-integer number of aluminum atoms leaves vacant cations positions in the lattice. Unlike the aluminum cations, the

oxygen anions are arranged into four distinct layers: A, B, C, and D. The A-layer represents the surface or top layer and the B-, C-, and D-layers are inner layers (Figure 1-3).

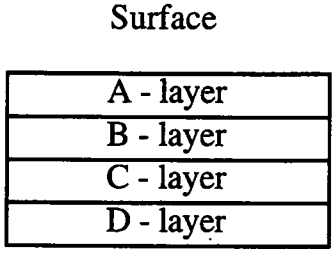


Figure 1-3. Layering of Alumina[13]

Each of the alumina layers is defined by the distribution of the cations in both octahedral and tetrahedral geometries. The 24 cation positions consist of 8 octahedral and 16 tetrahedral in the A-layer, 24 octahedral in the B-layer, 12 octahedral and 12 tetrahedral in the C-layer, and 24 octahedral in the D-layer (Figure 1-4).[13] Lower layers (B, C, and/or D) may be exposed if "clefts" or craters are present in the surface since the surface is better described as a mountainous region rather than a "flat" surface.

On the other hand, the anion layers, made-up of oxygen atoms, contain two different types which can hydrated or anhydrous. If hydrated, the A- and B-layers contain five types of hydroxyls that identify many of the reactive sites of alumina (see Figure 1-5).[14c] These hydroxyls have been distinctively identified by infrared spectrometry (Table 1-2)[14c] and ^{1}H NMR spectroscopy[15].

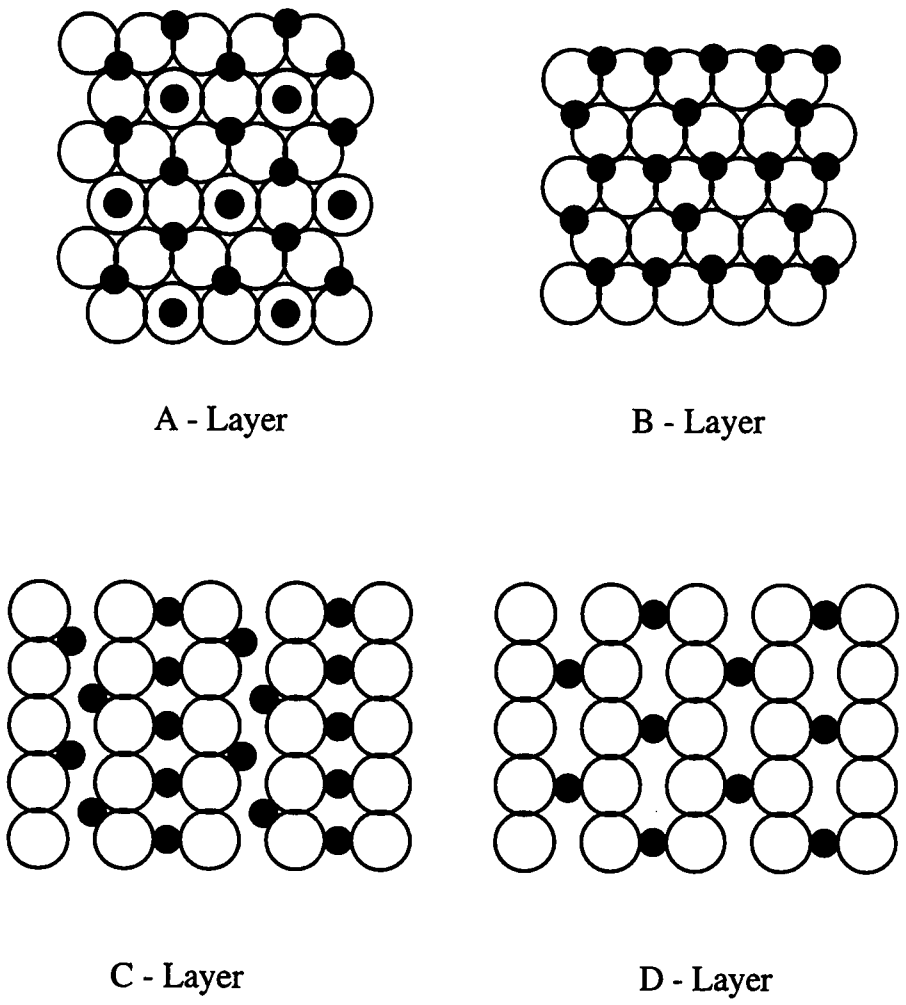


Figure 1-4. The Knözinger and Ratnasamy Layers of gamma-Alumina

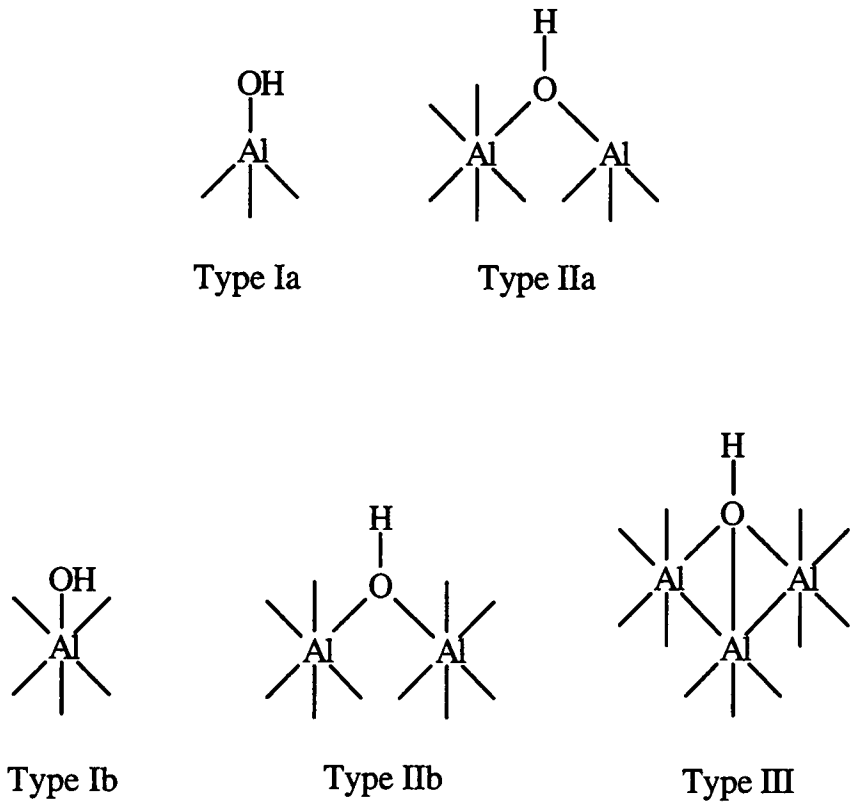


Figure 1-5. Hydroxyl Types on the A- and B-layers of gamma-Alumina

Table 1-2. IR Frequencies of Alumina Hydroxyls

Hydroxyl Type	IR Frequency (cm^{-1})
Ia	3760-3780
IIa	3730-3735
Ib	3785-3800
IIb	3740-3745
III	3700-3740

"Out of the bottle" or "off-the-shelf" gamma-alumina is naturally hydrated with approximately 3 mmols of surface hydroxyls per gram of alumina. This was confirmed by titrating the surface with methyllithium and measuring the volume of methane gas released by gasimetry. Alumina can be heated under vacuum, commonly called activation, to remove hydroxyls as water and expose aluminum cation and oxygen anion sites (Figure 1-6). The temperature of heating determines the amount of hydroxyl groups removed, and thus the extent of activation. The surface can be re-hydrated (except for highly activated surfaces heated to greater than 1000°C) by exposing the alumina to air. This reaction is extremely fast (~10 minutes) in humid East Tennessee compared to the lengthy four hour to two days activation time usually needed to remove the surface-bound hydroxyls.

Brockmann Grade I γ-alumina is a common form of alumina that is commercially available and is the solid usually studied by the Pagni and Kabalka

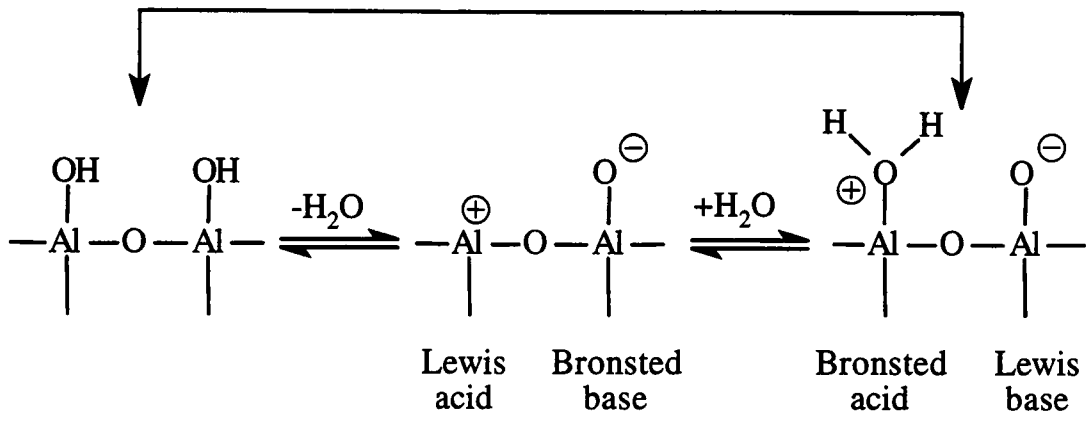


Figure 1-6. Activation and Dehydration of γ-alumina

research group. Earlier work by Posner[12a,12b] and co-workers, and more recently by Kropp[12c,12d] and co-workers, have shown the importance of γ-alumina in organic synthesis. Posner and Kropp have completed many studies of organic reactions on the activated and unactivated surfaces of alumina as well as on silica gel. Some of their reactions are detailed in Figures 1-7[11i,11e] and 1-8[12a-d]. Note that many of the reactions are performed in the absence of solvent. Interestingly, the products can be easily removed from the surface with a minimal amount of solvent with purification often taking place simultaneously. The diversity of reactions catalyzed by alumina is very large. These reactions will be studied for years to come.

Our group has shown that many reactions on alumina give excellent results.[6,7,11] For example, using alumina bound to a TLC plate, Kabalka and Gooch discovered that organoboranes react with sodium iodide to produce alkyl iodides (Figure 1-7, reaction 1).[11i] This was followed by a study that

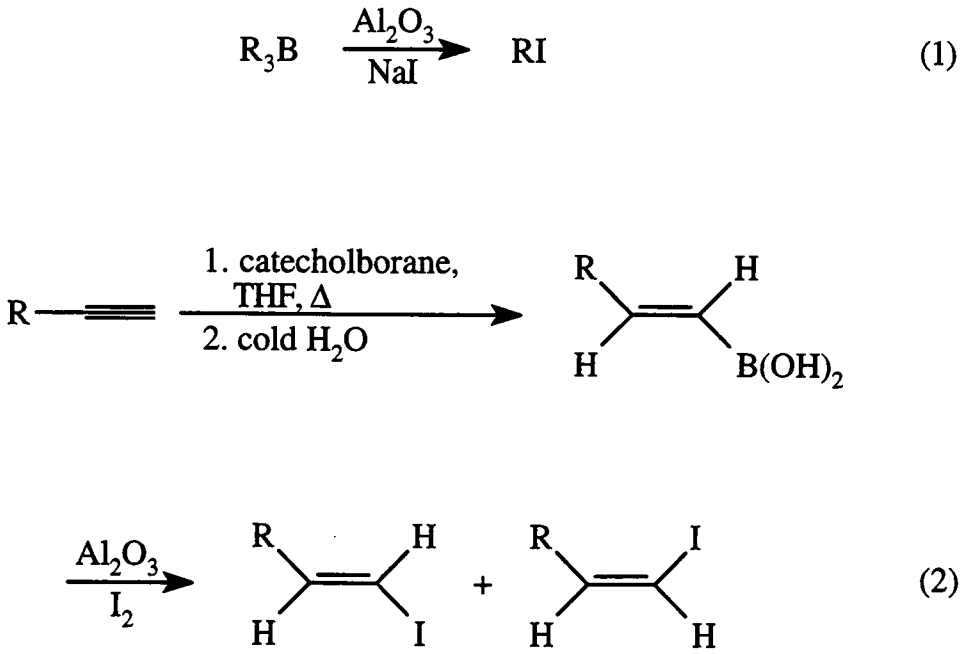


Figure 1-7. Iodinations using Alumina

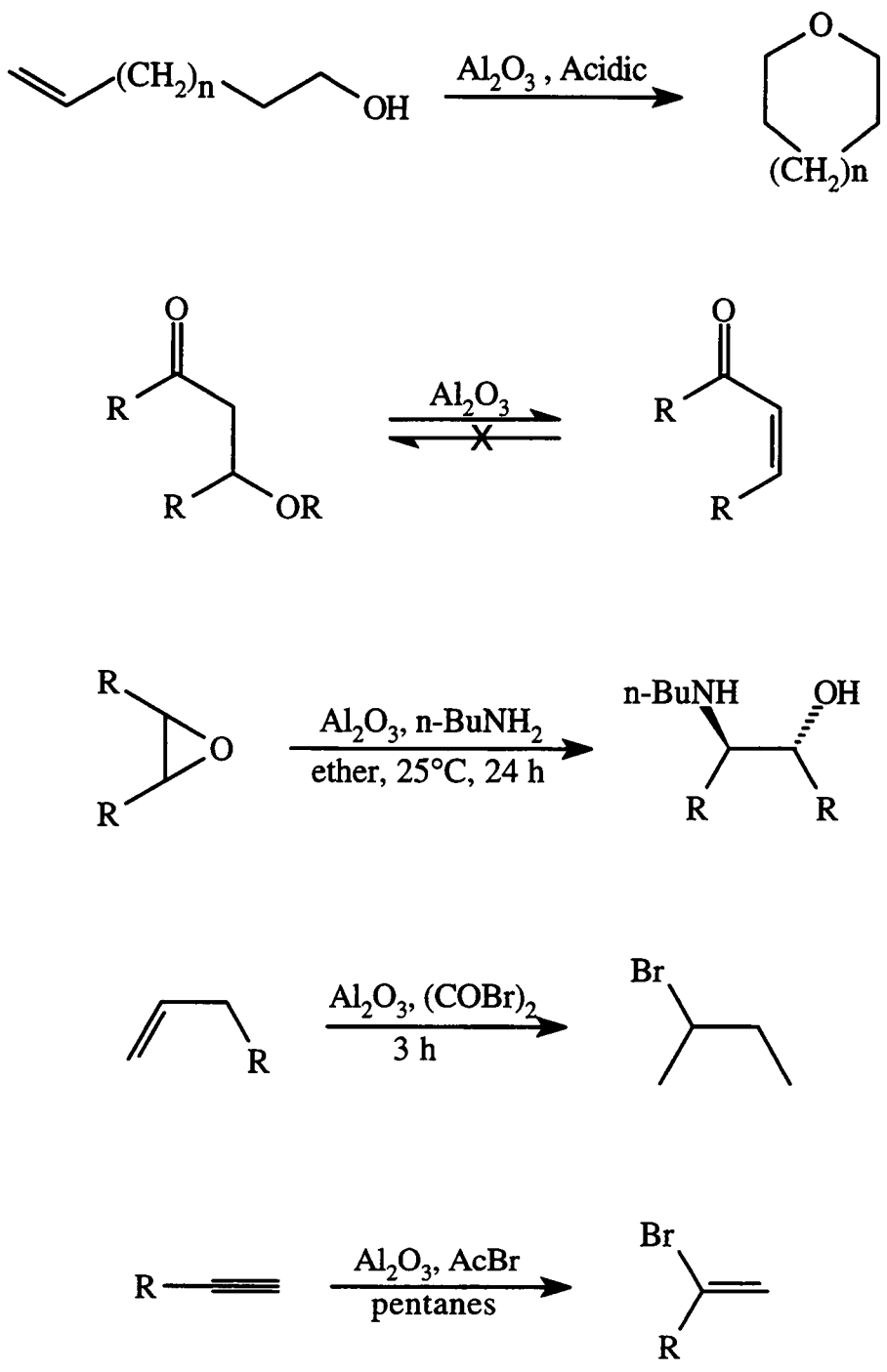


Figure 1-8. Reactions Catalyzed by Alumina

demonstrated that vinylboronic acids bound to the surface of alumina yielded *(E)* and *(Z)* vinyl iodides when treated with iodine. The major product was the *(E)* isomer, but the E/Z ratio could be modified by using different hydrated surfaces and activations.

Activation of alumina, in addition to removing hydroxyls, exposes additional acidic and basic sites to the surface in the form of aluminum cations and oxygen anions. These sites show much higher catalytic activity than those on less or unactivated alumina. The activity can be "regulated" by the temperature and time of activation. Several groups, including ours, have discovered that the most catalytically active alumina is the one activated at 400°C (Figure 1-9). This is due in part to the nearly equal number of exposed acid and basic sites and the fact that only 1 mmol of hydroxyls remains on the surface per gram of alumina; so-called defect sites also appear on this surface. The acidity of the 400°C activated alumina increases to a pK_a of between -3.0 and -8.2 from a value of $pK_a = 7.0$ for the unactivated, neutral alumina.[16]

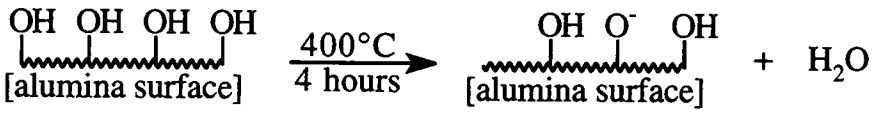


Figure 1-9. Activation of Alumina to 400°C

Our group has extensively studied the catalytic activity of Lewis acids as well as activated and unactivated alumina on the Diels-Alder reaction.[11c,11d] These catalysts have a dramatic effect on the reactivity of the D-A reactions, especially

when the dienophile contains an electron-withdrawing group (see Figure 1-1). They yield increased diastereoselectivity and enantioselectivity with superior regioselectivity as compared to the uncatalyzed reaction.

A quintessential D-A reaction studied is the cycloaddition of methyl acrylate (MA) and cyclopentadiene (CP) (Figure 1-10). The two products formed are the endo and exo adducts. The endo adduct is preferred for the uncatalyzed reaction due to the preferred HOMO-LUMO orbital overlap of MA and CP molecular orbitals and steric interactions in the transition state.[17] An uncatalyzed reaction produces only a 7.3:1 endo : exo ratio. Unactivated alumina yields an unimpressive 5.5:1, but the 400°C-activated alumina (Al_2O_3-400°C) increases that value to 50:1 due to the expanded acid sites on the surface. Although the homogeneous reaction with $AlCl_3$ produces an exceptional 99:1 endo : exo ratio[18], the results with Al_2O_3-400°C are better than those obtained with most other Lewis acids (see Table 1-3).

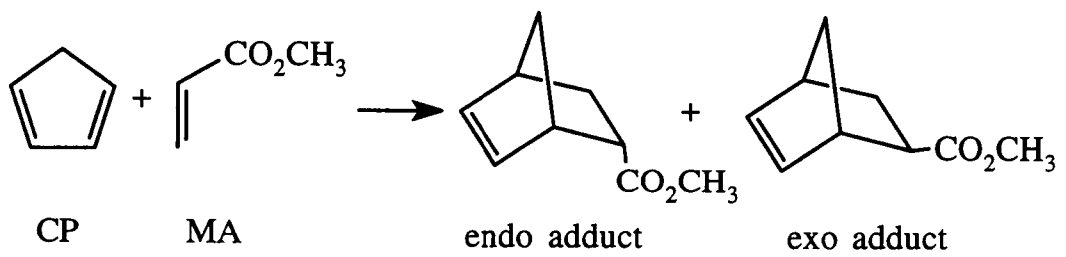


Figure 1-10. Cycloaddition of Methyl Acrylate and Cyclopentadiene

Table 1-3. Results of Methyl Acrylate and Cyclopentadiene Cycloaddition

Catalyst	endo	exo
CH_3CN [a]	4.9	1
Al_2O_3 [b]	5.5	1
none [a]	7.3	1
6 M $LiClO_4$/ether [c]	8.0	1
Al_2O_3-400°C	50	1
$AlCl_3$/benzene [d]	99	1

[a] reference 19. [b] reference 6a. [c] reference 20.
[d] reference 18.

To increase the acidity and catalytic activity of the alumina, the surface can be modified by either chemisorption or physisorption of a Lewis acid. A 1993 Tetrahedron article outlines the advantages of using $AlEt_2Cl$ and $TiCl_4$ adsorbed to the surfaces of alumina and silica gel as catalysts (Table 1-4).[21] The quantity of titanium or aluminum incorporated onto the surface ranged from zero (control experiment) to 1.43 millimoles per gram of solid. Also, the catalyst to dienophile (methyl acrylate) ratio, reaction time, activation method of the solid, and the Lewis acid amount were varied. The data revealed that Lewis acid incorporation onto alumina increased the adduct diastereoselectivity and percent conversion over the off-the-shelf and activated aluminas and silica gels. The uncatalyzed MA and CP reaction gave a 73:27 endo : exo adduct ratio with a modest yield of 9 % in 2 hours. Activated acidic alumina increased the adduct ratio to 92:8, with a 17 %

Table 1-4. Results Lewis Acid Incorporated Alumina and Silica Gel Catalyzed Methyl Acrylate and Cyclopentadiene Reaction

Solid	Activation	L.A. (meq/g)	Al or Ti (mmol/g)	Cat.:MA (g/meq)	% conversion 30 min	% conversion 2 hr	endo: exo [a]
-	-	-	-	-	-	9	73:27
Al_2O_3	b	-	-	0.13	7	17	92:8
Al_2O_3	none	Ti (1.0)	0.70	0.13	55	80	92:8
Al_2O_3	b	Al (1.0)	-	0.13	29	65	93:7
Al_2O_3	c	Al (1.0)	-	0.13	30	65	93:7
Al_2O_3	c	Al (2.5)	-	0.13	80	93	92:8
SiO_2	c	-	-	0.13	7	26	86:14
SiO_2	none	Al (2.5)	1.26	0.13	27	59	95:5
SiO_2	c	Al (2.5)	1.43	0.13	90	98	95:5
SiO_2	d	Al (2.5)	1.40	0.13	22	57	94:6

[a] Determined by GC. [b] Activated by heating at 400°C under vacuum. [c] Activated by heating at 140°C under vacuum [d] Activated by treatment with HCl
Al = $AlEt_2Cl$; Ti = $TiCl_4$
Reactions carried out in toluene at 20°C

conversion in 2 hours. Addition of the titanium or aluminum reagents retained the superb adduct ratios of the alumina catalyzed reaction (92:8) with conversions ranging from 65 % to 93 %.

The $AlEt_2Cl$ and $TiCl_4$ were chemisorbed to an activated neutral or activated acidic alumina or silica gel. The new surface provided a chemically bound Lewis acid for catalysis of organic reactions. The new catalysts could be recycled and regenerated, unlike the homogeneous aluminum and titanium catalysts. The concept of using Lewis acids chemisorbed on alumina to catalyze organic reactions has also been applied to $AlCl_3$,[22] BF_3,[23] and $ZrCl_4$[24] and can also be applied to other Lewis acids.

B. Results and Discussion

Boron trihalides are strong Lewis acids (see Figure 1-11) which have been used to catalyze many organic reactions.[25] They have also been used to catalyze the Diels-Alder reaction, but gave unacceptable results in specific cases. They often polymerize either the dienophile or the diene which leads to loss of product. If the acid was chemisorbed to a solid matrix, this problem might be avoided.

If the boron trihalide were chemisorbed to alumina, as described above for $AlEt_2Cl$ and $TiCl_4$ on alumina (see Table 1-4), their complexes with dienophiles would also be isolated from each other might then react with the diene to give the desired product. It is known that boron halides chemically bound to oxygen

Lewis Acidity

$BI_3 > BBr_3 > BCl_3 > BF_3$

Rate of Hydrolysis

$BI_3 > BBr_3 > BCl_3 > BF_3$

Figure 1-11. Boron Trihalides Acidity and Hydrolysis Character

($BX_3 \bullet OR_2$, BX_2OR, $BX(OR)_2$) are less acidic than the boron trihalides and thus are less prone to give side products during catalysis.

In addition to being strong Lewis acids, boron trihalides react with water (see Figure 1-11).[25] This is due, in part, to the strong oxophilic nature of boron. Not surprisingly, the reactivity of a boron halide is correlated with its Lewis acidity. Both the unactivated and activated γ-aluminas discussed earlier have their surfaces exposed with hydroxyl groups or oxide anions that react with the boron halide to create new, chemisorbed boronated surface (Figure 1-12).

Direct Method (X = F, Cl, Br)

$$BX_3 + Al_2O_3 \longrightarrow BX_n/Al_2O_3\ (n = 1\text{-}3) + (3\text{-}n)HX$$

Indirect Method (X = I)

$$BH_3 + Al_2O_3 \longrightarrow BH/Al_2O_3 + H_2$$

$$2BH/Al_2O_3 + I_2 \longrightarrow 2BI/Al_2O_3 + H_2$$

Figure 1-12. Chemisorption of BX_3 onto Alumina

Each of the four boron trihalides created a surface with unique characteristics. The reaction of boron trifluoride-etherate complex ($BF_3 \bullet Et_2O$) with γ-alumina did not liberate hydrogen fluoride (Figure 1-13). Boron-11 solid state NMR (SSNMR) of the resulting solid (BF_3/Al_2O_3) revealed a sharp, strong resonance at δ 6.5 and another weak one at δ 10.0, indicative of tetrahedral boron atoms. These signals indicated that there were two BF_3 species on the surface. The δ 6.5 signal is consistent with a BF_3 covalently bonded to a surface oxygen with the boron in a tetrahedral geometry. A solid state CPMAS (cross polarization magic angle spinning) NMR experiment confirmed the covalent bond of this species to the alumina surface.

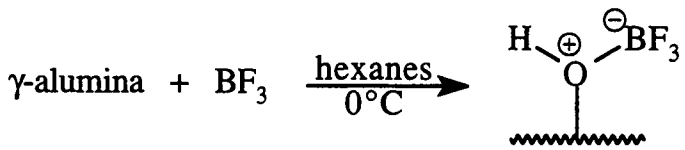


Figure 1-13. Reaction of BF_3 and Alumina

The δ 10.0 peak is presumably due to a physisorbed BF_3 on the surface, probably in the form of $BF_3 \bullet$etherate sitting on the surface. The physisorbed species was detected via a bilevel SSNMR experiment. The bilevel SSNMR experiment reveals species that are mobile on a surface unlike the CPMAS experiment which detects species that are immobile and chemically bound to the

surface. Since the two BF_3 species have borons in tetrahedral environments, the Lewis acidity of BF_3/Al_2O_3 is decreased compared to BF_3 itself.

BF_3/Al_2O_3 is a white solid that possessed a slightly higher acidity than alumina with an acidity function value (H_0) between 2.0 and 0.8. This was determined by a color change of a 1% fast garnet dye ($pK_a = 2.0$) from yellow to red, but no color change (blue to yellow) of a less basic species, crystal violet ($pK_a = 0.8$).

The BCl_3 and BBr_3 reactions were very similar in their reactions with γ-alumina. The chemisorption of these species produced new, boronated aluminas that offer promise as excellent solid catalysts. The addition of boron trichloride (1.0 M BCl_3 in hexanes) to alumina generated copious amounts of HCl gas and yielded a solid with two types of chemisorbed boron (see Figure 1-14). The reaction product possessed an overall stoichiometry of $BCl_{1.5}/Al_2O_3$. The $BCl_{1.5}/Al_2O_3$ solid is light brown in color and its ^{11}B SSNMR spectrum contains a single broad resonance at δ 7.0 indicating a trigonal boron species. Although only one resonance can be clearly identified, two types of boron presumably

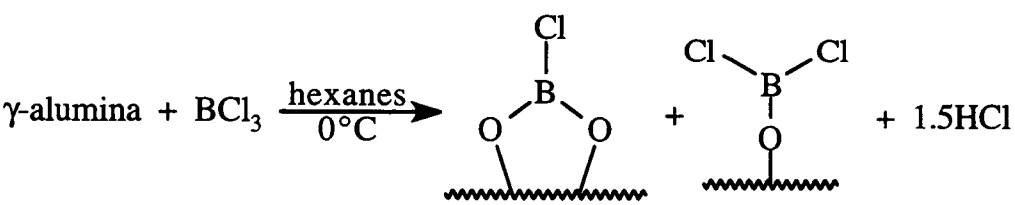


Figure 1-14. Reaction of BCl_3 and Alumina

exist. This is confirmed by the weight gain of the alumina (0.096g (1.5 mmols BCl) weight gain per gram of alumina) after the reaction is completed and the volume of hydrogen chloride gas released (1.5 mmols HCl gas measured by gasimetry). The acidity of the solid lies between H_o = -3.0 and -8.2, with indicators dicinnamalacetone (pK_a = -3.0) giving a positive test and anthraquinone (pK_a = -8.0) giving a negative test. The $BCl_{1.5}/Al_2O_3$ is a much stronger acid than the BF_3/Al_2O_3 due to the retention of the trigonal, electron deficient boron atom.

The bromoboronated alumina (BBr/Al_2O_3) was studied in the greatest detail. The BBr/Al_2O_3 was prepared via the previously described method (Figure 1-15). Unlike the fluorine and chlorine derivatives, the BBr/Al_2O_3 exhibited a surface with only one boron species. The boron-11 SSNMR spectrum contained a broad singlet with a chemical shift of 7.0, indicating a trigonal species (Figure 1-16). When pyridine was added to the surface, the ^{11}B resonance shifted upfield and sharpened as expected for tetrahedral, complexed boron atom (Figure 1-16).

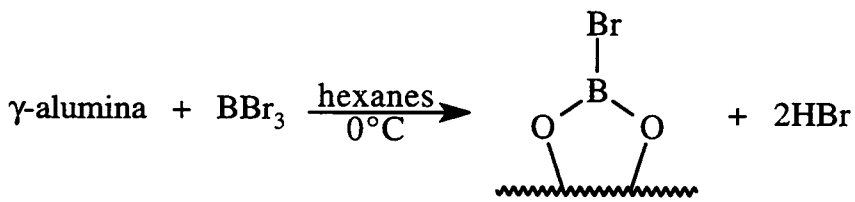


Figure 1-15. Reaction of BBr_3 and Alumina

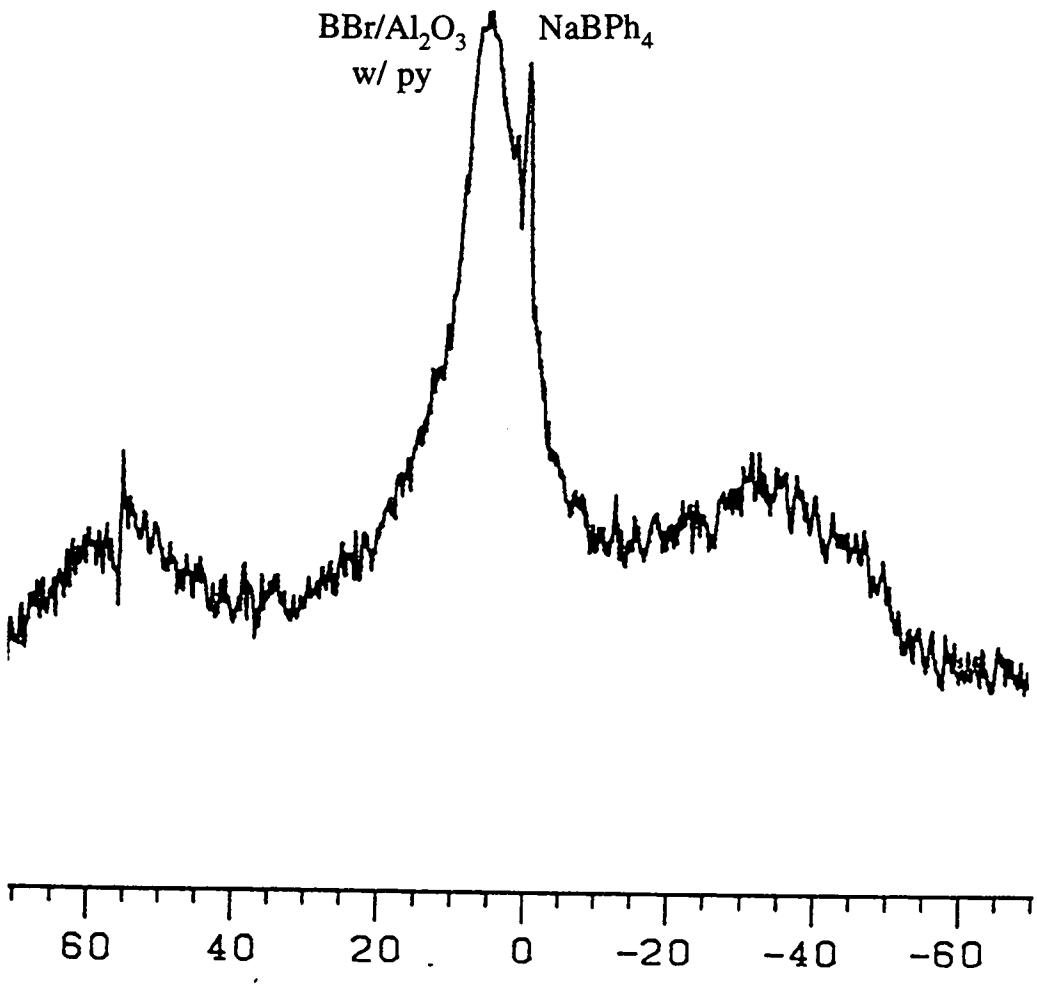


Figure 1-16. Boron-11 SSNMR of BBr/Al_2O_3 After the Addition of Pyridine

When 1 to 1.75 mmols of boron tribromide was added per gram of alumina, the weight gain of the solid corresponded to the addition of a lone B-Br absorbed onto the surface (see Figure 1-17 and Table 1-5). If less than 1 mmol was added, the weight increase of the alumina indicated that other species exist, but the SSNMR spectra was identical to that when higher amounts of BBr_3 were added. When greater than 2.0 mmol BBr_3 per gram Al_2O_3 was added, the alumina sites in which the BBr_3 react became saturated and the excess BBr_3 in solution was discarded in the work-up.

The HBr gas release was measured via gasimetry and supported the reaction release of 2 moles of HBr; this supported the proposed BBr/Al_2O_3 structure. In addition, aqueous washes of the surface were titrated and the results confirmed the existence of 1.0 mmol of boron and 1.1 mmol of bromine per gram of alumina. The titrations were performed with NaOH to determine the boron incorporation on alumina by formation of $B(OH)_3$ and Ag^+ ($AgNO_3$) to determine the bromide concentration by formation of AgBr.

FT-IR spectra of alumina before and after the treatment of BBr_3 showed that hydroxyl groups were consumed by the reaction (Figures 1-18, 1-19). Each analysis was performed with a small amount of solid placed in a reflectance apparatus cell inserted in the FT-IR.

Other spectral and experimental data obtained by previous graduate students of Pagni and Kabalka also support the postulated surface for BBr/Al_2O_3. Fast atom bombardment mass spectrometry (FAB-MS) gave negative results consistent with covalently bound BBr to the surface.[26] A positive result would have indicated that a boron species was able to enter the gas phase and, therefore

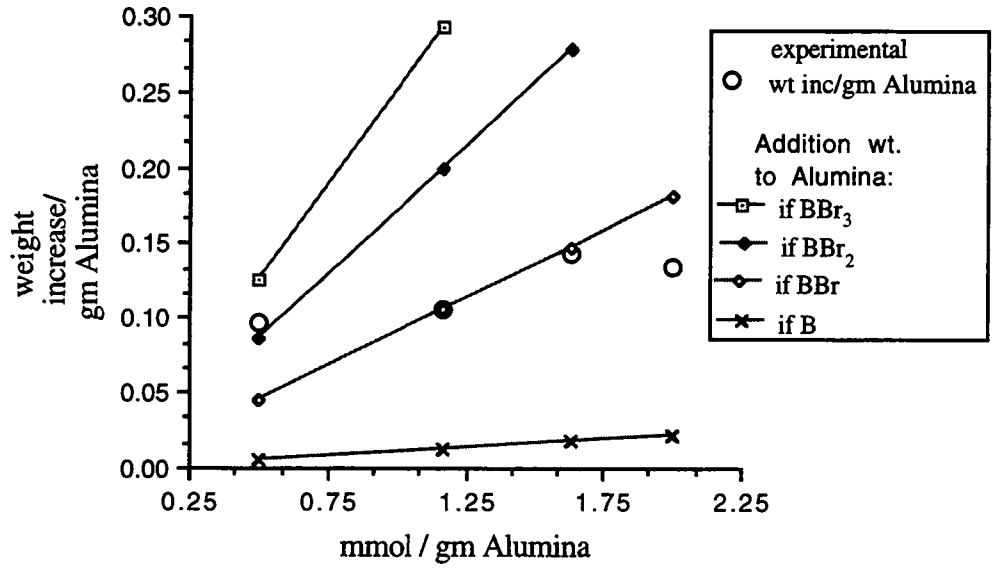


Figure 1-17 . Weight Increase of Adding Boron Tribromide to Alumina: Comparison of Experimental with Theoretical Predictions

Table 1-5. Weight Increase of Adding Boron Tribromide to Alumina: Comparison of Experimental with Theoretical Predictions

mmol BBr_3/ g Al_2O_3 added	Actual weight increase	Theoretical Weight Increase [a]			
		if BBr_3	if BBr_2	if BBr	if B
0.501	0.0976	0.1254	0.08539	0.04540	0.005400
1.17	0.1055	0.2936	0.1999	0.1063	0.01270
1.63	0.1431		0.2787	0.1482	0.01770
2.00	0.1354			0.1817	0.02170

[a] The theoretical weight increase of alumina if BBr_3, BBr_2, BBr, or B chemisorbed to the surface when adding 1.0 M BBr_3 to alumina.

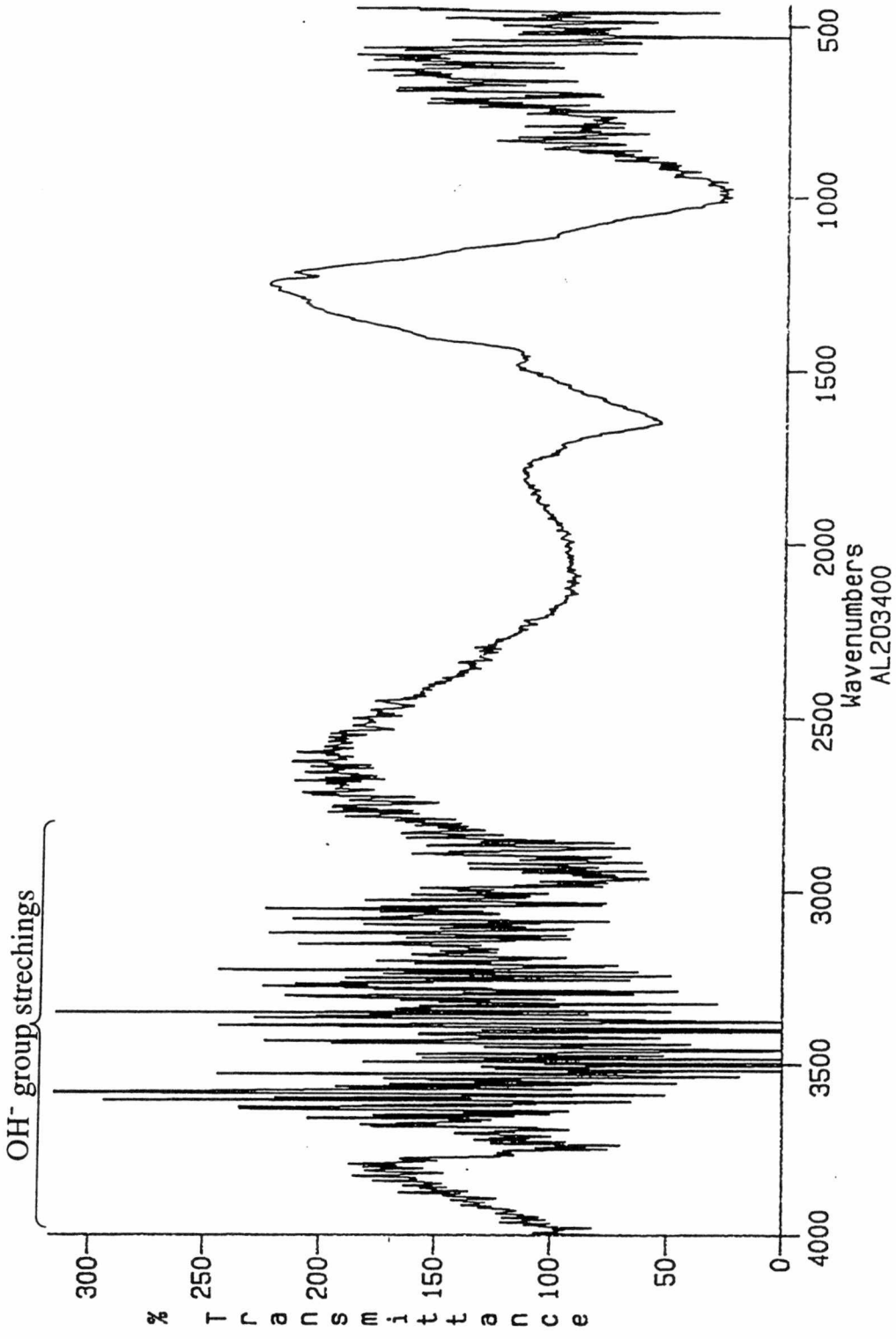


Figure 1-18. FT-IR Spectrum of Alumina

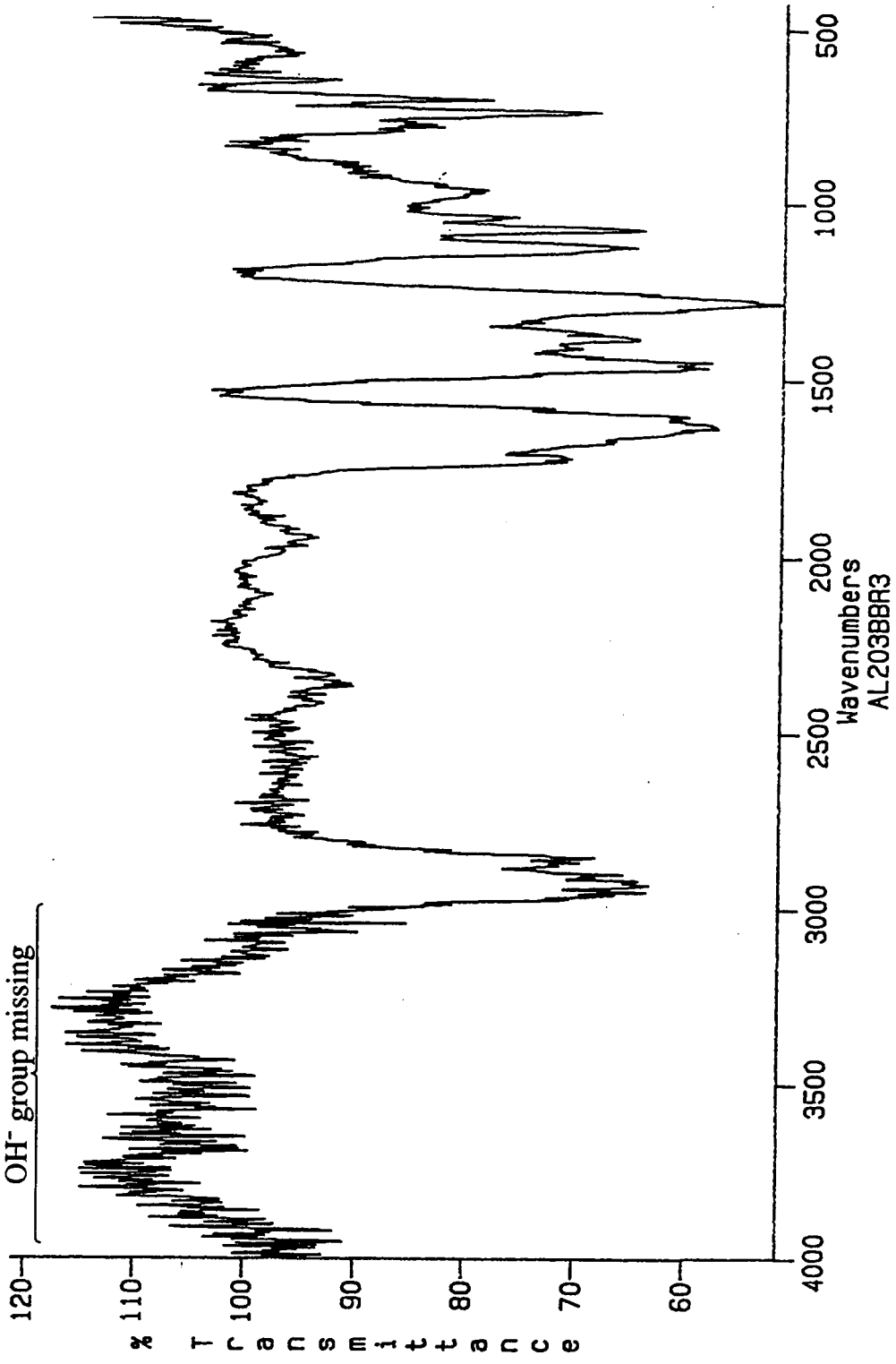


Figure 1-19. FT-IR Spectrum of BBr/Al_2O_3

was likely physisorbed on the surface. X-ray photoelectron spectroscopy or electron spectroscopy for chemical analysis (ESCA) revealed the expected presence of the four atoms on the surface: Al, O, B, and Br.[26]

The acidity of the BBr/Al_2O_3 was difficult to measure due to the brown color of the solid. The indicators used below $H_o = -13.2$ have color changes from yellow to colorless. These color changes are nearly impossible to detect with a highly colored solid. Although difficult to see, anthraquinone (pKa = -8.2) and m-nitrochlorobenzene (pKa = -13.2) gave positive color changes that confirmed that BBr/Al_2O_3 was a very acidic solid Therefore, the solid must have an acidity function greater than $H_o = -13.2$.

Acids can also be titrated with NMR sensitive bases. Phosphine oxides, strong Lewis bases, have been used, for example, as NMR probes to identify surface acidic sites on alumina.[27] Therefore, triethylphosphine oxide was used to probe the acids sites on BBr/Al_2O_3. The ^{31}P chemical shift of Et_3PO (δ 58.4 uncomplexed) changed markedly when added to BBr/Al_2O_3. Broad singlets at δ 90.5 and δ 104.8 were detected at lower concentrations of base because of the complexation of the base to the Lewis and Brønsted acidic sites on the solid. At higher concentrations of base, a resonance at δ 78.2 appeared due to the base being physisorbed to the alumina surface. The control NMR experiment with unmodified alumina revealed only the δ 77.0 resonance.

The final boron trihalide is unique. Boron triiodide is a very reactive, shock sensitive solid. Therefore, an alternative method was devised for the synthesis of BI_n/ Al_2O_3. First, BH_3•DMS (borane-dimethylsulfide complex) was added to

alumina to yield BH/Al_2O_3 (plus one equivalent of H_2). Then, iodine in a 1:1 ratio of I to B was added to yield BI/Al_2O_3 (plus one equivalent of H_2) (Figure 1-20). This achieved the desired result which was confirmed by boron-11 SSNMR which revealed a single resonance at δ 8.1. Although a tetrahedral species is shown in Figure 1-20, the exact nature of the species is not known. The BI/Al_2O_3 reacted violently with air and water, similar to boron triiodide, and has a high acidity function value. The BI/Al_2O_3 is a highly colored mustard yellow solid whose acidity was difficult to measure. The acidity function was determined to be less than -13.2.

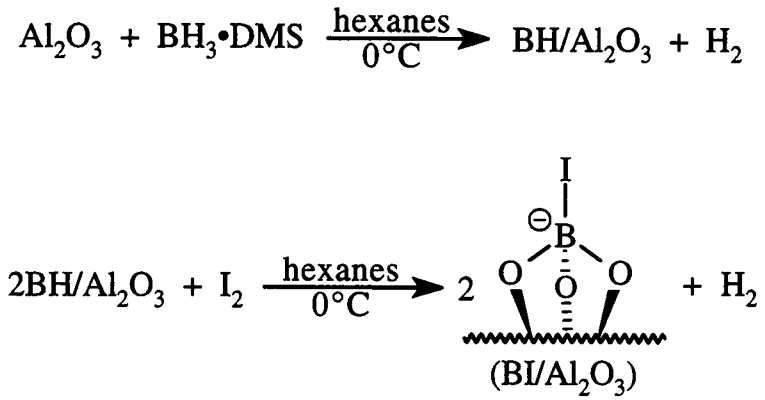


Figure 1-20. Addition of BI to Alumina

Table 1-6 summarizes and compares the data of the four boronated aluminas. These unique solids, especially the BCl, BBr, and BI derivatives, are very strong Lewis acids and can be used effectively to catalyze various organic reactions.

Table 1-6. Summary of BX_n/Al_2O_3 Characteristics

	BF_3/Al_2O_3	$BCl_{1.5}/Al_2O_3$	BBr/Al_2O_3	BI/Al_2O_3
Color	white	light brown	brown	mustard
^{11}B SSNMR	6.5, 10.0	7.0	7.0	8.1
Halide : Boron Stoichiometry	3 : 1	1.5 : 1	1 : 1	1 : 1
Acidity (H_o)	$\geq$ -3.0 $\leq$ 0.8	$\geq$ -8.2 $\leq$ -3.0	$\leq$ -13.2	$\leq$ -13.2
FT-IR	no OH^- present	no OH^- present	no OH^- present	no OH^- present
FAB-MS	-	-	negative	-
ESCA	-	-	showed Al, O, B, Br	-
^{31}P SSNMR of Et_3PO [a]	-	-	showed 3 resonances	-

[a] ^{31}P SSNMR of solid after the addition of Et_3PO.

Isomerizations

Two of the four boronated solids rapidly isomerized cis-alkenes to their trans configurations (Table 1-7). Dimethyl maleate (DMM) was transformed to its trans isomer, dimethyl fumerate (DMF), in as little as two minutes at room temperature. Other molecules, such as stilbene and maleic acid, were also isomerized from cis to trans on BX_n/Al_2O_3.

The isomerizations demonstrate that the boronated solids are strong Lewis acids and electron acceptors. The boron's empty 2p orbital readily accept one of the DMM's oxygen's lone pair electrons. Since a strong Lewis acid increases the single bond character of the carbon-carbon double bond, rotation about this bond to yield the trans isomer is thus possible (see Figure 1-21). Neat boron halides either isomerize at a very slow rate (BF_3•etherate) or polymerize the alkene (BCl_3, BBr_3). Experiments using unactivated and activated alumina revealed very slow isomerizations with some hydrolysis taking place.

Table 1-7. Isomerization of DMM to DMF with Boronated Solids

Catalyst	rate of isomerization
Al_2O_3	very slow [a]
Al_2O_3/BF_3	no isomerization
$Al_2O_3/BCl_{1.5}$	very slow
Al_2O_3/BBr	≤ 3 minutes
Al_2O_3/BI	≤ 2 minutes

5 mmols dienophile, 1 mmol BX_n/ 1 gm Al_2O_3, stoichiometric amount of catalyst, room temperature.
[a] some hydrolysis of the ester occured.

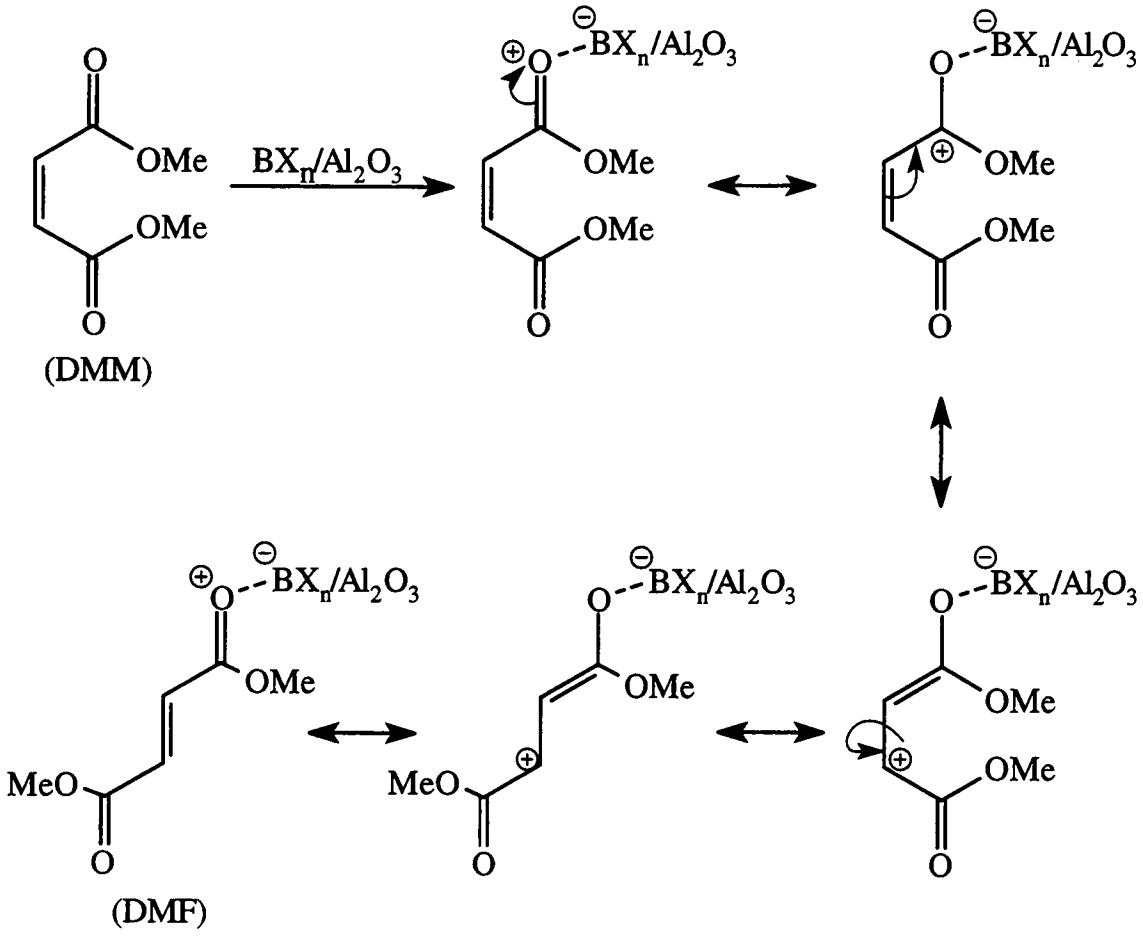


Figure 1-21. Isomerization of DMM to DMF by BX_n/Al_2O_3

Diels-Alder Reactions

Diels-Alder (D-A) reactions, as discussed earlier, are influenced by Lewis acids in several ways. Lewis acids will complex with the electron withdrawing substituent of the dienophile, thus making an even more electron deficient double bond (Figure 1-22). This results in a faster reaction and also a more selective reaction (Figure 1-23). The BX_n/Al_2O_3 solids exhibit enhanced Lewis acid due to the borons' empty 2p orbitals. Although back donation by bound surface oxygens is possible, the previous mentioned indicator tests confirm that the BCl, BBr and BI species are very acidic.

Typical D-A reactions were studied: methyl acrylate (MA) and cyclopentadiene (CP), isoprene (IP) and MA, and dimethyl maleate (DMM) and CP (Figure 1-24). These reactions were carried out on BX_n/Al_2O_3 due to the abundance of rate, stereochemical, and regiochemical data for comparable reactions in solution which were available. The reaction of MA and CP was first studied on the boronated alumina surface. In the absence of solvent, alumina acted as the "solvent" and catalyst (Table 1-8).

This reaction produced good endo : exo diastereochemical ratios, but unacceptable yields. The low yields are attributed to the slow diffusion of the starting materials on the alumina. Typically, MA was added to the solid first then, after 5 minutes of stirring, the CP was added. Frequently this produced a clumpy solid. The solventless reaction also produced black, polymer-like substances that were not isolated, but apparently reduced the yields of the desired adducts.

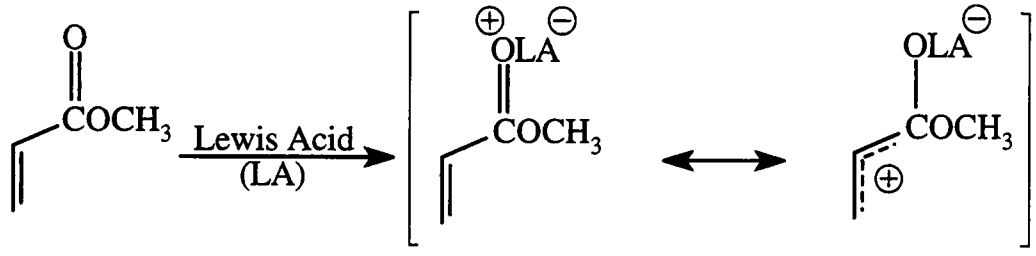


Figure 1-22. Lewis Acid Effect on a Dienophile

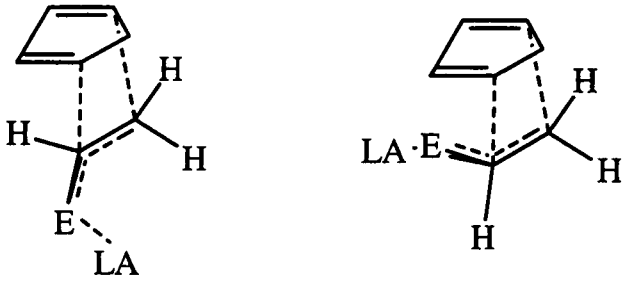
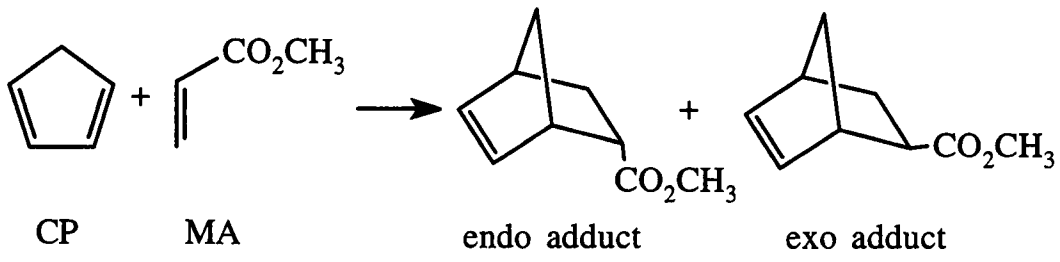
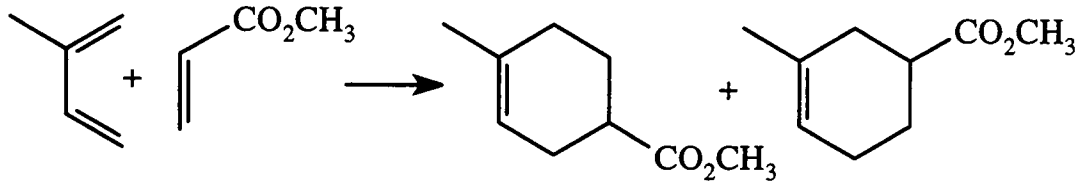


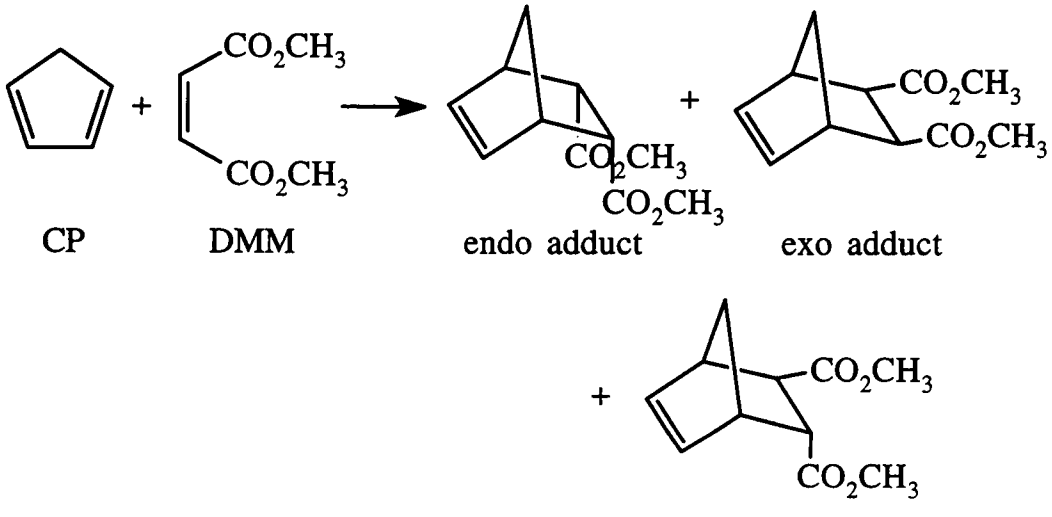
Figure 1-23. Lewis Acid-Catalyzed Diels-Alder Transition States



CP MA endo adduct exo adduct



IP MA "para" adduct "meta" adduct



CP DMM endo adduct exo adduct

trans adduct

Figure 1-24. Diels-Alder Reactions

Table 1-8. Neat Reactions of MA and CP with Boronated Solids

Catalyst	endo : exo	yield
a	4.9 : 1	–
Al_2O_3	5.8 : 1	–
Al_2O_3-400°C [b]	52 : 1	–
BF_3/Al_2O_3 [c]	4 : 1	<1 %
$BCl_{1.5}/Al_2O_3$ [c]	only endo	<1 %
BBr/Al_2O_3 [c]	8 : 1	18 %
BI/Al_2O_3 [c]	no adducts	–

5 mmol of reactants. [a] uncatalyzed in CH_3CN. [b] Al_2O_3 activated at 400°C. [c] 1 mmol BX_n/ 1 gm Al_2O_3, reaction time 4 hours, stoichiometric amount of catalyst, room temperature.

The MA and CP reaction was also carried out on the four boronated aluminas at elevated temperatures in hope of increasing the product yields. No D-A adducts were recovered, presumably because of decomposition of the products and starting materials.

A review of the literature revealed that toluene had been used successfully as a solvent system for alumina reactions.[21,28] A minimal amount of dry toluene was then added to the alumina to create a slurry before the reactants were added. As before, MA and CP were added successively and the reaction allowed to stir for one hour. With the exception of the BF_3/Al_2O_3, the reaction yields were acceptable (Table 1-9). A slight increase in selectivity was observed compared to the solventless reactions. The solvent allowed the starting materials to diffuse throughout the alumina surface and the reactions were catalyzed, as predicted.

Table 1-9. Reactions of MA and CP with Boronated Solids

Catalyst	endo : exo	yield
BF_3/Al_2O_3	24 : 1	31 %
$BCl_{1.5}/Al_2O_3$	12 : 1	78 %
BBr/Al_2O_3	13 : 1	88 %
BI/Al_2O_3	16 : 1	47 %

5 mmol of reactants, 1 mmol BX_n/ 1 gm Al_2O_3, toluene slurry, reaction time 1 hour, stoichiometric amount of catalyst, room temperature.

Most of the BF_3/Al_2O_3 Lewis acidic sites are masked because the original trigonal boron is complexed to oxygen. This produces a very poor catalyst. Even at longer reaction times, the fluoroboronated solid gave very poor yields, but product isomer ratios comparable to those obtained for the other boronated solids.

The $BCl_{1.5}/Al_2O_3$ and BBr/Al_2O_3 gave very good product isomer ratios and yields. Although these solids gave 12:1 and 13:1 endo : exo ratios, respectively, they do not compare favorably with the 99:1 product ratio of the $AlCl_3$ catalyzed reaction. However, the surface catalyzed reactions are accomplished with a minimal amount of solvent and the solids can be recycled, unlike the $AlCl_3$ catalyzed reactions. In addition, the products extracted form the surface are 99+ % pure due to the alumina surface doubling as a purification system.

The BI/Al_2O_3 catalyzed reaction produced acceptable product isomer ratios, but poor yields. This was due, in part, to many side reactions. The GC/MS scan revealed more than a dozen major products, with many minor ones. The mass

peaks indicated that they were derivatives of the starting materials, but none of them were isolated. The increased acidity of the iodoboronated solid also caused rapid degradation of the D-A adducts over moderate to long reaction times.

Since the BBr/Al_2O_3 furnished the best D-A results, further studies were performed to determine the best reaction conditions. First, the reaction time was varied (Table 1-10). The diastereotopic product ratios remained constant; however, the yields decreased over time. At 1 hour, the yield was 88 % and declined to 71 % over 16 hours. Beyond a 7 hour reaction time, the product resulting from the addition of HBr to the double bond of the D-A adduct was also detected. The HBr was presumably formed by the hydrolysis of the B-Br bond. The degradation occurred at about of 1 % per hour. Interestingly, product isomer ratios remained consistent throughout.

Table 1-10. Time Dependent Reactions of MA and CP with BBr/Al_2O_3

Catalyst	rxn time (hr)	endo : exo	yield
BBr/Al_2O_3	1	13 : 1	88 %
BBr/Al_2O_3	2	12 : 1	86 %
BBr/Al_2O_3	3.5	12 : 1	85 %
BBr/Al_2O_3	7	13 : 1	84 % [a]
BBr/Al_2O_3	16	13 : 1	71 % [a]

1 mmol BBr/ 1 gm Al_2O_3, toluene slurry, stoichiometric amount of catalyst, room temperature. [a] an additional product (HBr addition to the D-A adduct) of 5.5 % and 6.2 % yield respectively appeared.

All previously described reactions were carried out using 1 mmol of BBr per gram of alumina and stoichiometric amounts of the solid catalyst and the reactants. These parameters were then modified in an attempt to increase both the product isomer ratios and yields (Table 1-11). When excess catalyst (versus the reactant) was used (Table 1-11, entry 3), the product isomer ratios increased slightly, but the yields were reduced considerably when compared to the stoichiometric reaction in entry 1, Table 1-11.

When the quantity of BBr per gram of alumina was reduced, the product yield increased, but the diastereotopic ratio was lowered. Under these conditions, there are fewer catalytic sites and the BBr sites are further apart allowing for a slower, less selective reaction, but with fewer side products.

The D-A reactions were often run with excess CP (diene) due to its fast rate of dimerization via the D-A reaction with itself. When the 1 mmol BBr per gram alumina was used as the catalyst and CP was in excess, the yield of adducts increased to a remarkable 99+ % and the product isomer ratio to an excellent 16:1 (see Table 1-11). Thus, BBr/Al_2O_3 is a synthetically useful catalyst.

The turnover ratio was also determined to see if the solid was, in fact, serving a catalytic role in the reactions. This experiment used 2.2 grams of BBr/Al_2O_3 (2.2 mmol BBr) and 111 millimoles of each starting material. Over 40 mmols of D-A products were recovered after only 3 hours of reaction, with product ratios identical to those in previous reactions (see Table 1-11). The data indicate a high turnover rate and that BBr/Al_2O_3 is functioning as a catalyst.

Table 1-11. Stoichiometric Changes in the Reaction of MA and CP with BBr/Al_2O_3

mmol MA	mmol CP	mmol BBr / gm Al_2O_3	endo : exo	yield
5	5	1 : 1	13 : 1	88 %
5	5	0.5 : 1	12 : 1	95 %
2.5	2.5	1 : 1	24 : 1	72 %
2.5	2.5	0.5 : 1	16 : 1	74 %
6.5	15	1 : 1	13 : 1	95 %
5	15	1 : 1	16 : 1	99+ %
111	150	1 : 1	16 : 1	40 mmols [a]

toluene slurry, 5 gms Al_2O_3/BBr, reaction time 1 hour, room temperature. [a] turnover rate/catalytic activity rate experiment; 2.22 gms solid, 3 hour reaction time, 10 mL toluene, 40 mmols product recovered

The DMM with CP and IP with MA reactions were carried out using the results obtained in the MA and CP reactions. The reactions involved 1 mmol BX_3 per gram of alumina, excess CP (for the DMM + CP reaction), and a 1 hour reaction time. The DMM and CP reaction posed a different problem. As discussed earlier, the DMM isomerized to DMF in the presence of the boronated solids. This reaction, in fact, was faster than the D-A reaction and, in every case, the fumerate-CP (trans) adduct was detected. The BBr/Al_2O_3 was the only solid to catalyze the DMM and CP reaction in the absence of solvent, but the yield of products was low (5%) and only moderate selectivity of 4.2:10:1 trans : endo : exo product ratio was observed (Table 1-12). The other three solids gave only side products (polymers of the starting materials) in the absence of solvent.

When a toluene slurry was used, however, the DMM and CP reactions gave superior results to their solventless counterparts. The fluoro- and chloroboronated aluminas afforded nearly identical product isomer ratios of 1:10:0 and 1:14:0 respectively, but very different product yields of 24 % and 96 %. The low quantity of the fumerate product shows that only a small amount of DMM had isomerized prior to the Diels-Alder reaction, but the majority of the reactants yielded the endo adduct.

The bromoboronated alumina, again, gave a superior yield, 97 %, with outstanding selectivity for the trans adduct; the trans : endo ratio was 50:1. The isomerization of DMM was clearly very fast (see Table 1-7) and thus most of the product consisted of the trans adduct. Once again, the results show that BBr/Al_2O_3 can be synthetically useful.

Table 1-12. Reactions of DMM and CP with Boronated Solids

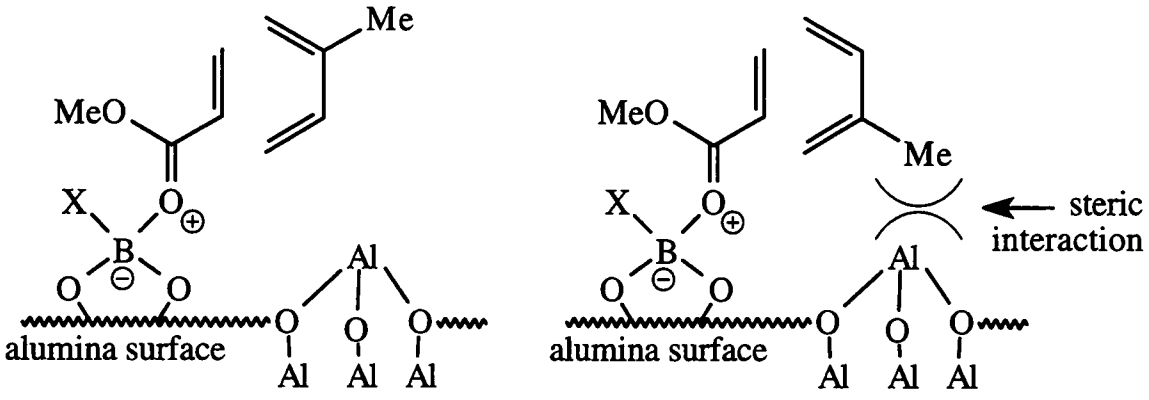
Catalyst	solvent slurry	trans : endo : exo	yield
BF_3/Al_2O_3	–	no adducts	–
	toluene	1 : 10 : 0	24 %
$BCl_{1.5}/Al_2O_3$	–	no adducts	–
	toluene	1 : 14 : 0	96 %
BBr/Al_2O_3	–	4.2 : 10 : 1	5 %
	toluene	50 : 1 : 0	97 %
BI/Al_2O_3	–	no adducts	–
	toluene	1 : 11 : 0	55 %

1 mmol BX_n/ 1 gm Al_2O_3, reaction time 1 hour, room temperature, stoichiometric amount of catalyst: 5 gms solid, 5 mmol DMM, 10-15 mmol CP.

The BI/Al_2O_3 catalyzed DMM plus CP reaction yielded a moderate product isomer ratio of 1:11:0, with a relatively poor product yield of 55 %. As with the MA and CP reaction, the iodoboronated alumina produced several side products that lowered the yield. The poor product isomer ratios are difficult to explain. The decomposition of one product might occur faster than another, but this is still unclear.

The IP and MA reactions produced remarkable results with the boronated solids. Neat reactions (solventless) using the boronated solids gave results similar to those of MA with CP and DMM with CP, but the toluene slurries generated results not previously observed (Table 1-13). Homogeneous catalysts, such as $AlCl_3$ in benzene and 6 M $LiClO_4$ in ether, only yielded para : meta product ratios of 20:1 and 3.4:1 respectively. Whereas the boronated solids BF_3/Al_2O_3, $BCl_{1.5}/Al_2O_3$, BBr/Al_2O_3, and BI/Al_2O_3 gave product isomer ratios of 5.8:1, 35:1, 49:1, and 23:1, better than has been previously achieved, particularly for the $BCl_{1.5}/Al_2O_3$ and BBr/Al_2O_3 catalysts. This large regioselectivity must be due to the steric interaction of the IP and the alumina surface (Figure 1-25). This steric interaction presumably forces the methyl group away from the surface, thus allowing the almost exclusive formation of the para product.

Product yields ranged from approximately 80 % for the $BCl_{1.5}/Al_2O_3$ and BBr/Al_2O_3 to a poor <1% for BF_3/Al_2O_3. The BF_3/Al_2O_3 once again showed that it is relatively inactive as a catalyst for the Diels-Alder reaction which may be a direct result of its lower acidity as compared to the other boronated solids.



para transition state

meta transition state

Figure 1-25. IP and MA Reaction Transition States

Table 1-13. Reactions of MA and IP with Boronated Solids

Catalyst	solvent slurry	para : meta	yield
$AlCl_3$ [a]	benzene	20 : 1	84
6M $LiClO_4$ [b]	ether	3.4 : 1	–
Al_2O_3/BF_3 [c]	–	no adducts	–
	toluene	5.8 : 1	< 1 %
$Al_2O_3/BCl_{1.5}$ [c]	–	32 : 1	5 %
	toluene	35 : 1	80 %
Al_2O_3/BBr [c]	–	49 : 1	15 %
	toluene	49 : 1	76 %
Al_2O_3/BI [c]	–	24 : 1	5 %
	toluene	23 : 1	56 %

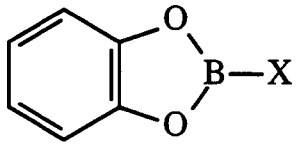
[a] reference 19. [b] reference 20, no yield reported. [c] 5 mmol reactants, 1 mmol BX_n/ 1 gm Al_2O_3, reaction time 1 hour, stoichiometric amount of catalyst, room temperature.

Homogeneous Diels-Alder Reactions

For comparison with the boronated solids, *B*-bromocatecholborane (BCB) and *B*-chlorocatecholborane (CCB) (Figure 1-26) were used to catalyze the reactions of MA with CP and MA with IP. BCB and CCB are Lewis acids with boron atoms in similar environments to those of the bromo- and chloroboronated aluminas, but they, can be used in homogeneous solutions. However, the empty 2p orbital of the boron atoms in BCB and CCB are conjugated with an aromatic system, thus reducing their Lewis acidity as compared to $BCl_{1.5}/Al_2O_3$ and BBr/Al_2O_3.

The BCB and CCB catalyzed reactions produced slightly better adduct ratios for the CP and MA reactions than did the boronated solid catalyzed reactions (Table 1-14). Nonetheless, the 19:1 endo : exo adduct ratio was not as good as the $AlCl_3$ catalyzed reaction in benzene (99:1). The catecholborane derivatives also produced lower yields of adducts (49 % and 47 %) as compared to the 88 % yield for the bromoboronated alumina catalyzed reaction. Longer reaction times did not result in higher product yields.

The BCB and CCB catalyzed reactions of MA and IP produced adduct ratios superior to the $AlCl_3$ catalyzed reaction (see Table 1-14). Although this selectivity is not fully understood, presumably steric interactions of the aromatic backbone of the Lewis acid must have an effect. The yields were slightly higher than those achieved on the bromo- and chloroboronated solids, but the adduct ratios observed in the boronated solids catalyzed reaction were not.



X = Cl : *B*-chlorocatecholborane (CCB)

X = Br : *B*-bromocatecholborane (BCB)

Figure 1-26. *B*-Halocatecholboranes

Table 1-14. Homogeneous versus Heterogeneous Diels-Alder Reactions

		MA + CP	MA + IP
Catalyst	solvent	endo : exo (yield)	para : meta (yield)
$AlCl_3$	benzene	99 : 1 (--) [a]	20 : 1 (84) [b]
CCB	CH_2Cl_2	19 : 1 (47) [c]	23 : 1 (94) [d]
BCB	CH_2Cl_2	19 : 1 (49) [c]	25 : 4 (63) [d]
$BCl_{1.5}/Al_2O_3$ [e]	toluene	12 : 1 (78)	36 : 1 (80)
BBr/Al_2O_3 [e]	toluene	13 : 1 (88)	49 : 1 (76)

[a] reference 18, no yield reported. [b] reference 19, 1.5 hour reaction time, room temperature. [c] 1.5 hour reaction time, room temperature. [d] 3 hour reaction time, room temperature [e] 1 mmol BX_n/ 1 gm Al_2O_3, reaction time 1 hour, stoichiometric amount of catalyst, room temperature.

C. CONCLUSIONS

A series of boronated aluminas was prepared, characterized, and used to catalyze isomerizations of alkenes and the Diels-Alder reactions of MA with CP, MA with IP, and DMM with CP. Results showed excellent selectivity with MA and IP, good selectivity with MA and CP, and excellent selectivity for the trans adduct with DMM and CP. When compared to the homogeneous reactions catalyzed by the *B*-halocatecholboranes, the boronated solids led to increased yields for the MA with CP reaction and exceptional adduct ratios for the MA and IP reaction. Product yields exceeded 90 % for most reactions while the purity of the products surpassed 95 % for all solid catalyzed reactions.

D. EXPERIMENTAL

General

Solution ^{1}H, ^{11}B and ^{13}C NMR spectra were recorded on JEOL FX90Q (Tecmag interface), Brüker AC-250, and Brüker AMX-400 instruments. $CDCl_3$ and CD_2Cl_2 were used as solvents with 1% TMS ($\delta = 0$) as the internal standard. Solid state ^{11}B, ^{13}C, and ^{31}P NMR spectra were recorded on a Nicolet NT-200 instrument with Doty Scientific solid state probe. The standard was measured externally with a Doty rotor (titanium) filled with sodium tetraphenylborate ($NaB(C_6H_5)_4$, $\delta = 0$) for ^{11}B, triphenylphosphine ($P(C_6H_5)_3$, $\delta = 0$) for ^{31}P, and hexamethylbenzene ($C_6(CH_3)_6$, $\delta_{methyl} = 17.36$, $\delta_{aromatic} = 132.30$) for ^{13}C spectra. FT-IR spectra were recorded on a Biorad Spec 3200 FTS-60 and FTS-7

instruments. A reflectance apparatus was inserted into the Biorad FTS-7 instrument for solid FT-IR spectra. The FAB mass spectra were recorded on a VG ZAB-EQ hybrid spectrometer, while ESCA were obtained using a Perkin-Elmer (P-E) I #5100 instrument. Gas chromatography was carried out on Varian Model 3700 and Hewlett-Packard (HP) 5890 instruments, and GC/MS on a HP 98785A instrument. Surface areas were measured using a NOVA 1000 surface analyzer. Acidity function (H_O) measurements were carried out by standard procedures.

All yields reported, except where noted, were calculated from peak areas generated on a Hewlett-Packard 5790 gas chromatograph fitted with a mass spectrometer detector or a Hewlett-Packard 5790 gas chromatograph. Decane, undecane, dodecane, and hexadecane were used as internal standards. Correction factors were calculated using calibration standards containing pure samples of the desired product along with an internal standard.

Solid reagents that were oxygen or moisture sensitive were transferred in an AtMos glove bag under an argon atmosphere. Liquid reagents that were oxygen or moisture sensitive were transferred via doubled-ended needle under positive argon pressure. All syringes and needles were oven dried and purged with argon prior to use. Glassware was oven dried and then flame dried while being flushed with argon (mercury bubbler exit) before each reaction.

Synthesis of BF_3/Al_2O_3

In a 250-mL, round-bottomed flask equipped with a septum-sealed side arm and a magnetic stir bar was placed 50 g of unactivated Brockmann grade I

neutral alumina. The flask was then fitted with a vacuum adapter, flushed with argon, and flame dried. The flask was allowed to cool while maintaining the argon purge. The flask was charged with hexanes (30 mL) to make a slurry, $BF_3 \cdot Et_2O$ (7.1 g; 6.1 mL, 50 mmol) was then added via syringe. The reaction flask was flushed with argon to remove any HF in the system. The slurry was allowed to stir for three hours and then the solvent removed *in vacuo*. Heat was applied to the flask, while under vacuum, until the solid was completely dry. The solid was transferred, under argon, to a flame-dried, septum-sealed Erlenmeyer flask for later use.

Synthesis of $BCl_{1.5}/Al_2O_3$

In a 250-mL, round-bottomed flask equipped with a septum-sealed side arm and a magnetic stir bar was placed 50 g of unactivated Brockmann grade I neutral alumina. The flask was then fitted with a vacuum adapter, flushed with argon, and flame dried. The flask was allowed to cool while maintaining the argon purge. The flask was charged with hexanes (30 mL) to make a slurry, BCl_3 (50 mmol; 50 mL of 1.0 M solution in hexanes) was then added via double-ended needle dropwise over 10 minutes. Copious quantities of HCl were liberated during the reaction. The reaction flask was flushed with argon to remove the HCl. The slurry was then allowed to stir for three hours. The solvent was removed *in vacuo* and solid was transferred, under argon, to a flame-dried, septum-sealed Erlenmeyer flask for later use.

Synthesis of BBr/Al_2O_3

In a 250-mL, round-bottomed flask equipped with a septum-sealed side arm and a magnetic stir bar was placed 50 g of unactivated Brockmann grade I neutral alumina. The flask was then fitted with a vacuum adapter, flushed with argon, and flame dried. The flask was allowed to cool while maintaining the argon purge. The flask was charged with hexanes (30 mL) to make a slurry, BBr_3 (50 mmol; 50 mL of 1.0 M solution in hexanes) was then added via double-ended needle dropwise over 10 minutes. Copious quantities of HBr were liberated during the reaction. The reaction flask was flushed with argon to remove the HBr. The slurry was then allowed to stir for three hours. The solvent was removed *in vacuo* and solid was transferred, under argon, to a flame-dried, septum-sealed Erlenmeyer flask for later use.

Synthesis of BI/Al_2O_3

In a 250-mL, round-bottomed flask equipped with a septum-sealed side arm and a magnetic stir bar was placed 50 g of unactivated Brockmann grade I neutral alumina. The flask was then fitted with a vacuum adapter, flushed with argon, and flame dried. The flask was allowed to cool while maintaining the argon purge. The flask was charged with hexanes (30 mL) to make a slurry, then $BH_3 \cdot Me_2S$ (3.8 g; 4.7 mL; 50 mmol) was added via syringe. After the slurry stirred for three hours, iodine (25 mmol; 6.3 g) in hexanes (50 mL) was added via double-ended needle. The solvent was removed *in vacuo*. The solid was transferred, under argon, to a flame-dried, septum-sealed Erlenmeyer flask for later use.

Reaction of Methyl Acrylate with Isoprene, Methyl Acrylate with Cyclopentadiene, and Dimethyl Maleate with Cyclopentadiene on Boronated Alumina.

To a flame-dried 250-mL, round-bottomed flask equipped with a septum-sealed side arm and a magnetic stir bar was transferred, under argon BX_n/Al_2O_3 (5 g). The flask was sealed with a septum and charged with toluene (10 mL). Methyl acrylate (0.43 g; 5.0 mmol) was then added via syringe and the reaction flask allowed to stir for five minutes. Isoprene (1.0 g; 1.5 mmol) was then added via syringe. The reaction was stirred at room temperature for 3 hr, then methanol (15 mL) was added and the mixture was allowed to stir for 15 min. The product was then removed from the alumina by washing with methanol (2 x 15 mL) and then ether (2 x 15 mL). After filtering the solution through a glass-fritted filter packed with celite, the mixture was concentrated *in vacuo* and decane (0.2 g; 1.4 mmol) was added as an internal standard for GC analysis.

The reactions of methyl acrylate and dimethyl maleate with cyclopentadiene, prepared by cracking the dicyclopentadiene dimer, were run and analyzed similar to that described above except for the reaction time.

***B*-Halocatecholborane Catalyzed Reaction of Methyl Acrylate with Isoprene and Cyclopentadiene.**

B-Halocatecholborane (5.0 mmols) (halogen = chlorine or bromine) was transferred, under argon, to a flame-dried 100-mL, round-bottomed flask equipped with a septum-sealed side arm and a magnetic stir bar. After the flask was sealed

with a septum, it was charged first with methylene chloride (20 mL) and then with methyl acrylate (3.0 g; 35 mmols). The mixture was then stirred for 5 min. and isoprene (3.4 g; 50 mmols) was added. After 3 hours at room temperature, 10 mL of cold 50% aqueous methanol was added to the reaction mixture. The reaction mixture was extracted with methylene chloride (3 x 15 mL). The combined organic phase was dried over anhydrous $MgSO_4$ (5 g) and vacuum filtered through a glass-fritted filter packed with celite. The mixture was concentrated *in vacuo*, and decane (0.20 g; 1.4 mmols) was added as an internal standard for GC analysis.

The reaction of methyl acrylate and cyclopentadiene, prepared by cracking the dicyclopentadiene dimer, was run and analyzed similar to that described above.

Reaction of Methyl Acrylate and Isoprene with $AlCl_3$

To a flame-dried 250-mL, round-bottomed flask equipped with a septum-sealed side arm and a magnetic stir bar was transferred, under argon, $AlCl_3$ (0.25 g, 1.9 mmol). The flask was sealed with a septum and charged with benzene (20 mL) and then with methyl acrylate (3.0 g, 35 mmol). The mixture was then stirred for 5 min. and isoprene (3.4 g; 50 mmols) was added. After the reaction mixture was stirred for 3 hr, aqueous $NaHCO_3$ (10 mL) was added. The reaction mixture was extracted with 3 x 15-mL aliquots of methylene chloride. The organic phase was dried over $MgSO_4$ (5 g) and vacuum filtered (through a glass fritted filter packed with Celite). The solvent was removed in vacuo and the residue purified

via flash chromatography. The mixture was concentrated *in vacuo*, and decane (0.20 g; 1.4 mmols) was added as an internal standard for GC analysis.

Titration of γ-Alumina with Methyllithium

Gasimetric titrations were performed by the method developed by Brown and co-workers.[29] Standardization of the methyllithium concentration was determined by gasimetry prior to the titration. Solid γ-alumina (0.90 - 1.20 g) was transferred to a septum-sealed 25-mL round-bottomed flask in a glove bag. A Brown gasimeter was connected to the flask by either a two-way adapter already connected to the flask or via a short 16-gauge needle. A known amount of methyllithium was added to the flask. When no more gas evolved, the volume of gas released was recorded and converted to moles using the gas law equation for gaseous volumetric titration.[29]

Gasimetric titrations were performed on the BH/Al_2O_3 in a similar fashion except that a methanol/water (80:20) mixture was used as the titrant.

Solid State NMR Spectra

The solid samples were transferred in an AtMos glove bag under argon to a zirconium solid state rotor. The ends of the rotor were closed with Kel-F end caps (minor components included C, F, and N). The SSNMR rotor was placed in a ziploc® bag and transfered to the NMR instrument. The rotor was placed in the probe and the spectrum was acquired.

Acidity Function (H_0) Measurements of BX_n/Al_2O_3 [30]

A 1% (wt. to vol.) of indicator dye solution was made for the following dyes: methyl red ($pK_a = 4.8$), p-dimethylaminoazobenzene (dimethyl yellow, $pK_a = 3.3$), fast garnet ($pK_a = 2.0$), crystal violet ($pK_a = 0.8$), dicinnamalacetone ($pK_a = -3.0$), anthraquinone ($pK_a = -8.2$), and m-nitrochlorobenzene ($pK_a = -13.2$). To a flame-dried 25-mL, round-bottomed flask equipped a magnetic stir bar was transferred 0.2 grams of solid. The flask was septum-sealed and 2 mL of 1% indicator dye solution was added. The solution stirred for 3-5 minutes. The color of the solution was recorded and compared with the known color change of the indicator.

E. MATERIALS

Solvents

Benzene, Fisher Chemical Company

Cyclohexane, Fisher Chemical Company

Dichloromethane (methylene chloride), Fisher Chemical Company

Diethylether, Fisher Chemical Company

Ethanol (absolute), Mallinkrodt Chemical Company

Hexanes, Fisher Chemical Company

Methanol (dry, HPLC grade), Fisher Chemical Company

THF, Fisher Chemical Company

Toluene, Fisher Chemical Company

NMR solvents

Dichloromethane-d_2 (methlene chloride-d_2), Aldrich Chemical Company

Chloroform-d, Aldrich Chemical Company

Gases

Argon (prepurified), MG Industries

Nitrogen (prepurified), MG Industries

Reagents

Alumina, Brockmann activity grade I-neutral, Fisher Chemical Company

Aluminum chloride, Aldrich Chemical Company

B-Bromocatecholborane, Aldrich Chemical Company

B-Chlorocatecholborane, Aldrich Chemical Company

Borane dimethylsulfide complex (~10.2 M), Aldrich Chemical Company

Boron tribromide (99+%), Aldrich Chemical Company

Boron trichloride (1.0 M in hexanes), Aldrich Chemical Company

Boron trifluoride etherate, Aldrich Chemical Company

Celite, Aldrich Chemical Company

Decane, Aldrich Chemical Company

Dicyclopentadiene, Aldrich Chemical Company

Dimethyl maleate, Aldrich Chemical Company

Dodecane, Aldrich Chemical Company

Hexadecane, Aldrich Chemical Company

Iodine, Aldrich Chemical Company

Isoprene, Aldrich Chemical Company

Magnesium Sulfate, Aldrich Chemical Company

Methyl Acrylate, Aldrich Chemical Company

Methyllithium, Aldrich Chemical Company

Sodium tetraphenylborate, Aldrich Chemical Company

Stilbene, Aldrich Chemical Company

Undecane, Aldrich Chemical Company

LIST OF REFERENCES

1. a. March, J. *Advanced Organic Chemistry, 3rd Ed.* John Wiley & Sons: New York, 1985. b. Carey, F.A.; Sundberg, R.J. *Advanced Organic Chemistry, 3rd Ed.* Plenum Press: New York, 1990.

2. Fringuelli, F.; Taticchi, A. *Dienes in the Diels-Alder Reaction*; Wiley-Interscience: New York, 1990.

3. Kieselev, V.D.; Konovalov, A.I. *Russ. Chem. Rev.* **1989**, *58*, 230.

4. a. *Polymer-Supported Reactions in Organic Synthesis*; Hodge, P.; Sherrington, D.C., Eds.; John Wiley & Sons: New York, 1980. b. *Syntheses and Separations Using Functional Polymers*; Sherrington, D.C.; Hodge, P., Eds.; John Wiley & Sons: New York, 1988.

5. a. *Solid Supports and Catalysts in Organic Synthesis*; Smith, K. Ed.; Ellis Harwood and Prentice Hall: New York, 1992. b. *Catalyst Supports and Supported Catalysts: Theoretical and Applied Concepts*; Stiles, A.B., Ed.; Butterworths: Boston, 1987. c. *Preparative Chemistry Using Supported Reagents*; Laszlo, P., Ed.; Academic Press: New York, 1987.

6. See Pagni, R.M.; Kabalka, G.W.; Hondrogiannis, G.; Bains, S.; Anosike, P.; Kurt, R. *Tetrahedron* **1993**, *49*, 6743 and Bains, S.; Pagni, R.M.; Kabalka, G.W.; Pala, C. *Tetrahedron: Asymmetry* **1994**, *5*, 821 for leading references.

7. Kabalka, G.W.; Wang, Z. *Organometallics*, **1990**, *8*, 1093.

8. ref 5a, pp 100-129.

9. ref 5a, pp 130-170.

10. ref 5a, pp 3-39.

11. a. Willis, D.A.; McGinnis, M.B.; Kabalka, G.W.; Pagni, R.M. *J. Organomet. Chem.* **1995**, *487*, 35. b. Hondrogiannis, G.; Tan, L.C.; Pagni, R.M.; Kabalka, G.W.; Herold, S.; Ross, E.; Green, J.F.; McGinnis, M.B. *Tetrahedron Lett.* **1994**, *35*, 6211. c. Bains, S.; Green, J.F.; Tan, L.C.; Pagni, R.M.; Kabalka, G.W. *Tetrahedron Lett.* **1992**, *33*, 7475. d. Hondrogiannis, G.M.; Plesco, M.; Kurt, R.; Cox, D.; Green, J.F. *Tetrahedron Asym.* **1991**, *2*, 1283. e. Sponholtz, W.R.; Pagni, R.M.; Kabalka, G.W.; Green, J.F.; Tan, L.C. *J. Org. Chem.* **1991**, *56*, 5700. f. Gaetano, K.; Pagni, R.M.; Kabalka, G.W.; Bridwell, P.; Walsh, E.; True, J.; Underwood, M. *J. Org. Chem.* **1985**, *50*, 499. g. Varma, R.S.; Kabalka, G.W.; Evans, L.T.; Pagni, R.M. *Synth. Commun.* **1985**, *15*, 279. h. Varma, R.S.; Kabalka, G.W. *Heterocycles* **1985**, 139. I. Kabalka, G.W.; Gooch, E.E. *J. Org. Chem.* **1981**, *46*, 2582.

12. a. Posner, G.H. *Angew. Chem. Int. Ed. Engl.* **1978**, *17*, 487. b. Posner, G.H.; Hulce, M. *J. Catal.* **1980**, *64*, 497. c. Kropp, P.J.; Daus, K.A.; Crawford, S.D.; Tubergen, M.W.; Kepler, K.D.; Craig, S.L.; Wilson, V.P. *J. Am. Chem. Soc.* **1990**, *112*, 7433. d. Kropp, P.J.; Daus, K.A.; Tubergen, M.W.; Kepler, V.P.; Wilson, V.P.; Craig, S.L.; Baillargeon, M.M.; Breton, G.W. *J. Am. Chem. Soc.* **1993**, *115*, 3071. e. McKillop, A.; Young, D.W. *Synthesis*, **1979**, 401. f. McKillop, A.; Young, D.W. *Synthesis*, **1979**, 481.

13. Knözinger, H.; Ratnasamy, P. *Catal. Rev. Sci. Eng.* **1978**, *17*, 31.

14. a. Peri, J.B. *J. Phys. Chem.* **1965**, *69*, 231. b. Peri, J.B. *J. Phys. Chem.* **1965**, *69*, 211. c. Peri, J.B. *J. Phys. Chem.* **1965**, *69*, 220.

15 DeCanio, E.C.; Edwards, J.C.; Bruno, J. *J. Cat.* **1994**, *148*, 76.

16. *Aldrich Catalog and Handbook of Fine Chemicals*; Aldrich Chemical Company: Milwaukee, 1996.

17. Lowry, T.H.; Richardson, K.S. *Mechanism and Theory in Organic Chemistry, 3rd. Ed.*; Harper & Row: New York, 1987.

18. Isaacs, N.S. *Physical Organic Chemistry*; Wiley: New York, 1987; p 705.

19. McGinnis, M.B.; Vagle, K., Green, J.F.; Tan, L.C., Palmer, R.; Siler, J.; Pagni, R.M.; Kabalka, G.W. *J. Org. Chem.* **1996**, *61*, 3496.

20. Pagni, R.M.; Kabalka, G.W.; Bains, S.; Plesco, M.; Wilson, J.; Bartmess, J. *J. Org. Chem.* **1993**, *58*, 3130.

21. Cativiela, C.; Fraile, J.M.; Garcia, J.I.; Mayoral, J.A.; Pires, E.; Royo, A.J. *Tetrahedron*, **1993**, *49*, 4073.

22. Marczewski, M. *Catalysis by Acids and Bases*; Imelik, B., et al., Eds.; Elsevier: Amsterdam, 1985; p 213.

23. Marczewski, M.; Marczewska, H.; Witoslawski, K. *Bull. Soc. Chim. Fr.* **1991**, *128*, 366.

24. Juszczyk, W.; Marczewski, M. *J. Chem. Soc.* **1992**, *88*, 3591.

25. a. Cotton, F.A.; Wilkinson, G. *Advanced Inorganic Chemistry*, 4th ed.; Wiley: New York, 1980. b. Yates, P.; Eaton, P. *J. Am. Chem. Soc.* **1960**, *82*, 4437.

26. a. Green, J.F. Ph.D. Dissertation, University of Tennessee, 1994. b. Tan, L.C. Ph.D. Dissertation, University of Tennessee, 1993. c. Bains, S. Ph.D. Dissertation, University of Tennessee, 1993.

27. a. Baltusis, L.; Frye, J.S.; Maciel, G.E. *J. Am. Chem. Soc.* **1986**, *108*, 7119. b. Lunsford, J.H.; Rothwell, W.P.; Shen, W. *J. Am. Chem. Soc.* **1985**, *107*, 1540. c. Rothwell, W.P.; Shen, W.; Lunsford, J.H. *J. Am. Chem. Soc.* **1984**, *106*, 2452.

28. a. Liu, H.; Lu, H.; Wang, P.; Sun, P.; Zhang, F. *J. Chem. Soc. Perkin Trans I* **1990**, 2624. b. Reichardt, C. *Solvents and Solvent Effects in Organic Chemistry*; VCH: Weinheim, 1988.

29. Pelter, A.; Smith, K.; Brown, H.C. *Borane Reagents*; Academic Press: San Diego, 1988.

30. Benesi, H.A. *J. Am. Chem. Soc.* **1956**, *78*, 5490.

PART 2

The *s-cis* and *s-trans* Pi-Complexes

of

(*E*)-2-Butenal and *B*-Bromocatecholborane

A. INTRODUCTION

Complexes of carbonyl compounds with a Lewis acids have been known since the 1870s.[1] The subject has been summarized in a recent review by Schreiber and Shambayati.[2] The favorable effect of a Lewis acid on the Diels-Alder reaction was discussed in Chapter 1. In this case, the Lewis acid complexes with the electron withdrawing-substituent of the dienophile, thus lowering the electron density in the carbon-carbon double bond and increasing the dipole moment of the molecule.[2] In turn, this lowers the LUMO energy of the dienophile and produces a more reactive species. This increased reactivity results from the smaller energy gap in the dienophile's LUMO and diene's HOMO energies (Figures 2-1, 2-2).[3] Earlier studies using $AlCl_3$ in solution[4] and the solid acid BBr/Al_2O_3 demonstrated the effectiveness of Lewis acids on organic chemistry and the Diels-Alder reaction.

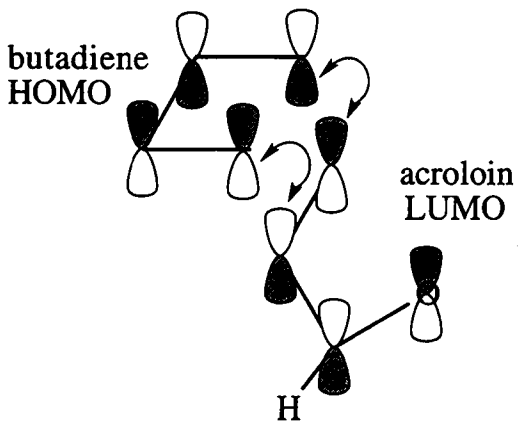


Figure 2-1. Favorable Orbital Overlap for Acrolein and Butadiene

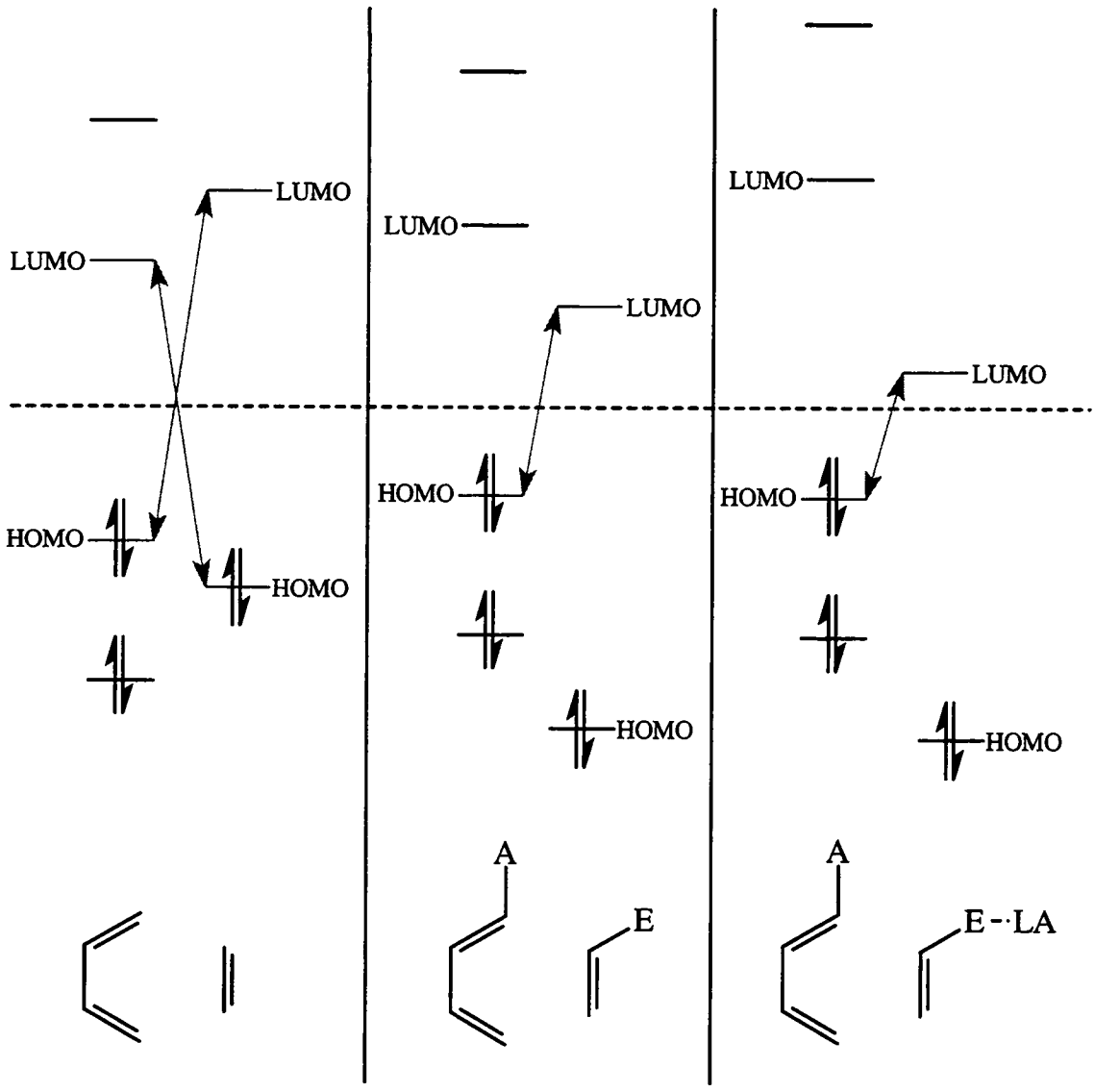


Figure 2-2. Frontier Orbital Interactions of a Dienophile and a Diene in the Diels-Alder Reaction [3]

Theoretical studies, X-ray crystallography, and NMR spectroscopy have shed light on the conformations of the Lewis acid - dienophile complexes.[2,5] These investigations showed that there are four distinct conformations in which complexed, conjugated aldehydes and ketones may exist. Rotation around the C_1 and C_2 carbons and around the oxygen and Lewis acid create molecular conformations (Figure 2-3) with different relative energies. As theory predicts, the *s-trans*, E conformation has the lowest energy due to its minimized steric interactions. The equilibrium between these species can be affected by the strength and size of the Lewis acid and carbonyl substrate. Temperature will also effect the conformational equilibria.

NMR studies of boron-containing Lewis acids and their complexes are extensive. Boron trifluoride complexes, for example, were studied with low temperature ^{1}H, ^{11}B, ^{13}C, and ^{19}F NMR.[2,6] To complement the NMR studies, IR and UV spectroscopies were used to identify the presence of the carbonyl group in the complexes.[2,7] These techniques were effective in yielding structural information about the environment and conformation of the boron acid and complexed base.

NMR spectroscopy is perhaps the most widely used technique for structural determination. Furthermore, proton and ^{13}C NMR chemical shifts can be used to determine environmental effects. An upfield (lower ppm or delta (δ) units) shift, for example, indicates that the nucleus is in an electron rich environment; whereas a downfield shift indicates a less electron rich environment. When a Lewis acid complexes to a conjugated carbonyl group, electron density is removed from the

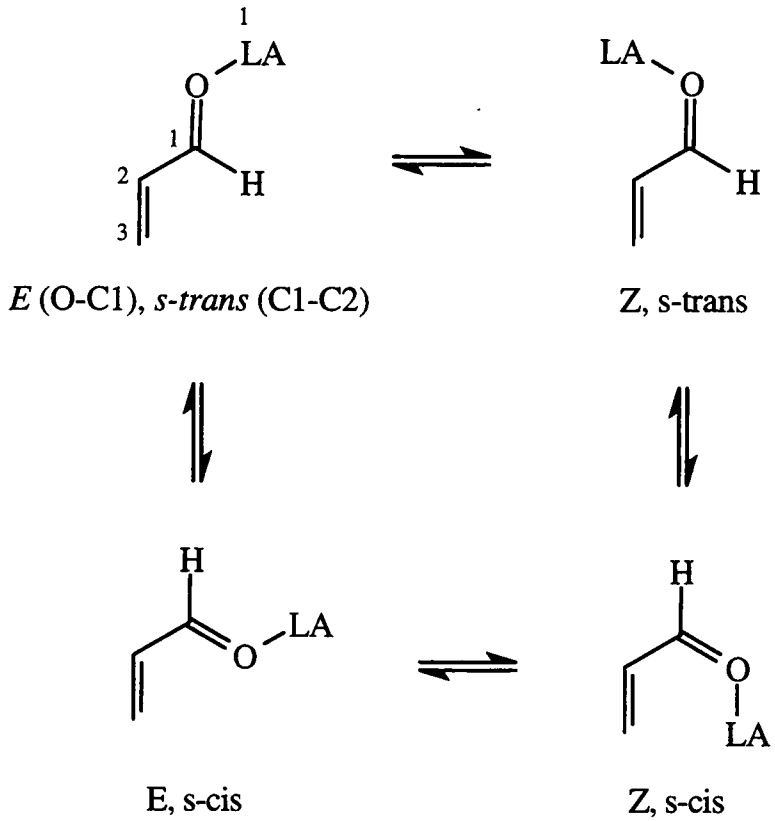


Figure 2-3. Conformations of Acrolein - Lewis Acid Complexes

pi-system and a downfield proton chemical shift is generally observed for the vinylic hydrogens. In fact, Laszlo[8] and Childs[9] have formulated Lewis acid strength scales based on the LUMO energy of the complex and the downfield chemical shift of α,β-unsaturated compounds, respectively. Laszlo also showed that the LUMO energies correlated reasonably well with the NMR scale and the rates of Lewis-acid catalyzed ene reactions.[8]

The discovery that there is a correlation between chemical shifts and Lewis acidic strengths gives organic chemists a simple method for determining relative acid strengths among Lewis acids.[9] The bases that Childs and co-workers used to formulated their Lewis acid scale consisted of crotonaldehyde, tiglaldehyde, pent-3-en-2-one, 2-cyclohexanone, methyl crotonate, and crotononitrile. Childs complexed a base with a Lewis acid at -78°C in CD_2Cl_2 and then recorded the ^1H NMR spectrum at -20°C. The bases were chosen for their stability when complexed with a Lewis acid. Each of the bases showed the predicted downfield shift of the proton resonances when complexed to a Lewis acid.

Crotonaldehyde (CA) produced the most significant shifts with protons 2, 3, and 4 shifting downfield for all the Lewis acids studied. The greatest chemical shift change occurred for H3. When CA complexes with a Lewis acid, the positive charge around C3 increases the most; whereas charge around C2 and C4 increases less (Figure 2-4, Table 2-1). A linear correlation was found between the changes (Δ) of δ's of H2 and H4 and that for H3 as the Lewis acid varied. This correlation was used to determine relative acid strength of the Lewis acids as shown in Table 2-1.[9] Child's method can be used to determine relative acid strengths for other acids of interest.

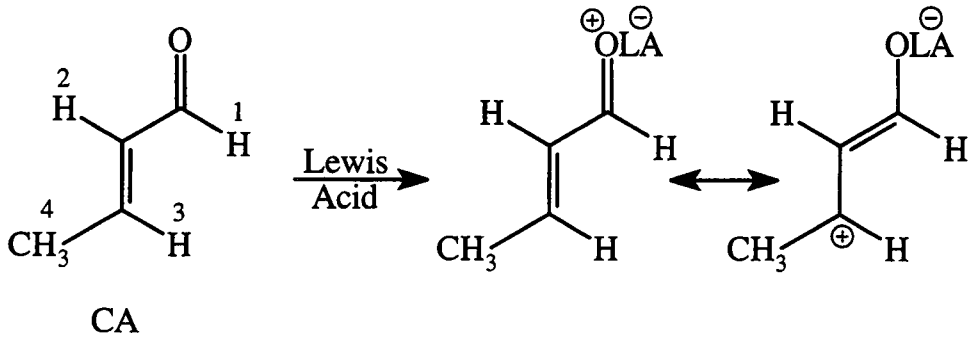
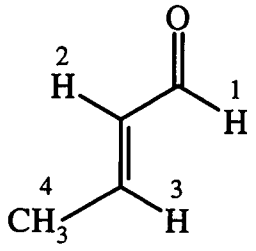


Figure 2-4. Reaction of a Lewis Acid with Crotonaldehyde

Table 2-1. Proton Chemical Shifts of Crotonaldehyde on Complexation with Lewis Acids at -20°C [a]

Crotonaldehyde (CA):



Lewis acid complex [a,b]	H1 (Δδ, ppm) [c]	H2 (Δδ, ppm) [c]	H3 (Δδ, ppm) [c]	H4 (Δδ, ppm) [c]	Relative power [d]
none	9.47	6.10	6.93	2.02	–
BBr_3	9.58 (0.11)	7.03 (0.93)	8.42 (1.49)	2.53 (0.51)	1.00
BCl_3	8.82 (-0.65)	6.95 (0.85)	8.28 (1.35)	2.51 (0.49)	0.93
$AlCl_3$	9.27 (-0.20)	6.86 (0.76)	8.16 (1.23)	2.49 (0.47)	0.82
BF_3	9.20 (-0.27)	6.84 (0.74)	8.10 (1.17)	2.46 (0.44)	0.77

[a] reference 9. [b] Approximately 0.3 M solution in CD_2Cl_2 at -20°C. [c] $\Delta\delta = \delta_{complexed} - \delta_{uncomplexed}$. [d] Relative Lewis acid strength based on Δδ-values of H3 resonances of various bases.

B. Results and Discussion

To compare the acid strengths of the homogeneous *B*-bromocatecholborane (BCB) and *B*-chlorocatecholborane (CCB) with the corresponding *B*-bromo- and *B*-chloroboronated aluminas, each was treated with an equivalent of trans-crotonaldehyde (CA) in a 1 : 1 ratio of CA to Lewis acid. The solids posed several difficult problems. First, the boron acid was present in only a concentration of 1 mmol per gram of solid. Second, proton NMR could be obtained for the solid only with difficulty and even the carbon-13 SSNMR required more than 30,000 scans. The low natural abundance of ^{13}C (~1.1%) and low concentration of carbon on the surface made the carbon SSNMR experiment nearly impossible. A spectrum was recorded for the CA + BBr/Al_2O_3, but the carbons could not be assigned because additional resonances arising from the carbons in the Kel-F end caps were also present as were those for trace amounts of toluene. The observed signal to noise ratio of 3 was also poor. A background SSNMR spectrum of the solid state rotor and end caps (SSNMR cell) was acquired, but the resonances due to CA could still not be assigned unambiguously.

The NMR experiments in solution were much more interesting. When BCB (and CCB) was treated with one equivalent of CA in CD_2Cl_2 at -20°C, no downfield shifts of the protons were recorded in the NMR spectrum (Figures 2-5 and 2-6; for comparison, ^1H NMR spectra of CA and BCB are shown in Figures 2-7 and 2-8). Instead, eight new resonances, dramatically upfield from those of CA, appeared. The protons must be in a more shielding environment. The

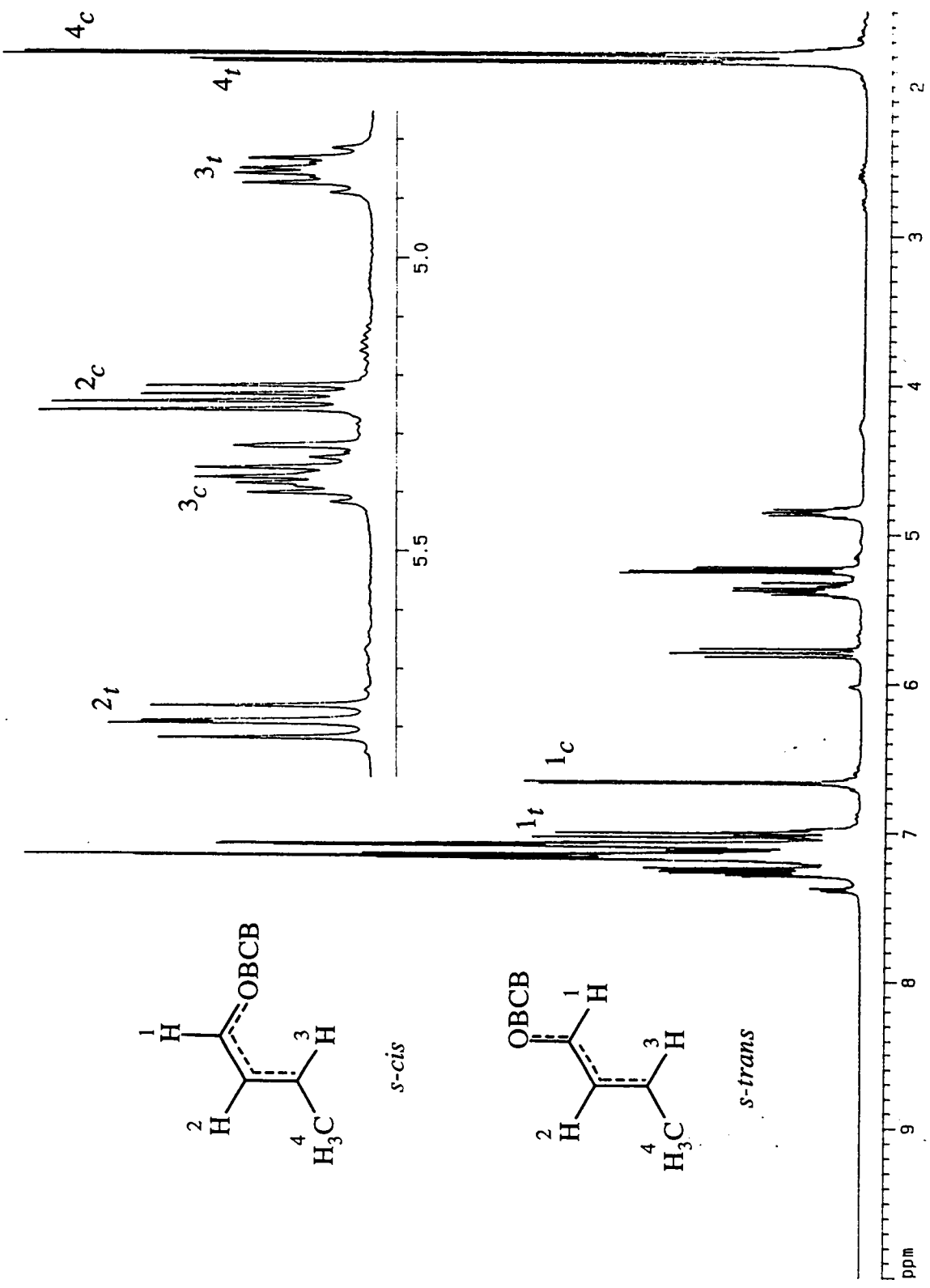


Figure 2-5. Proton NMR Spectrum of CA:BCB Complex at -20°C in CD_2Cl_2

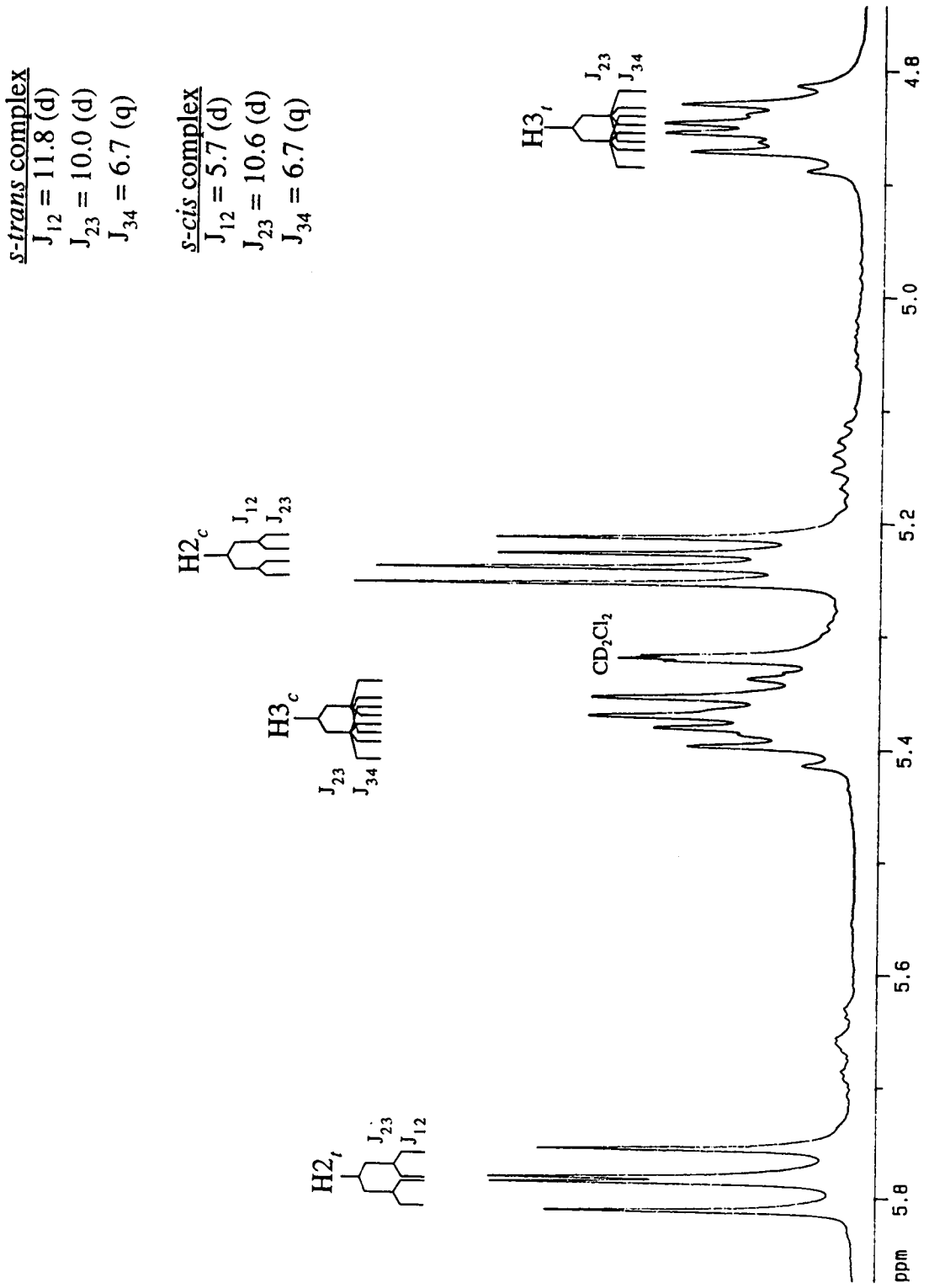


Figure 2-6. Expanded Vinylic Region of Proton NMR Spectrum of CA:BCB Complex at -20°C in CD_2Cl_2

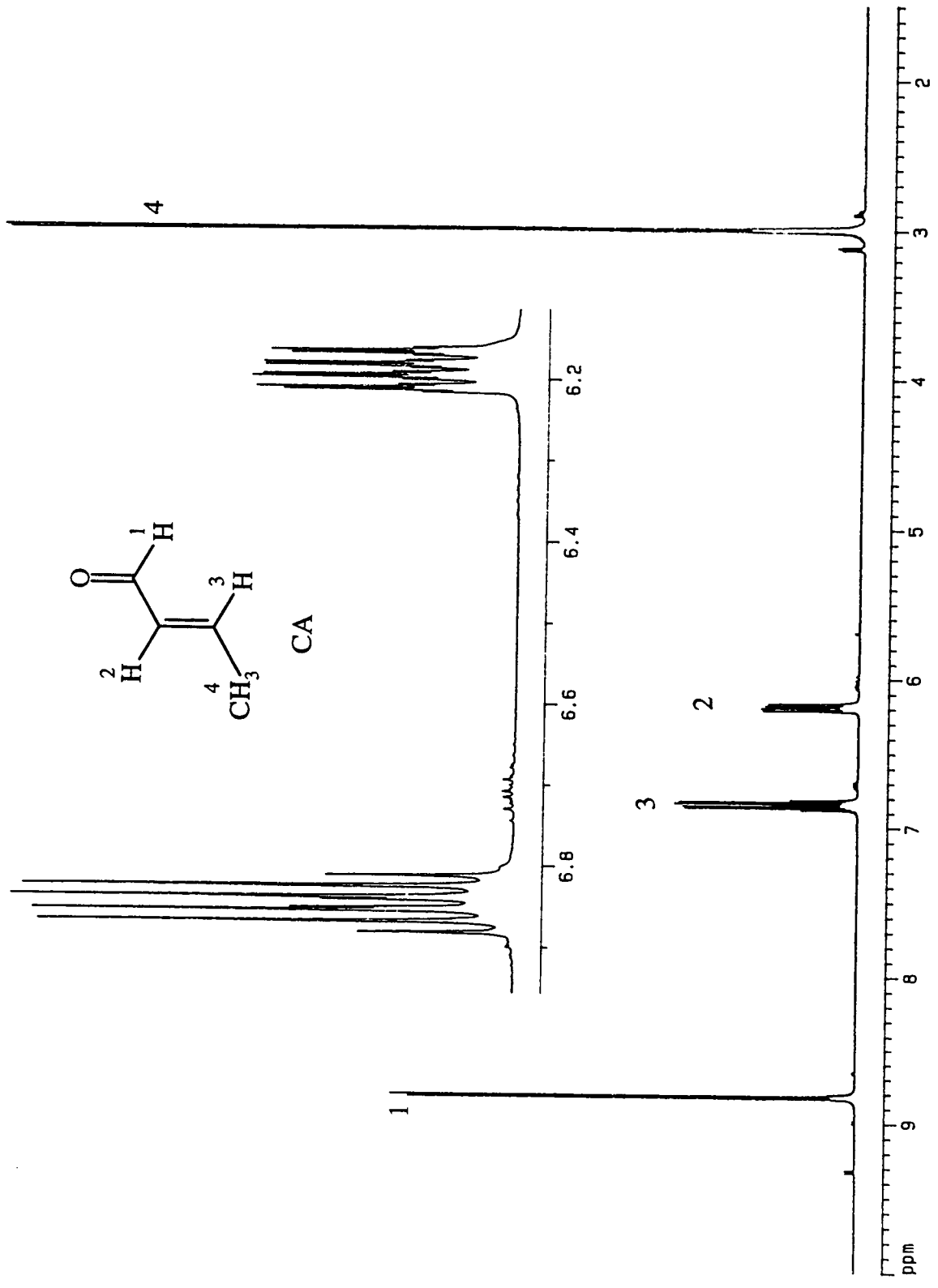


Figure 2-7. Proton NMR Spectrum of CA at -20°C in CD_2Cl_2

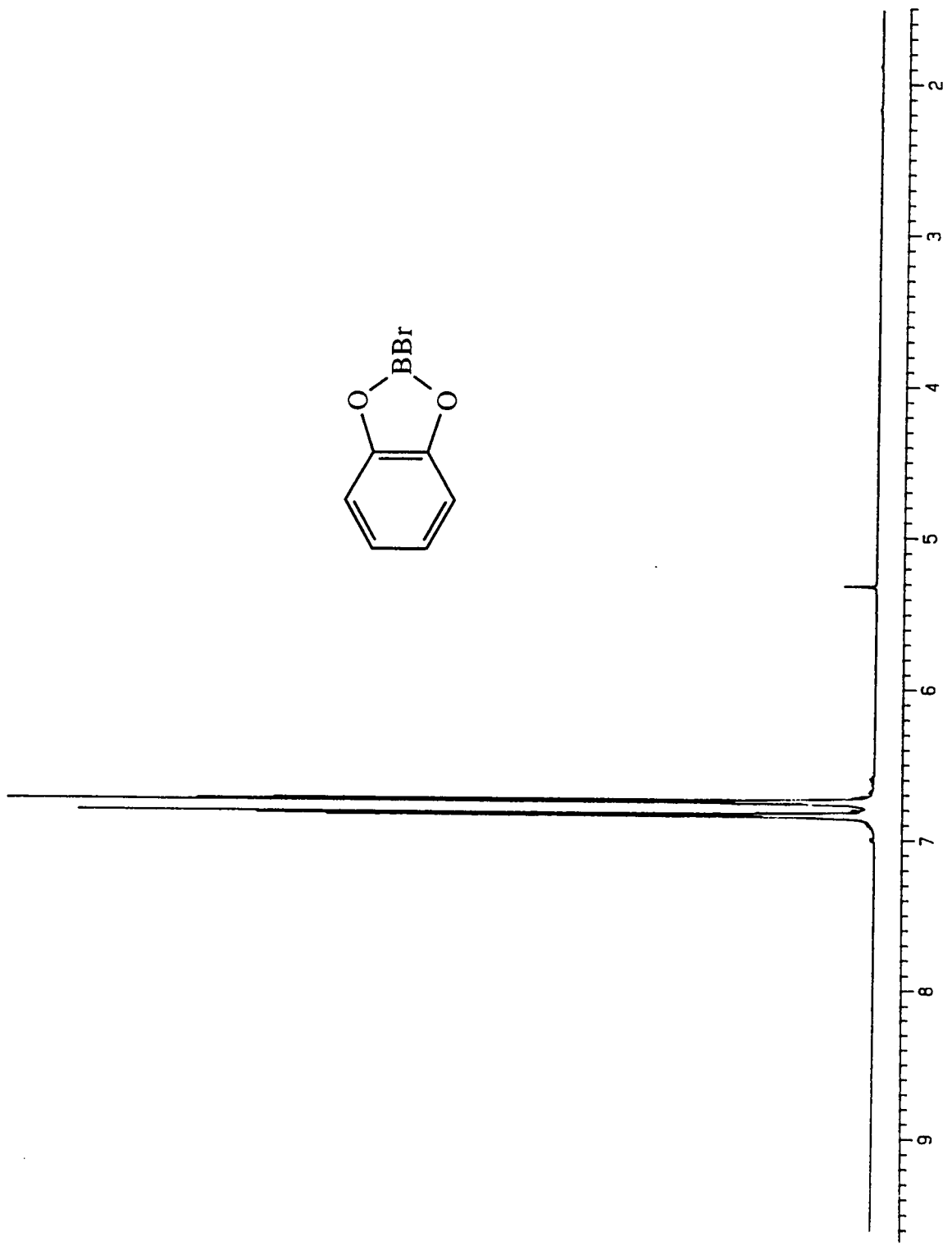


Figure 2-8. Proton NMR Spectrum of BCB at -20°C in CD_2Cl_2

spectrum suggested that *s-cis* and *s-trans* conformations of the aldehyde were pi-complexed to the Lewis acid (Figure 2-9). Integration implied the two species were present in equal amounts. The chemical shift data for the complexes, protonated CA and uncomplexed CA are recorded in Table 2-2.

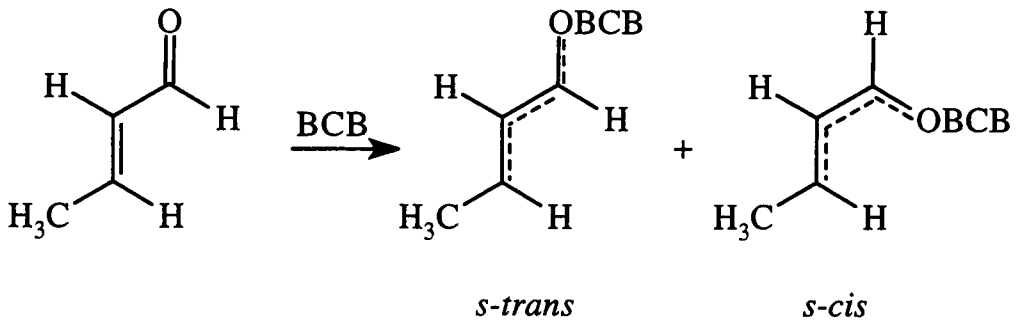


Figure 2-9. Reaction of *B*-Bromocatecholborane with Crotonaldehyde

Coupling constants and splitting patterns (Table 2-3, Figure 2-7) of the 1D proton spectrum and ^1H-^1H COSY (correlated spectroscopy) (Figure 2-10) were used to confirm the existence of the *s-cis* and *s-trans* complexes. The H_1-H_2 coupling constants for the *s-cis* and *s-trans* compounds differed greatly. The J_{12} of the trans species had a much larger coupling constant than that for the cis (see Table 2-3). J_{12} for the trans complex was larger than for the corresponding Js in CA and CAH^+, which exist in the trans conformation. Likewise, J_{23} decreased in both complexes due to the weakening of the C2-C3 double bond of CA. The small allylic J_{24} coupling for the *s-trans* was also observed in the CA:BCB complex.

Table 2-2. Proton Chemical Shifts of Crotonaldehyde and *B*-Halocatecholborane Complexes at -20°C in CD_2Cl_2

Lewis acid	configuration, conformation	H1 ($\Delta\delta$ ppm) [c]	H2 ($\Delta\delta$ ppm) [c]	H3 ($\Delta\delta$ ppm) [c]	H4 ($\Delta\delta$ ppm) [c]
none	E	9.42	6.05	6.88	1.97
	Z	10.81	5.79	6.65	2.10
H^+ [a]	E	9.59 (+0.17)	7.07 (+1.02)	8.61 (+1.73)	2.67 (+0.70)
BCB [b]	E, *s-trans*	7.02 (-2.40)	5.82 (-0.23)	4.86 (-2.02)	1.86 (-0.11)
	E, *s-cis*	6.68 (-2.74)	5.25 (-0.80)	5.39 (-1.49)	1.81 (-0.16)
CCB [b]	E, *s-trans*	d	5.69 (-0.36)	4.70 (-2.18)	1.68 (-0.29)
	E, *s-cis*	6.73 (-2.69)	5.12 (-0.93)	5.29 (-1.59)	1.64 (-0.33)

[a] reference 9. [b] Approximately 0.27 M solution in CD_2Cl_2 at -20°C.
[c] $\Delta\delta = \delta_{complexed} - \delta_{uncomplexed}$. [d] undetectable in aromatic region.

Table 2-3. Coupling Constants (Hz) of Crotonaldehyde and *B*-Halocatecholborane Complexes at -20°C in CD_2Cl_2

Lewis acid	configuration, conformation	J_{12}	J_{23}	J_{24}	J_{34}
none	E	8.0	15.9	1.5	6.9
	Z	8.3	11.1	1.8	7.8
H^+ [a]	E	10.0	16.0	–	8.0
BCB [b]	E, *s-trans*	11.8	10.0	c	6.7
	E, *s-cis*	5.7	10.6	c	6.7
CCB [b]	E, *s-trans*	11.9	9.5	–	6.7
	E, *s-cis*	5.8	10.1	–	6.6

[a] reference 9. [b] Approximately 0.27 M solution in CD_2Cl_2 at -20°C. [c] very small.

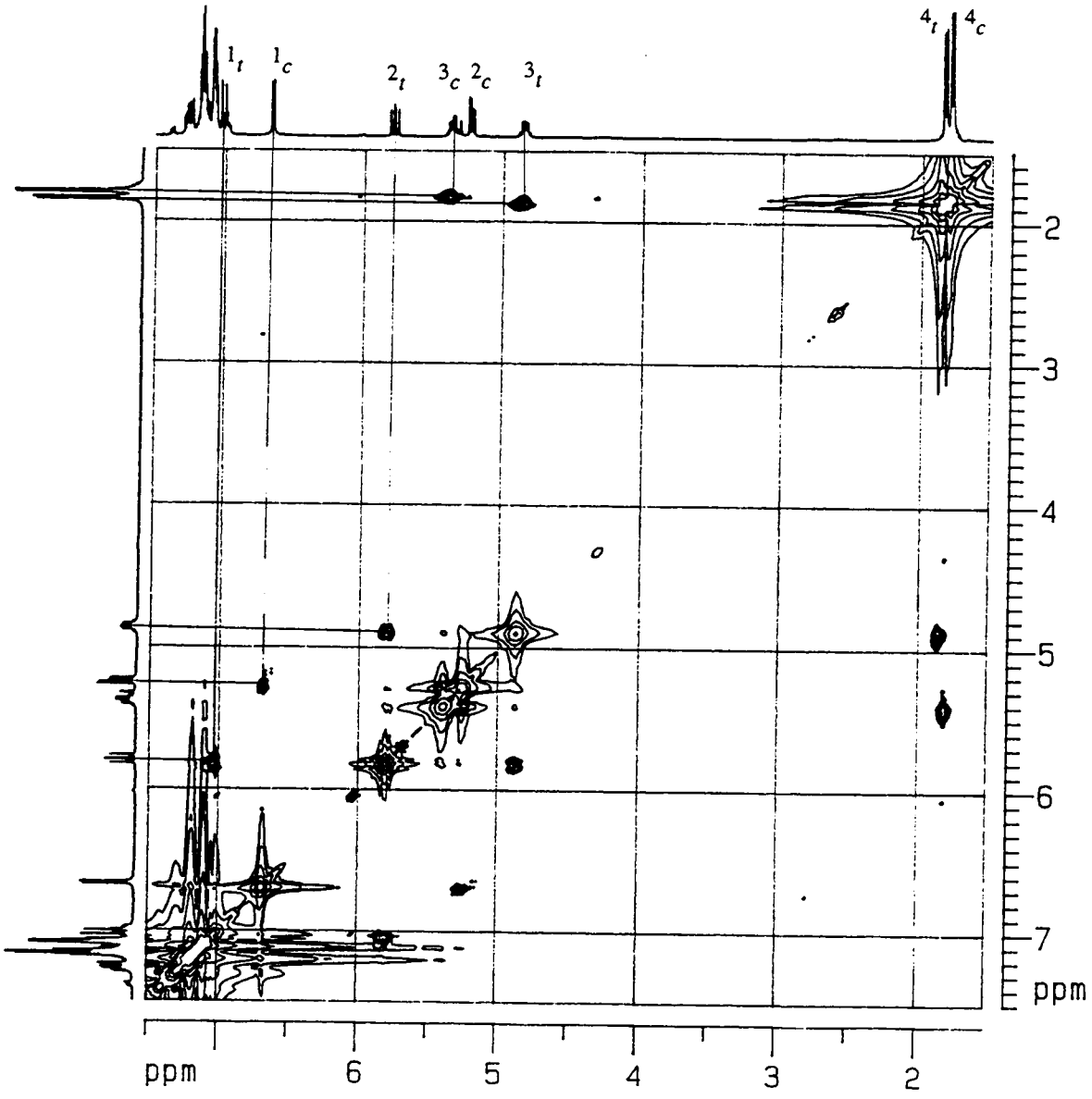


Figure 2-10. ^1H-^1H COSY Spectrum of CA:BCB Complex at -50°C in CD_2Cl_2

Two-dimensional ^{1}H-^{1}H COSY NMR was also used to confirm the proton connectivities. COSY is one of the most useful 2-D NMR experiments, it reveals off-diagonal crosspeaks (or contours) of protons which are coupled to one another.[10] COSY of the CA:BCB complex clearly showed the through-bond interactions. Figure 2-10 shows the COSY spectrum of the complexes with the conformations labeled as *t* for *s-trans* and *c* for *s-cis*. The *s-trans* was easily distinguished from the *s-cis* by the larger J_{12} coupling, as already noted.

Carbon-13 NMR at -20°C also revealed two species in equal amounts (Figure 2-11; for comparison, ^{13}C NMR spectra of CA and BCB are shown in Figures 2-12 and 2-13). The ^{13}C resonances were also dramatically shifted upfield. The chemical shift data for the complexes, protonated CA and uncomplexed CA are recorded in Table 2-4.

Boron-11 NMR spectroscopy was utilized to confirm that complexation to boron had occurred. A titration of BCB with CA was performed (Figure 2-14). When CA was added to BCB, a resonance upfield from that due to BCB appeared, indicative of a tetrahedral boron species. A 1:1 mixture of CA and BCB produced only the upfield resonance. Although 2 complexes exist, only a single ^{11}B resonance was observed. ^{11}B NMR could not differentiate between the two perhaps because the boron resonance was broad.

Several X-ray crystallography studies have shown that protons in alkenes, nitrones, and imines adopt non-classical intramolecular conformations with "edge-to-face aromatic interactions".[2,11] Although X-ray crystallography of the CA:BCB and CA:CCB complexes would definitely have shown the pi-complex

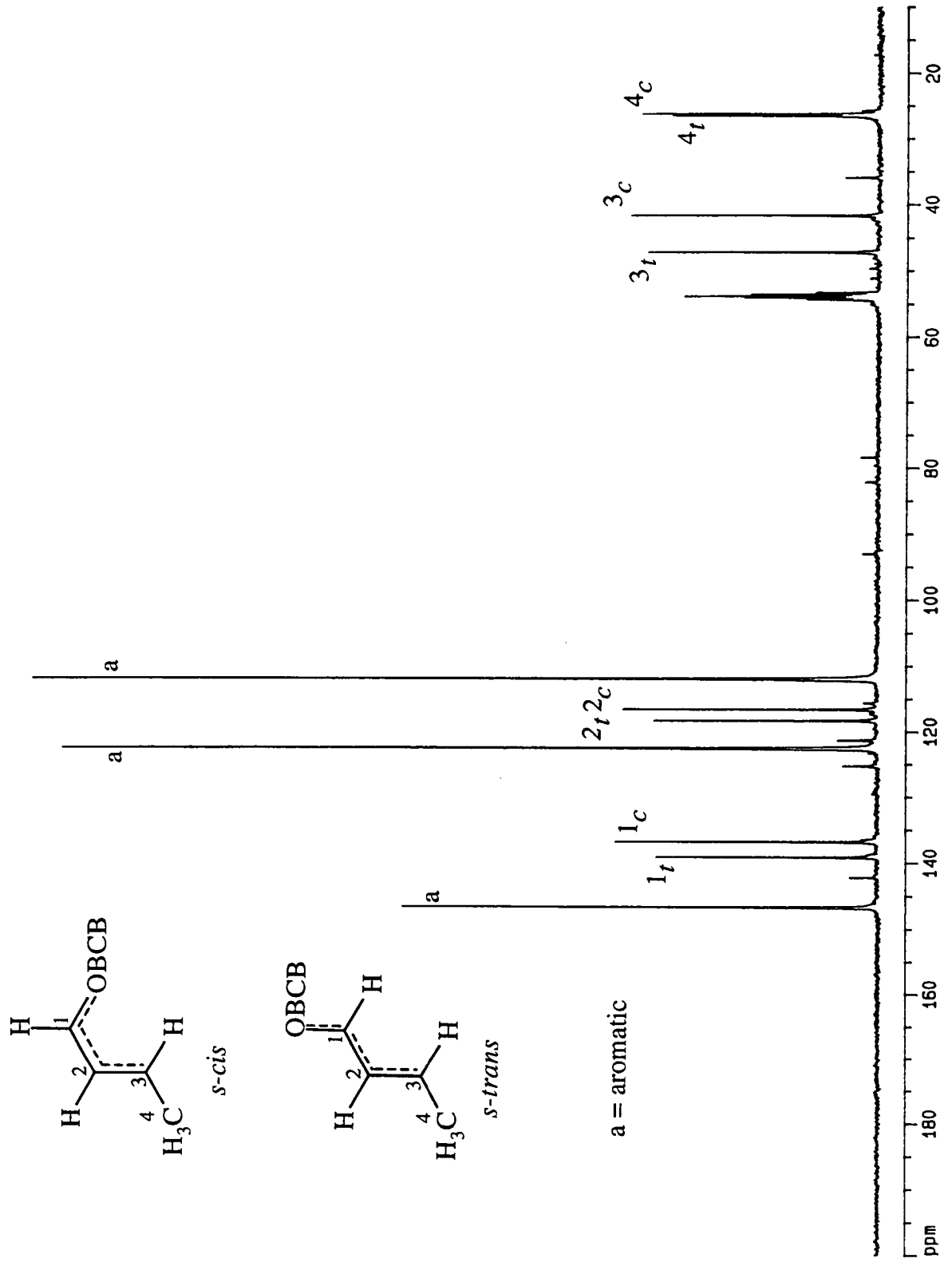


Figure 2-11. Carbon-13 NMR Spectrum of CA:BCB Complex at -20°C in CD_2Cl_2

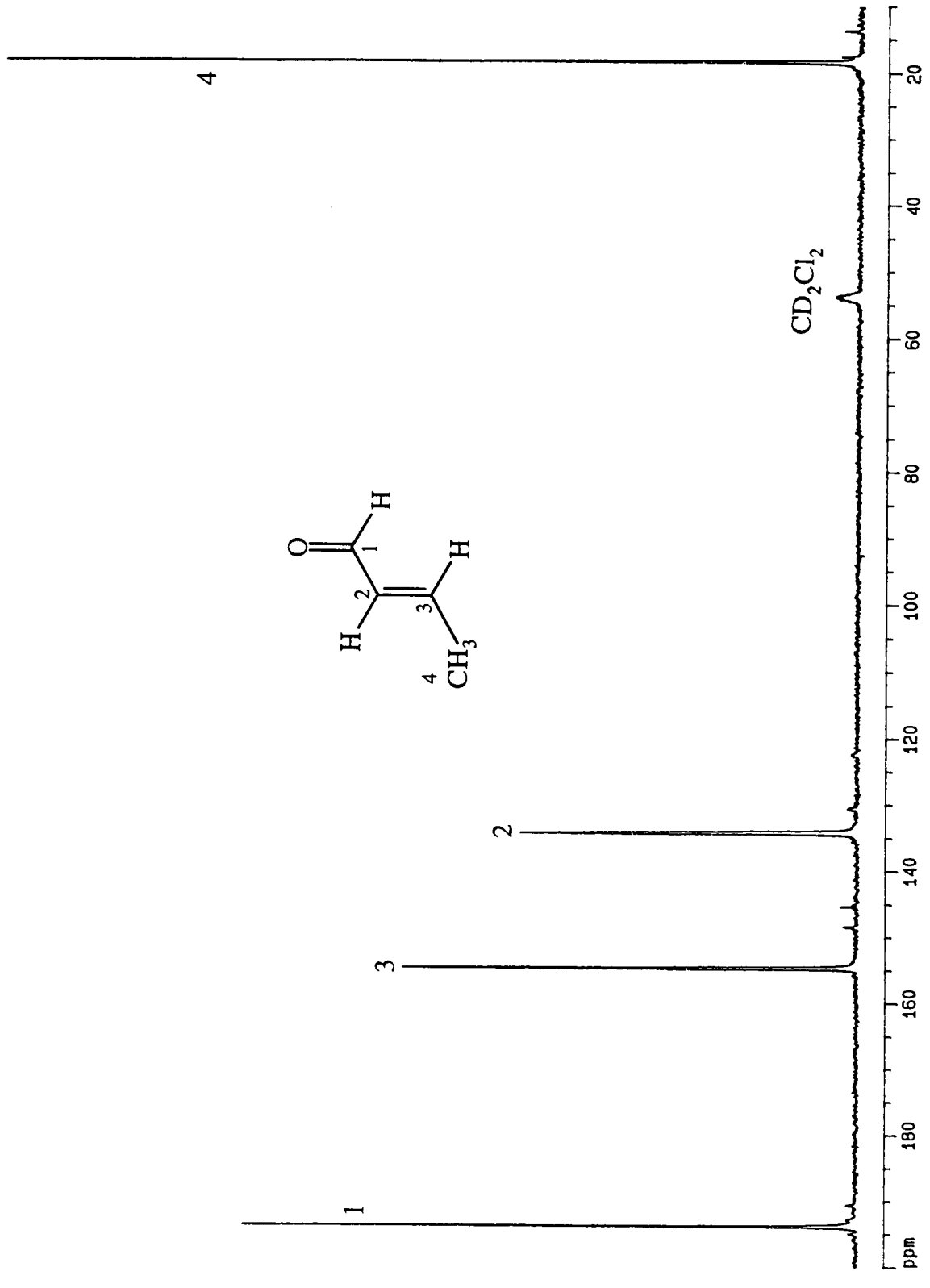


Figure 2-12. Carbon-13 NMR Spectrum of CA at -20°C in CD_2Cl_2

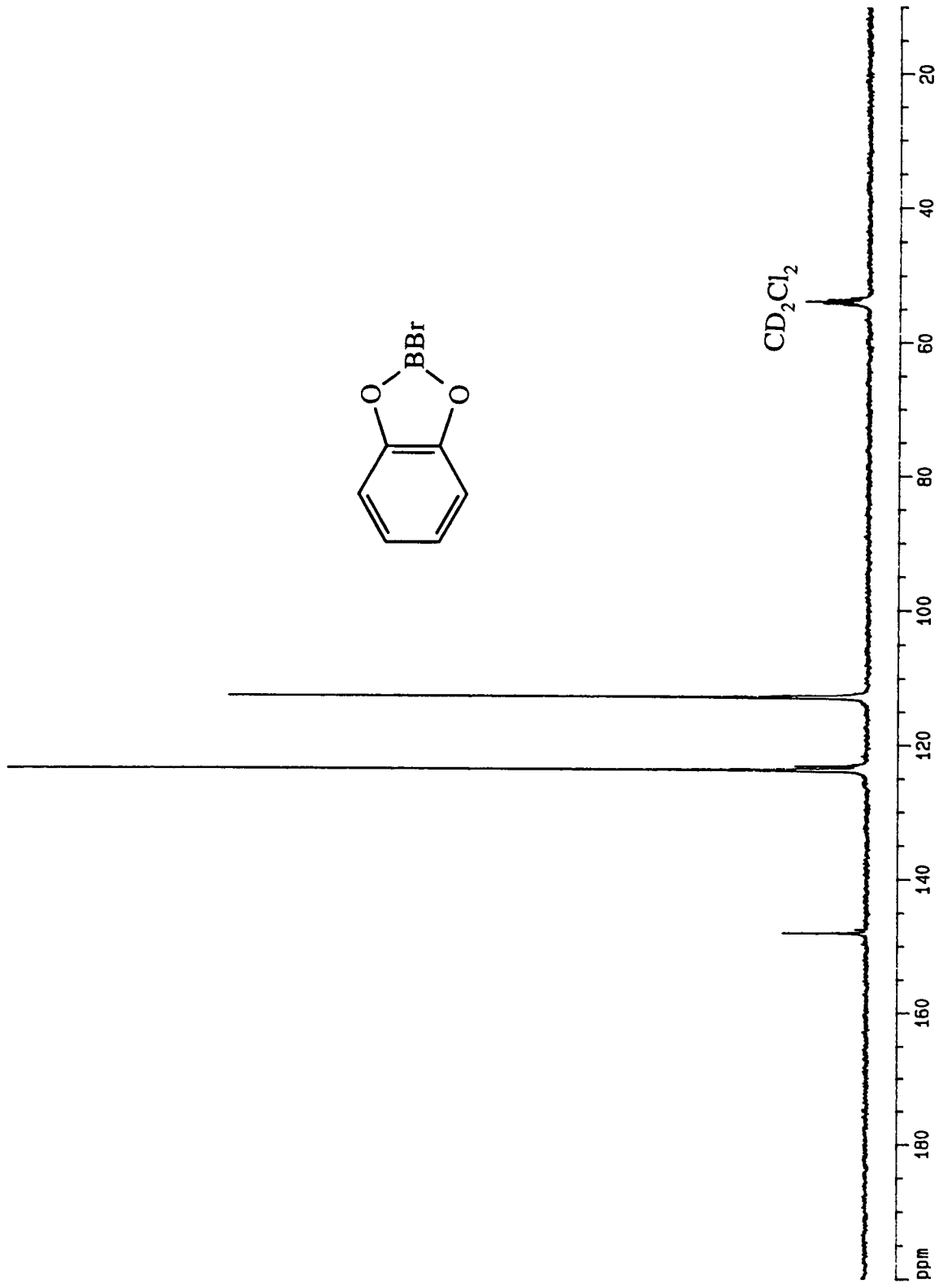


Figure 2-13. Carbon-13 NMR Spectrum of BCB at -20°C in CD_2Cl_2

Table 2-4. Carbon Chemical Shifts of Crotonaldehyde and *B*-Halocatecholborane Complexes at -20°C in CD_2Cl_2

Lewis acid	configuration, conformation	C1 ($\Delta\delta$ ppm) [e]	C2 ($\Delta\delta$ ppm) [e]	C3 ($\Delta\delta$ ppm) [e]	C4 ($\Delta\delta$ ppm) [e]
none	E [a]	194.0	134.5	154.9	18.6
	E [b]	193.4	134.8	153.9	18.5
H^+ [c]	E	206.1 (+12.1)	130.4 (-4.1)	193.2 (+38.3)	23.6 (+5.0)
BCB [d]	E, *s-trans*	139.7 (-54.3)	119.3 (-15.2)	46.7 (-108.2)	26.9 (+8.3)
	E, *s-cis*	137.2 (-56.8)	117.5 (-17.0)	41.4 (-113.5)	26.7 (+8.1)
CCB [d]	E, *s-trans*	140.1 (-53.9)	118.2 (-16.3)	55.4 (-99.5)	26.0 (+7.4)
	E, *s-cis*	137.4 (-56.6)	116.7 (-17.8)	50.3 (-104.6)	25.7 (+7.1)

[a] this work. [b] reference 12. [c] reference 13. [d] Approximately 0.27 M solution in CD_2Cl_2 at -20°C. [e] $\Delta\delta = \delta_{complexed} - \delta_{uncomplexed}$ (this work).

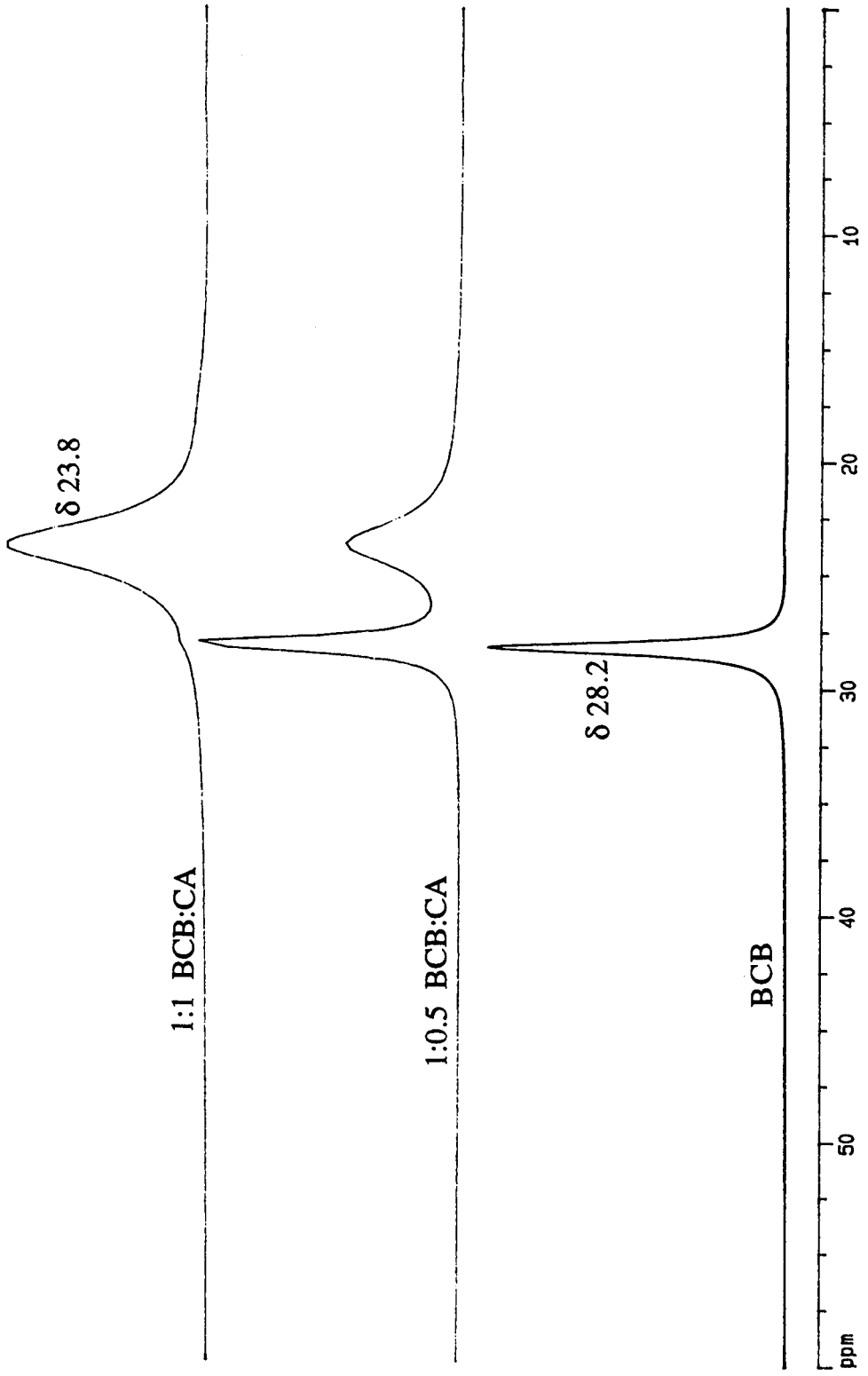


Figure 2-14. Boron-11 NMR Spectrum: Titration of BCB with CA at -20°C in CD_2Cl_2

nature of the two species, the reality of isolating a single crystal from a mixture that degrades quickly above -20°C was improbable. Therefore, 2-dimensional NMR and IR techniques were used to corroborate the nature of the complexes.

Heteronuclear chemical shift correlation (HETCOR) was utilized to identify the carbon chemical shifts. ^{1}H-^{13}C HETCOR shows crosspeak contours of correlated protons and carbons. Since the proton assignments for the CA:BCB complex were already made, ^{1}H-^{13}C HETCOR helped in the assignment of the complex's complicated carbon spectrum. The ^{1}H-^{13}C HETCOR spectrum (Figure 2-15) of the CA:BCB complex at -50°C in CD_2Cl_2 clearly identified the carbons as indicated in Figure 2-11 and Table 2-4. Dramatic upfield shifts for the CA's C1, C2, and C3 occurred in the carbon-13 spectrum, while the methyl carbons (C4) showed minor shifts (+8.3, +8.1) for the *s-trans* and *s-cis* complexes. The upfield chemical shifts of the sp^2 carbons of CA verified the pi-complexed nature of the two species, as previously proposed.

ROESY 2D spectroscopy, a NMR technique related to NOESY spectroscopy, confirmed the pi-complex nature of CA:BCB. ^{1}H-^{1}H NOESY (nuclear Overhouser spectroscopy) detects through-space proton interactions within a molecule. The CA:BCB complex, like many medium-sized molecules, gave very small NOE interactions in a ^{1}H-^{1}H NOESY NMR experiment. ^{1}H-^{1}H ROESY (rotating frame Overhouser enhancement spectroscopy), also known as CAMELSPIN (cross-relaxation appropriate for mini-molecules emulated by spin-locking) reduces the scalar coupling, the coupling which is caused by adjacent protons in the COSY spectrum, and reveals the through-space interactions.

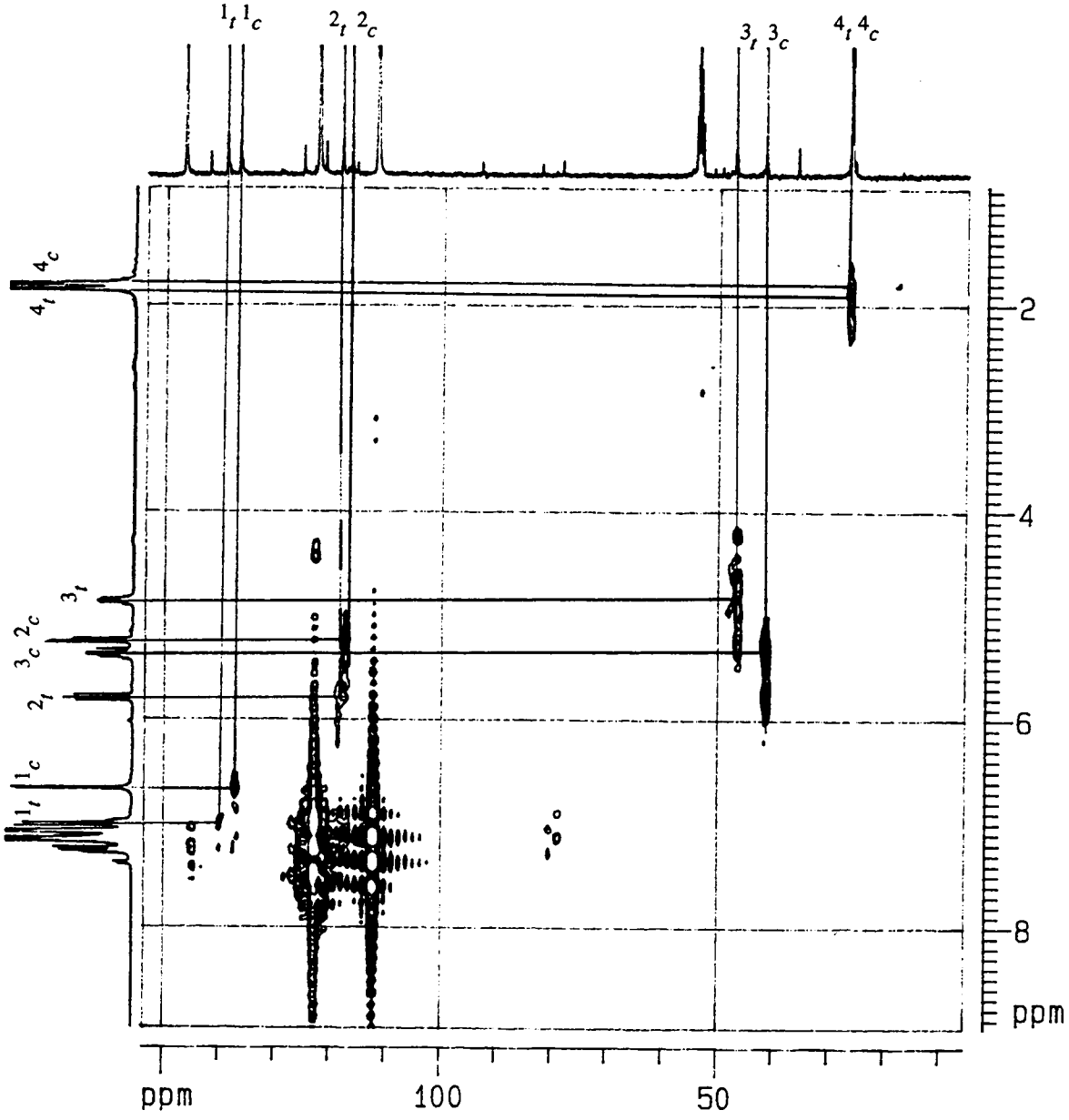


Figure 2-15. ^{1}H-^{13}C HETCOR Spectrum of CA:BCB Complex at -50°C in CD_2Cl_2

The advantage of ROESY is that all molecules give positive NOE interactions, unlike NOESY in which the NOE changes sign depending on the molecular correlation time.[14] Although COSY correlations frequently break through in ROESY, this technique must be utilized instead of NOESY.

In fact, ^{1}H-^{1}H ROESY revealed the through-space interactions of the CA protons with the BCB aromatic protons of the ring (Figure 2-16). Both the methyl protons and vinylic protons of both complexes showed through-space interactions with the aromatic protons. This supports the pi-complex structure that was proposed earlier, confirming that the upfield shifts of the CA proton resonances were caused by the additional electron density from the aromatic ring. In addition, the H1-H3 through space interaction of the *s-trans* complex was detected, thus confirming the initial assignment of the *s-trans* conformation. No such H1-H3 interaction was seen for the *s-cis* complex, as expected. Additional COSY correlations were also observed in the ROESY spectrum.

The temperature of the solution containing the two complexes was varied to determine if the *s-cis* and *s-trans* species were interconverting. Proton NMR spectra were recorded in 10°C increments from -20°C to -100°C. No change, except for the expected loss in resolution and slight chemical shift change, was detected. A 1:1 ratio of *s-trans* and *s-cis* complexes was detected at all temperatures. On the other hand, an EXSY 2D spectrum proved that, in fact, the species do interconvert (Figure 2-17). EXSY (exchange spectroscopy) uses the NOESY experiment protocol with different processing parameters for the data and shows cross peaks of atoms that chemically exchange with one another.

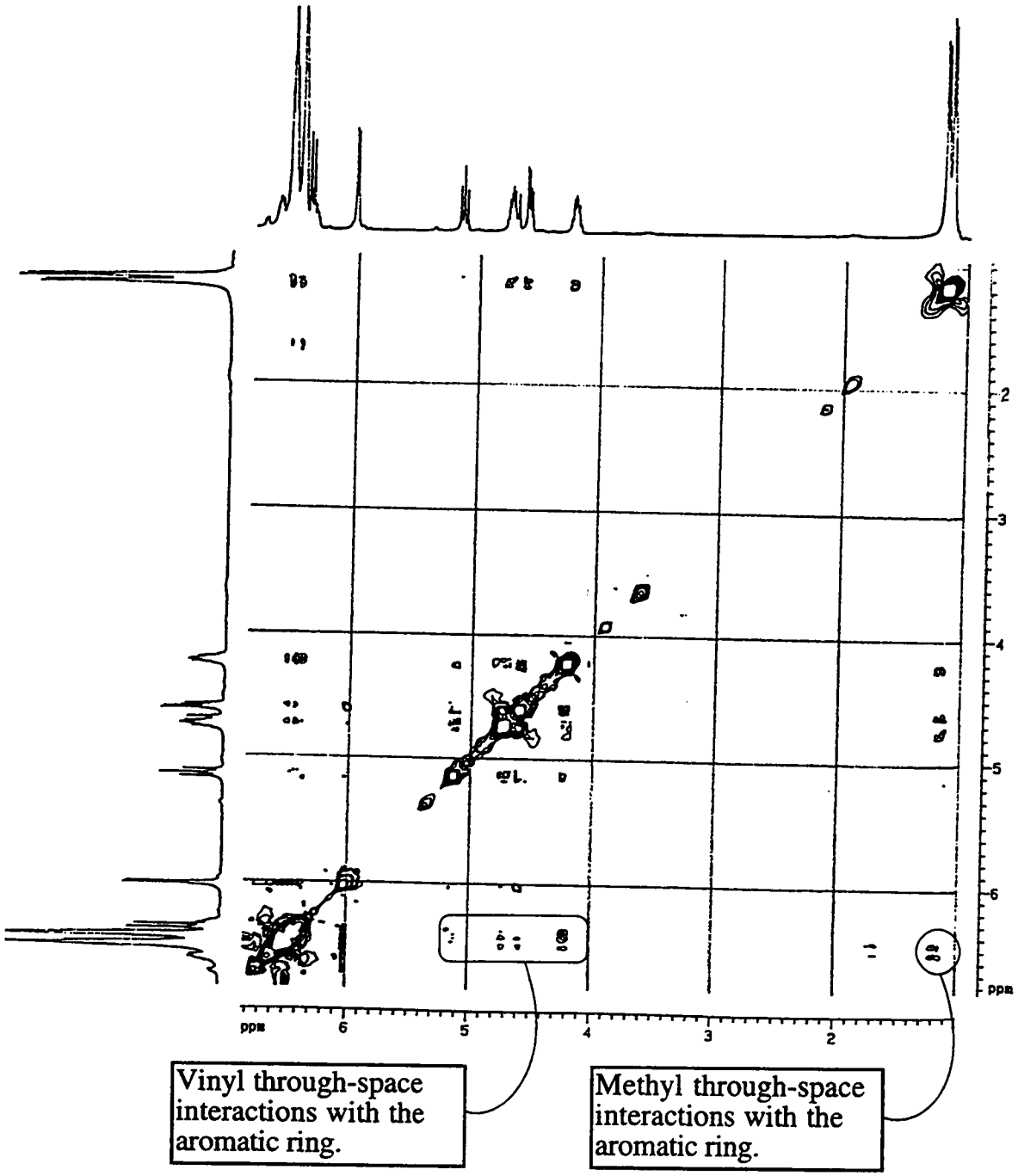


Figure 2-16. ^{1}H-^{1}H ROESY Spectrum of CA:BCB Complex at -50°C in CD_2Cl_2

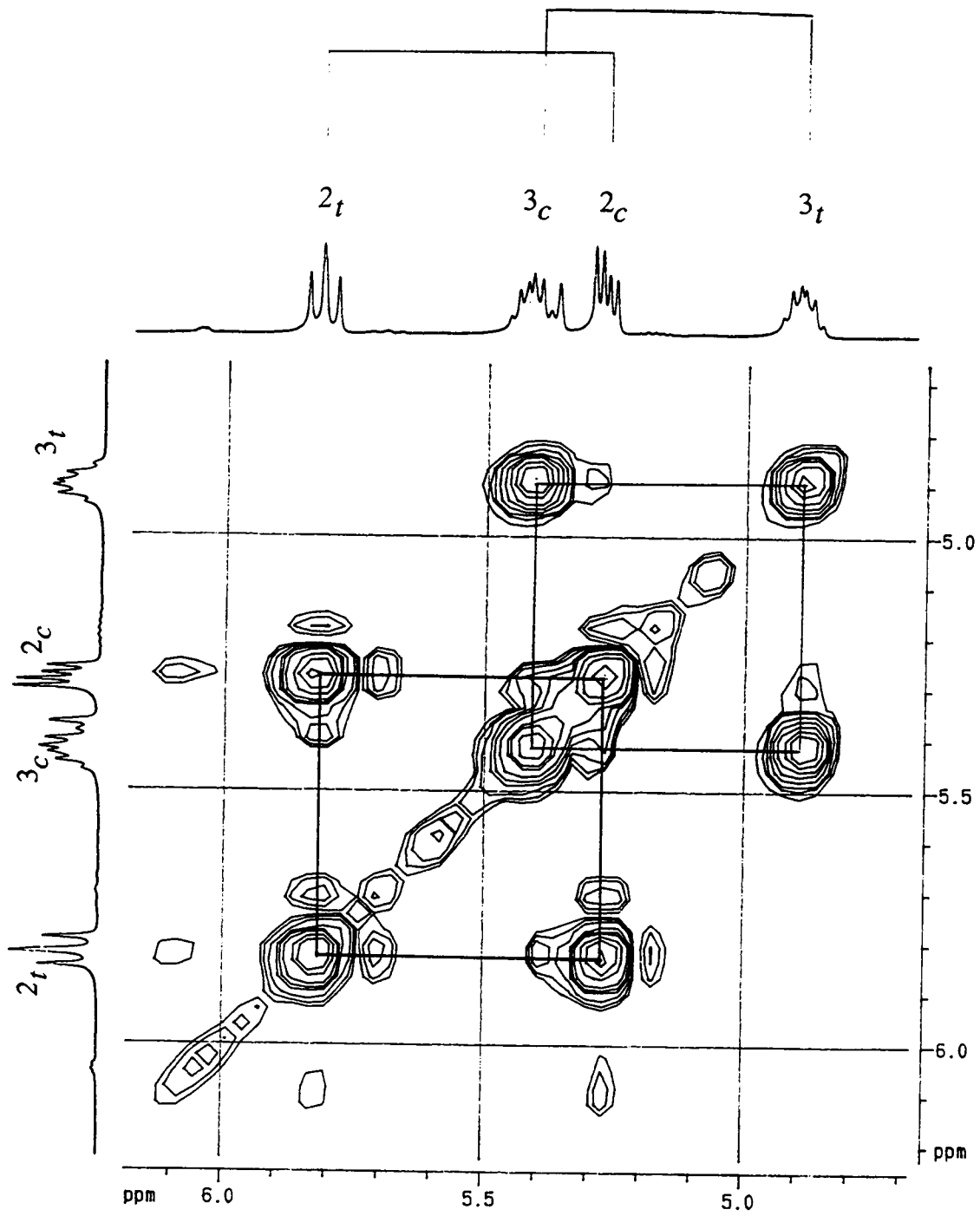


Figure 2-17. EXSY of CA:BCB Complex at -50°C in CD_2Cl_2

The ^1H-^1H EXSY of the CA:BCB complex showed that the vinylic protons of the *s-cis* and *s-trans* exchange at -50°C (Figure 2-17). This proves that the complexes do interconvert but that temperature does not affect the equilibrium distribution; therefore the equilibrium constant must be 1. The temperature dependent behavior is only possible if the entropy term is close to zero.

The NMR results were used to formulate the three-dimensional structures of the *s-cis* and *s-trans* complexes with a CaCHe molecular modeling program. Unfortunately, the results were disappointing. CaCHe did find a local minimum for the *s-trans* CA:BCB complex, but needed the *s-cis* conformation "locked" before a minimum was found for it. In addition, the *s-cis* minimum was clearly inaccurate because the carbonyl oxygen-boron bond was more than twice as long as expected. The structure depicted in Figure 2-18 is the CaCHe molecular mechanics output using the MNDO bases set for the *s-trans* complex. This structure is inconsistent with the NMR data obtained for the CA:BCB *s-trans* complex, but is consistent with a normally complexed substrate with a Lewis acid. Figures 2-19 and 2-20 are more representative structures for the *s-cis* and *s-trans* structures.

Raman spectroscopy was used to confirm the absence of a C-Br bond. The C-Br stretching would occur if the CA reacted with the BCB in a 1,4 HBr addition (Michael addition) or 1,2 HBr addition to create a boron enolate (see Figure 2-21). Brominated organic compounds absorb in the 690-515 cm^{-1} region, for example.[10] The Raman spectrum of molecules with C-Br bonds (as models) were compared to the Raman spectrum of the CA:BCB. Clearly, there were no

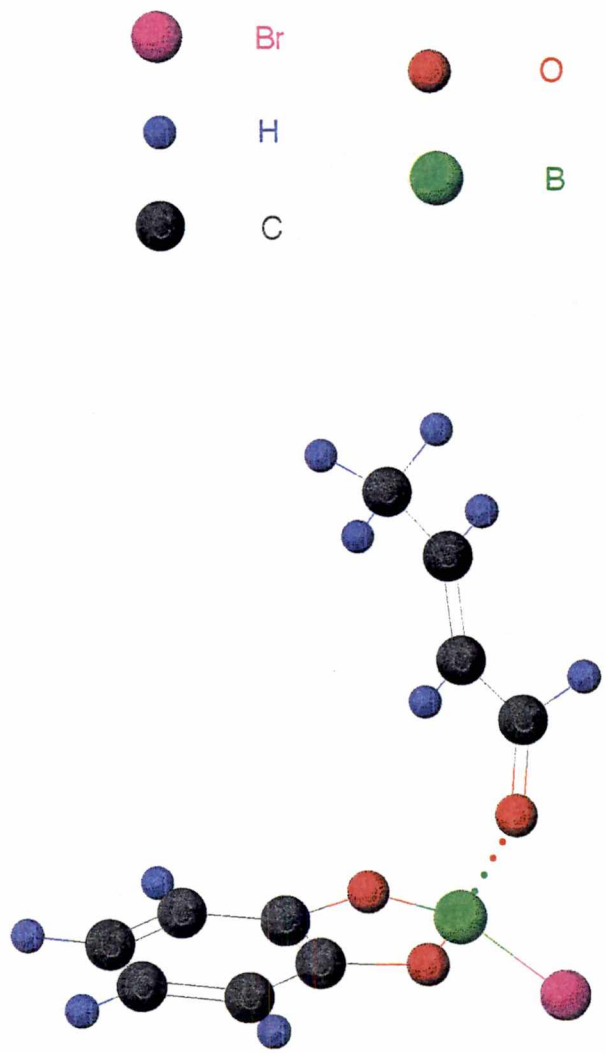


Figure 2-18. The CA:BCB Complex Created by MNDO Theoretical Minimization Using CaCHe Software

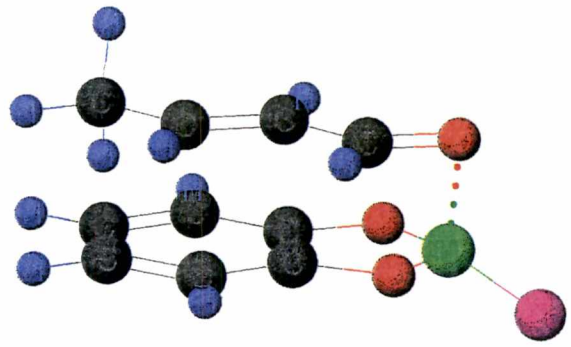


Figure 2-19. The *s-trans* Conformation of the CA:BCB Complex

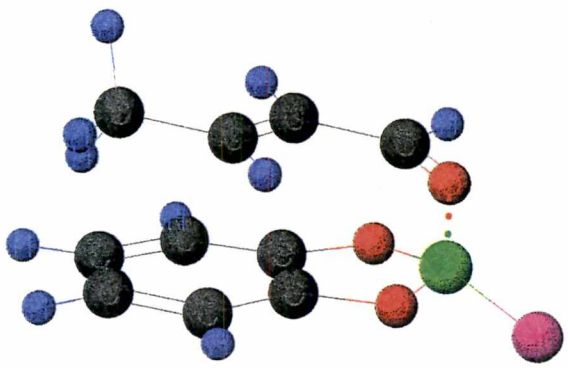
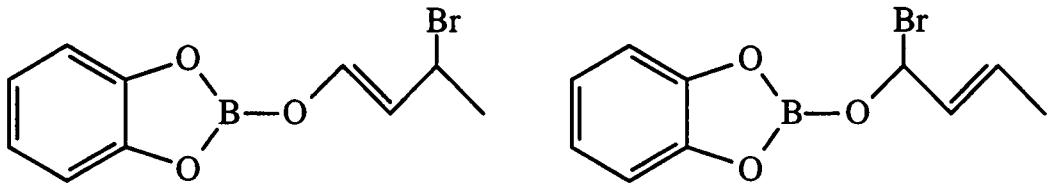


Figure 2-20. The *s-cis* Conformation of the CA:BCB Complex

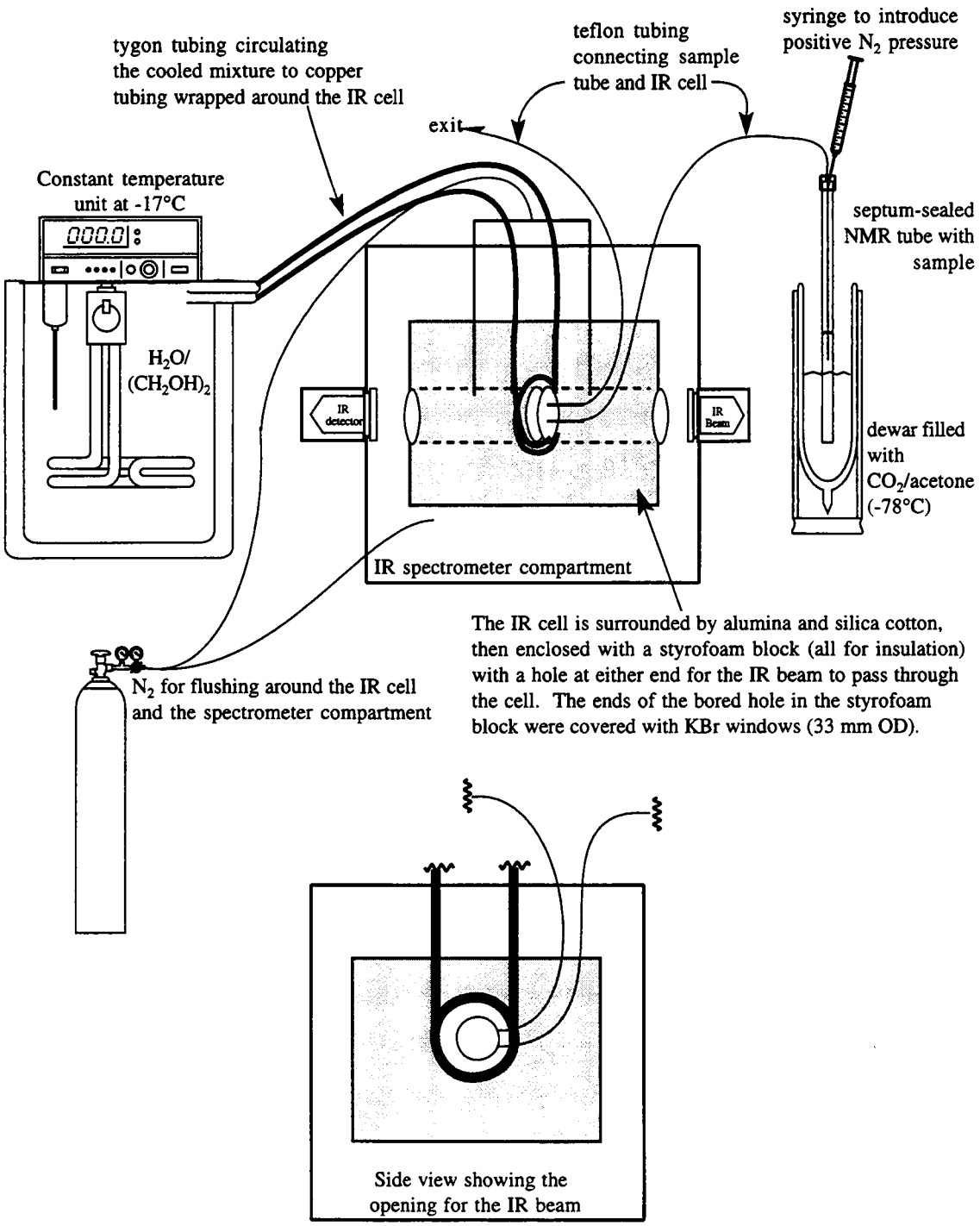


1,4 HBr addition 1,2 HBr addition

Figure 2-21. Possible Boron Enolate Products if CA Reacted with BCB

C-Br stretchings in the region of IR spectrum where a C-Br bond would be detected in the CA:BCB complex. However, the C-Cl stretching of the CD_2Cl_2 was observed in each spectrum at 674 cm^{-1}.

Infrared spectroscopy was used to confirm the existence of the carbonyl groups in the complex. A carbonyl group complexed to a Lewis acid will yield a carbonyl stretch in its IR spectrum, whereas a boron enolate-type molecule would show a C-O stretch (a boron enolate would exist if hydrogen bromide, from BCB, added 1,2 or 1,4 to CA; see Figure 2-21). The difficulty posed with the CA:BCB complex was that the infrared spectrum had to be obtained at temperatures ≤ -20°C or the complex decomposed quickly above -20°C. A rough, but elaborate apparatus was constructed to keep an IR cell at -17°C (Figure 2-22). Liquid was introduced via positive nitrogen pressure to a previously-cooled, sealed cell and spectra was recorded of neat CD_2Cl_2, neat CA, CA in CD_2Cl_2, BCB in CD_2Cl_2, and the CA:BCB complex in CD_2Cl_2 (Figures 2-23, 2-24, 2-25). The carbonyl was clearly detected in the complex (1672 cm^{-1}) with the stretching frequency shifting to lower energy (lower wavenumbers) as compared to CA itself (1687 cm^{-1}), as expected when a carbonyl group is complexed to a Lewis acid.



* The IR spectrometer used was a BioRad FTS-60 instrument connected to a BioRad Spec3200 workstation. The IR cell was a Wilmad sealed cell with KBr (25 mm OD) plates.

Figure 2-22. Low Temperature IR Instrument Set-up

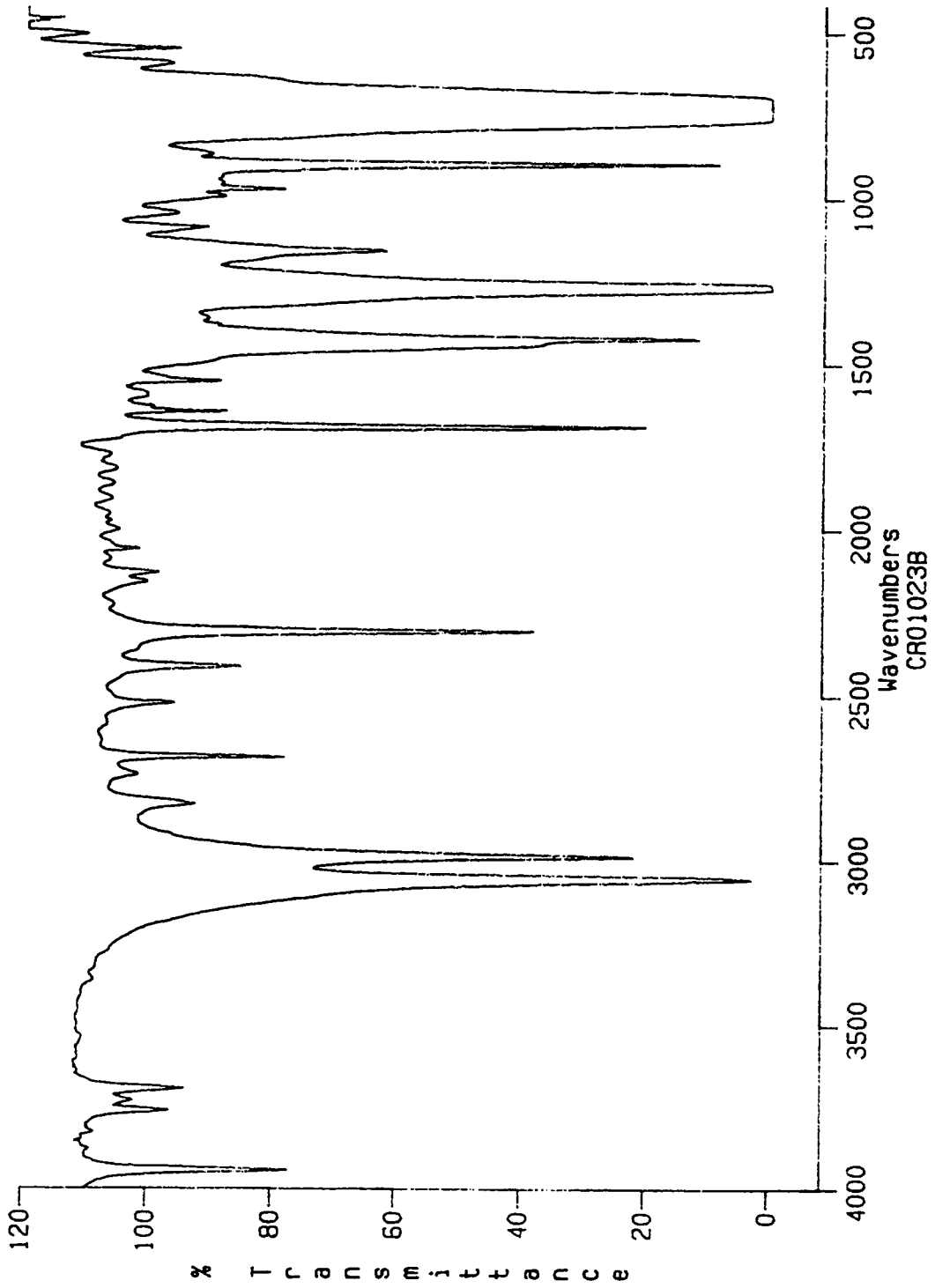


Figure 2-23. IR Spectrum of CA at -17°C in CH_2Cl_2

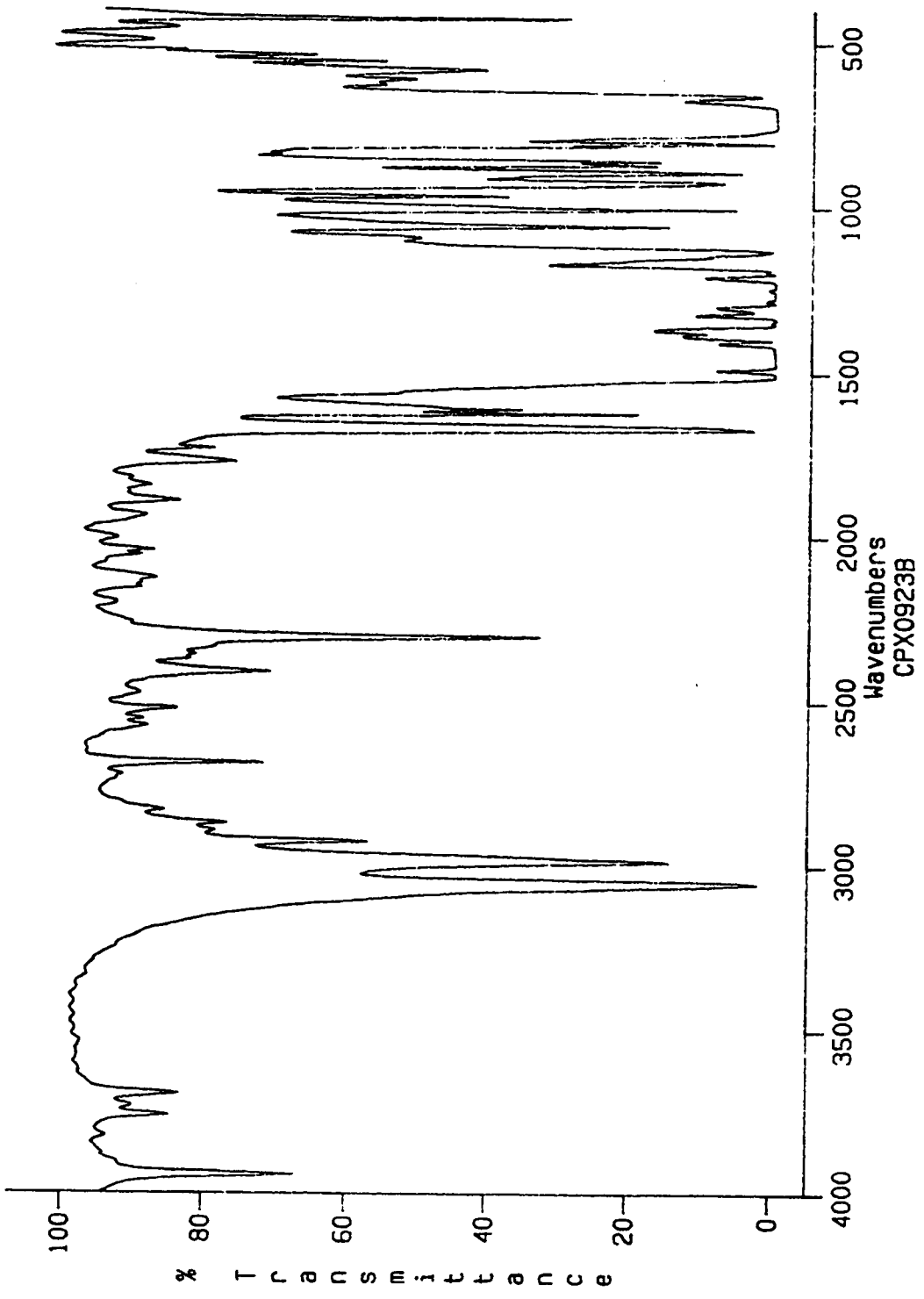


Figure 2-24. IR Spectrum of CA:BCB Complex at -17°C in CH_2Cl_2

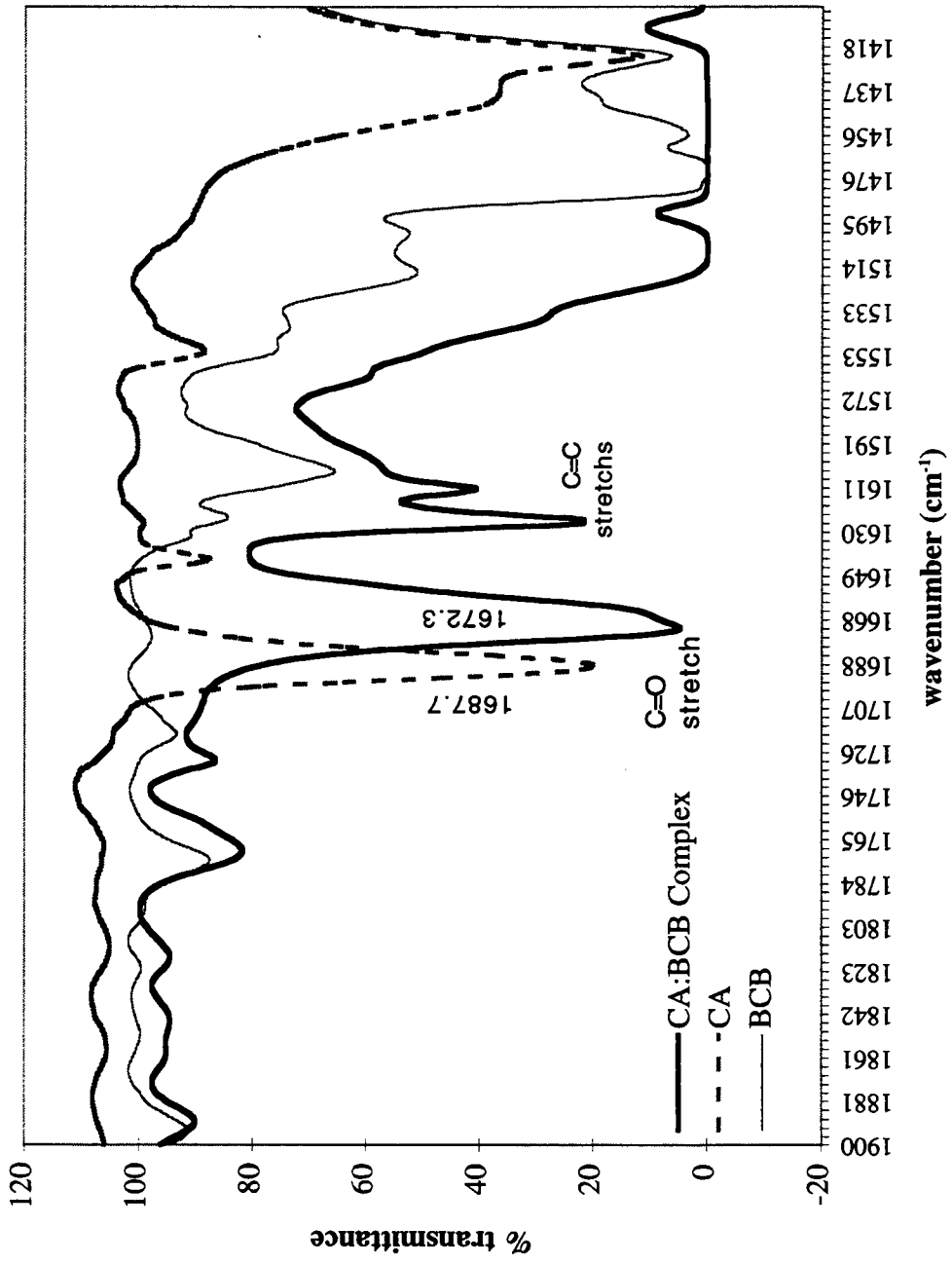


Figure 2-25. Expanded Region of IR Spectra of CA, BCB and CA:BCB Complex at -17°C in CH_2Cl_2

In order to confirm that the complex contained only CA and BCB, the solution was quenched with water. After extraction with methylene chloride, catechol, *(E)*-2-butenal, and 3-bromobutanal were detected in the organic layer, as expected. The aqueous layer generated boric acid after evaporation.

Reaction of the CA:BCB complex with cyclopentadiene afforded the Diels-Alder adducts from the E configuration cleanly (Figure 2-26). Proton NMR spectroscopy at room temperature and GC/MS were used to identify the products which are comparable with literature values and the $TiCl_4$ catalyzed reaction of CA and CP.[16] The endo and exo adducts that would have been formed had (*Z*)-2-butenal been present were not detected, further demonstrating that neither CA:BCB complex contained the *Z*-isomer of crotonaldehyde. If CA was not present in the complexes, e.g. if CA had reacted with BCB (see Figure 2-21), then the expected D-A adduct of CA and CP would not have been afforded.

The CA and CP reaction at different temperatures also gave unusual results (Table 2-5). Product ratios should have a linear correlation with the reaction temperature, i.e. a plot of ln(endo:exo) versus 1/temperature should yield a straight line, if they arise from a common precursor. The D-A adduct ratios of BCB catalyzed reaction of CA and CP were not linear. Such behavior is possible if the products arise from two precursors, i.e. the *s-trans* and *s-cis* complexes, each giving its own temperature dependent product ratio.

Previously, Yamamoto and coworkers discovered that enones pi-complexed with aluminum tris(2,6-diphenylphenoxide), a stericly hindered propeller-shaped Lewis acid, are exo-selective when reacted with CP.[15] The data in Table 2-5 show that other pi-complexed species also give interesting chemistry.

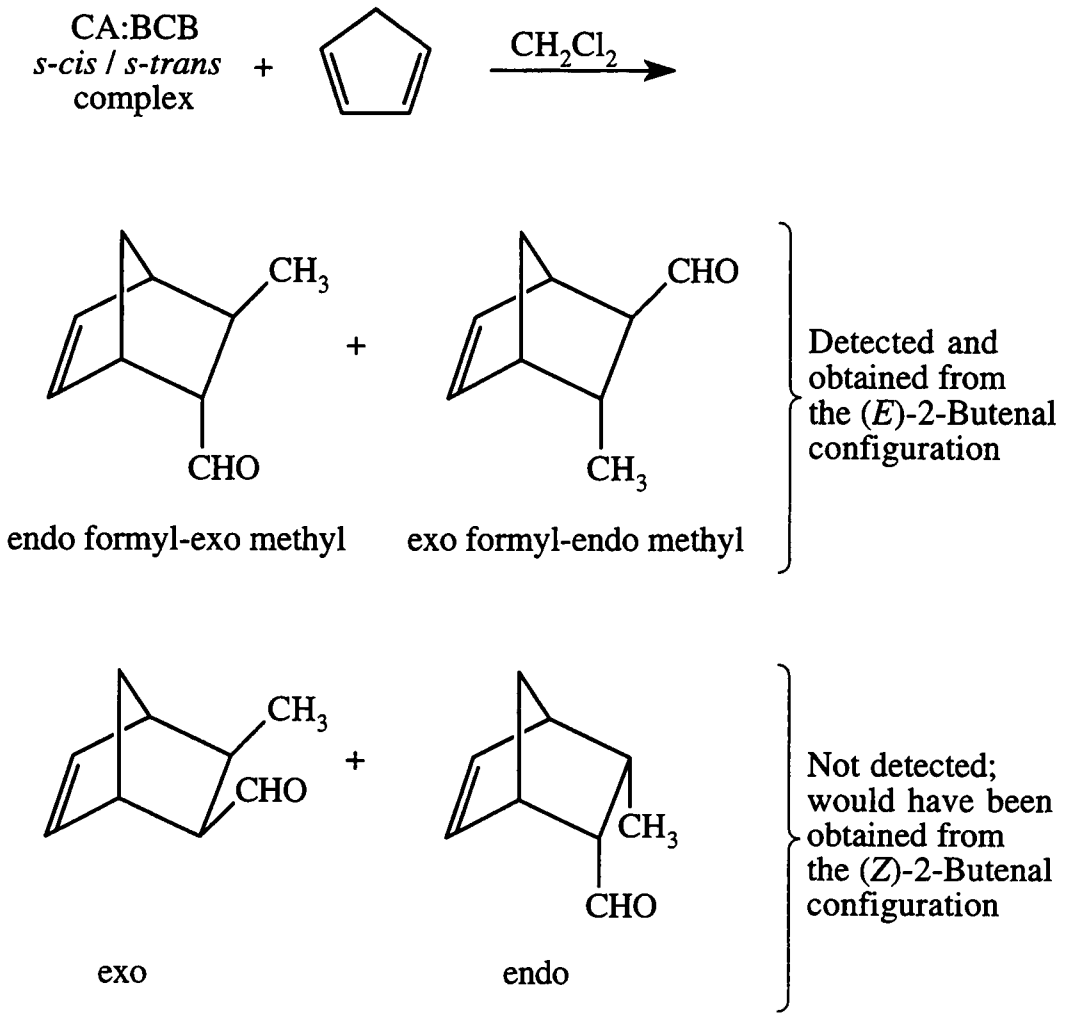


Figure 2-26. The BCB Catalyzed Reaction of CA and CP

Table 2-5. *B*-Bromocatecholborane Catalyzed D-A Reaction of CA and CP at Various Temperatures

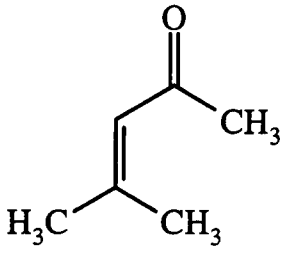
Reaction temperature (°C)	Product ratio [a] endo : exo
24	79 : 21
-22	86 : 14
-78	83 : 17

[a] endo and exo 2-Formyl-3-methylbicyclo [2.2.1]hept-5-ene. note: the thermal reaction of CA + CP gave 51 : 49 endo : exo adduct ratios.[16]

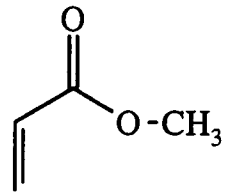
As a comparison with the behavior of CA and BCB, other possible pi-complexed bases were treated with BCB (Figure 2-27). Mesityl oxide (MSO), for example, showed minor downfield shifts of the C1 methyl group, but a small upfield shift of the allylic methyls (Table 2-6). A larger (-0.34) upfield shift of the H2 proton revealed that mesityl oxide, when complexed with BCB, does not necessarily pi-complex with the benzene aromatic ring system in the same way that CA does, but is still influenced by the aromatic pi-electrons of the oxygen-containing ring (Figure 2-28). After MSO's carbonyl oxygen bonds to the BCB's boron, the large size of the 3 methyl groups prevents MSO from pi-bonding to the aromatic rings of BCB. The H2 proton, nonetheless, resides over the BCB; thus a dramatic upfield shift occurs with H2. The small upfield shift of the allylic methyls suggested that they, in addition to the H2 proton, are influenced by the aromatic ring current; consequently their electron density is increased.

The carbon-13 spectrum corroborated the proton data (Table 2-7). Slight shifts in the ^{13}C resonances occurred, except for the carbonyl carbon, as expected. The carbonyl carbon, due to its weakened double-bond caused by Lewis acid complexation, shifted upfield 37.6 ppm to δ160.9.

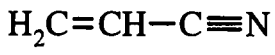
In addition to yielding the complexed MSO, another reaction of BCB with MSO was observed; i.e. the addition of HBr. The resulting 1,2 HBr addition product (MSO-Br; 4-bromo-2-pentanone) was clearly identified in the proton and carbon-13 NMR spectra (see Table 2-6 and Table 2-7). BCB will react with traces of H_2O in the solvent and on the glass to produce HBr, which, in turn, reacts with unsaturated carbon-carbon double bonds (Figure 2-29).



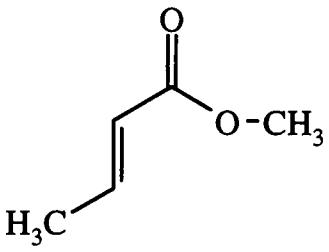
Mesityl Oxide
(MSO)



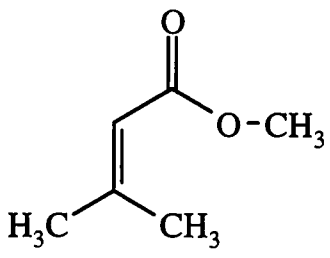
Methyl Acrylate
(MA)



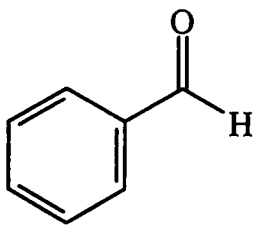
Acroylnitrile
(AN)



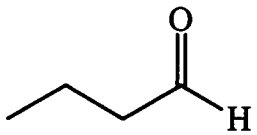
Methyl Crotonate
(MC)



Methyl 3,3-Dimethylacrylate
(MDA)



Benzaldehyde
(BZ)



Butyraldehyde
(Butanal)
(BTA)

Figure 2-27. Conjugated Bases Complexed with BCB

Table 2-6. Proton Chemical Shifts of Mesityl Oxide and BCB

	$(CH_3)1$	H2	$(CH_3)3$	$(CH_3)4$
MSO	1.82	6.05	2.08	2.06
MSO : BCB	1.90	5.71	1.98	1.95
MSO-Br [a]	3.13	5.51	2.25	2.14

[a] MSO-Br is 4-bromo-2-pentanone; the product of 1,2 HBr addition to mesityl oxide after a reaction with BCB.

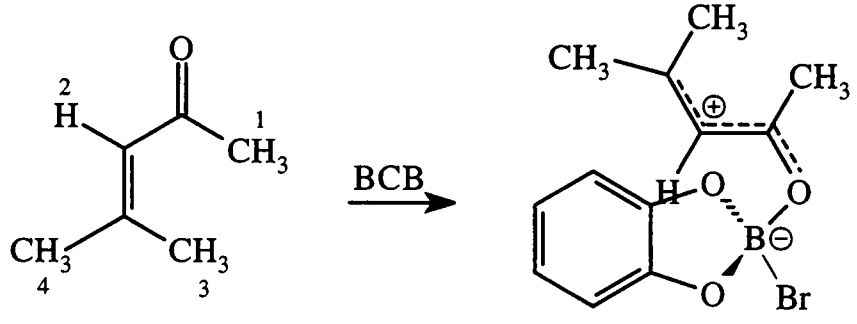
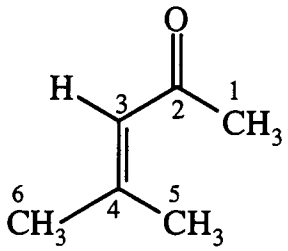


Figure 2-28. Complex of Mesityl Oxide and *B*-Bromocatecholborane

Table 2-7. Carbon-13 Chemical Shifts of Mesityl Oxide and BCB



	C1	C2	C3	C4	C5	C6
MSO	31.7	198.5	123.9	155.1	27.5	20.3
MSO : BCB	62.5	160.9	124.0	155.8	24.5	20.7
MSO-Br [a]	57.8	109.1	112.2	122.2	33.9	31.8

[a] MSO-Br is 4-bromo-2-pentanone; the product of 1,2 HBr addition to mesityl oxide after a reaction with BCB.

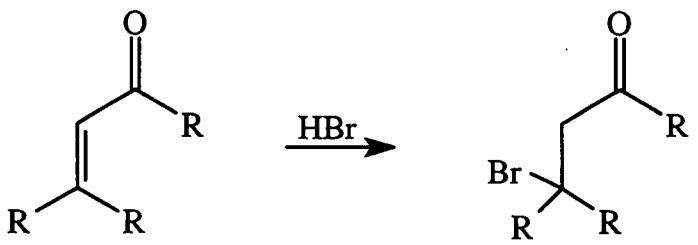


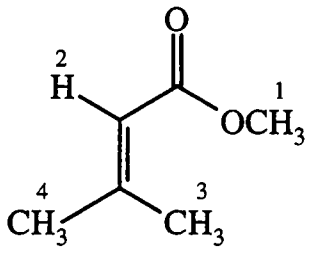
Figure 2-29. Hydrogen Bromide Addition to Conjugated Carbonyls

The conjugated esters methyl 3,3-dimethylacrylate (MDA) and methyl crotonate (MC) produced downfield shifts for all their protons in their respective NMR spectra when complexed to BCB, as expected for normal, non-pi-complexed species (Table 2-8 and Table 2-9). The small shifts relative to those of uncomplexed MDA and MC showed that these esters are not strong bases, as most ester are not. Carbon-13 resonances of the two complexes were similar to those of the individual compounds. The MC also reacted with the BCB to produce a small amount of methyl 3-bromobutanoate, the HBr addition product of MC.

Methyl acrylate (MA) was also treated with BCB. Methyl acrylate is very reactive and is sold commercially with added hydroquinone monomethyl ether as an inhibitor; it is also a good proton donor (MA polymerizes very quickly without an inhibitor present). Distillation of MA failed to remove all the inhibitor. Thus, when MA was treated with BCB the hydroquinone reacted with the BCB to produce HBr, which added to MA to yield methyl 3-bromo propanoate (see Table 2-10). Although the proton resonances of the MA and BCB mixture showed very minor downfield shifts relative to MA itself, the carbon-13 resonance of C2, the carbonyl carbon, did not shift and, therefore, no complex was formed between MA and BCB (Table 2-11).

Acrylonitrile (AN), with an electronegative nitrogen atom, was also subjected to BCB in CD_2Cl_2. Although no complex was recorded, AN did react with BCB to produce the 1,2 and 1,4 HBr addition products (see Table 2-12 and Table 2-13).

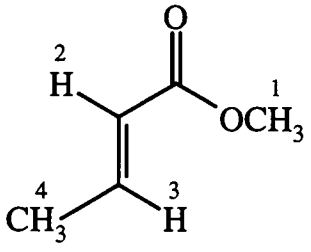
Table 2-8. Proton Chemical Shifts of Methyl 3,3-Dimethyl Acrylate and BCB



	OCH_3	H2	$(CH_3)3$	$(CH_3)4$
MDA	3.53	5.57	1.78	2.05
MDA : BCB	3.70	5.74	1.90	2.16

NMR was recorded at -20°C in CD_2Cl_2.

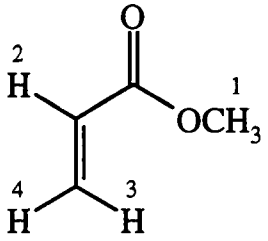
Table 2-9. Proton Chemical Shifts of Methyl Crotonate and BCB



	OCH_3	H2	H3	$(CH_3)4$
MC	3.62	5.79	6.91	1.81
MC : BCB [a]	3.66	5.96	7.01	1.89
MC-Br	3.62 (s)	2.86 (d)	4.45 (6)	1.71 (d)

NMR was recorded at -20°C in CD_2Cl_2. [a] MC-Br is methyl 3-bromobutanoate, the product of 1,2 HBr addition to methyl crotonate after a reaction with BCB.

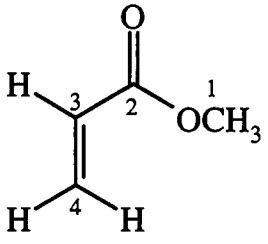
Table 2-10. Proton Chemical Shifts of Methyl Acrylate and BCB



	OCH_3	H2	H3	H4
MA	3.68	6.09	6.34	5.80
MA : BCB	3.74	6.20	6.42	5.87
MA-Br	3.68	2.91	3.57	

NMR was recorded at -20°C in CD_2Cl_2. [a] MA-Br is methyl 3-bromopropanoate, the product of 1,2 HBr addition to methyl acrylate after a reaction with BCB.

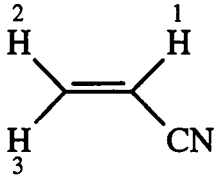
Table 2-11. Carbon-13 Chemical Shifts of Methyl Acrylate and BCB



	OCH_3	C2	C3	C4
MA	51.7	166.6	130.9	128.2
MA : BCB	52.1	168.0	127.8	123.7
MA-Br	53.7	171.2	37.3	26.7

NMR was recorded at -20°C in CD_2Cl_2. [a] MA-Br is methyl 3-bromopropanoate, the product of 1,2 HBr addition to methyl acrylate after a reaction with BCB.

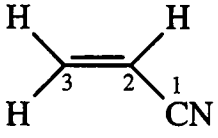
Table 2-12. Proton Chemical Shifts of Acrylonitrle and BCB



	H1	H2	H3
AN	5.67 (dd)	6.08 (d)	6.22 (d)
AN : BCB	5.68 (dd)	6.10 (d)	6.24 (d)
AN-Br (1,2) [a]	2.97 (t)	3.52 (t)	
AN-Br (1,4) [b]	2.27 (s)	7.00 (t)	4.21 (d)

NMR was recorded at -20°C in CD_2Cl_2. [a] AN-Br(1,2) is 3-bromopropionitrile; the product of 1,2 HBr addition to acrylonitrile after a reaction with BCB. [b] AN-Br(1,4) is $NH=C=CHCH_2Br$; the product of 1,4 HBr addition to acrylonitrile after a reaction with BCB.

Table 2-13. Carbon-13 Chemical Shifts of Acrylonitrle and BCB



	C1	C2	C3
AN	117.3	107.5	137.9
AN : BCB	117.7	107.3	138.1
AN-Br (1,2) [a]	127.3	21.9	25.3
AN-Br (1,4) [b]	151.9	148.2	29.7

NMR was recorded at -20°C in CD_2Cl_2. [a] AN-Br(1,2) is 3-bromopropionitrile; the product of 1,2 HBr addition to acrylonitrile after a reaction with BCB. [b] AN-Br(1,4) is $NH=C=CHCH_2Br$; the product of 1,4 HBr addition to acrylonitrile after a reaction with BCB.

Butyraldehyde (butanal; BTA) has the same 4-carbon chain as CA, but without the conjugated carbon-carbon double-bond. When BTA was complexed with BCB in CD_2Cl_2 at -20°C, the resulting proton NMR spectrum showed that the chemical shifts for H2, H3 and H4 shifted slightly downfield from the uncomplexed BTA values, but the H1 resonance showed a significant upfield shift (Table 2-14, Figure 2-30; for comparison, ^1H NMR spectrum of BTA is shown in Figure 2-31). The boron-11 spectrum of the complex indicated the boron was in a similar environment as the boron in the CA:BCB complex; that is, the boron atom was complexed to the carbonyl oxygen. That hypothesis was disproved by the absence of a carbonyl stretch in the low-temperature FT-IR spectrum of the adduct (Figures 2-32, 2-33, 2-34). Although no carbonyl was detected by IR, the oxygen was presumably still bonded to the boron as shown in Figure 2-35. A theoretically calculated value of δH1 in this σ-bonded species from shielding constants[10,17] is approximately 6 ppm, close to value obtained.

Table 2-14. Proton Chemical Shifts of Butyraldehyde (butanal) and BCB

	chemical shifts (J/Hz)			
	H1 (J_{12})	H2	H3	H4 (J_{34})
BTA	9.65	2.35	1.55	0.85
BTA : BCB [a]	6.55 (5.8)	2.21	1.57	1.00 (7.4)

NMR was recorded at -20°C in CD_2Cl_2. [a] Upon complexation of BTA with BCB, a 1,3 bromine shift occurred.



Figure 2-30. Proton NMR Spectrum of BTA and BCB at -20°C in CD_2Cl_2

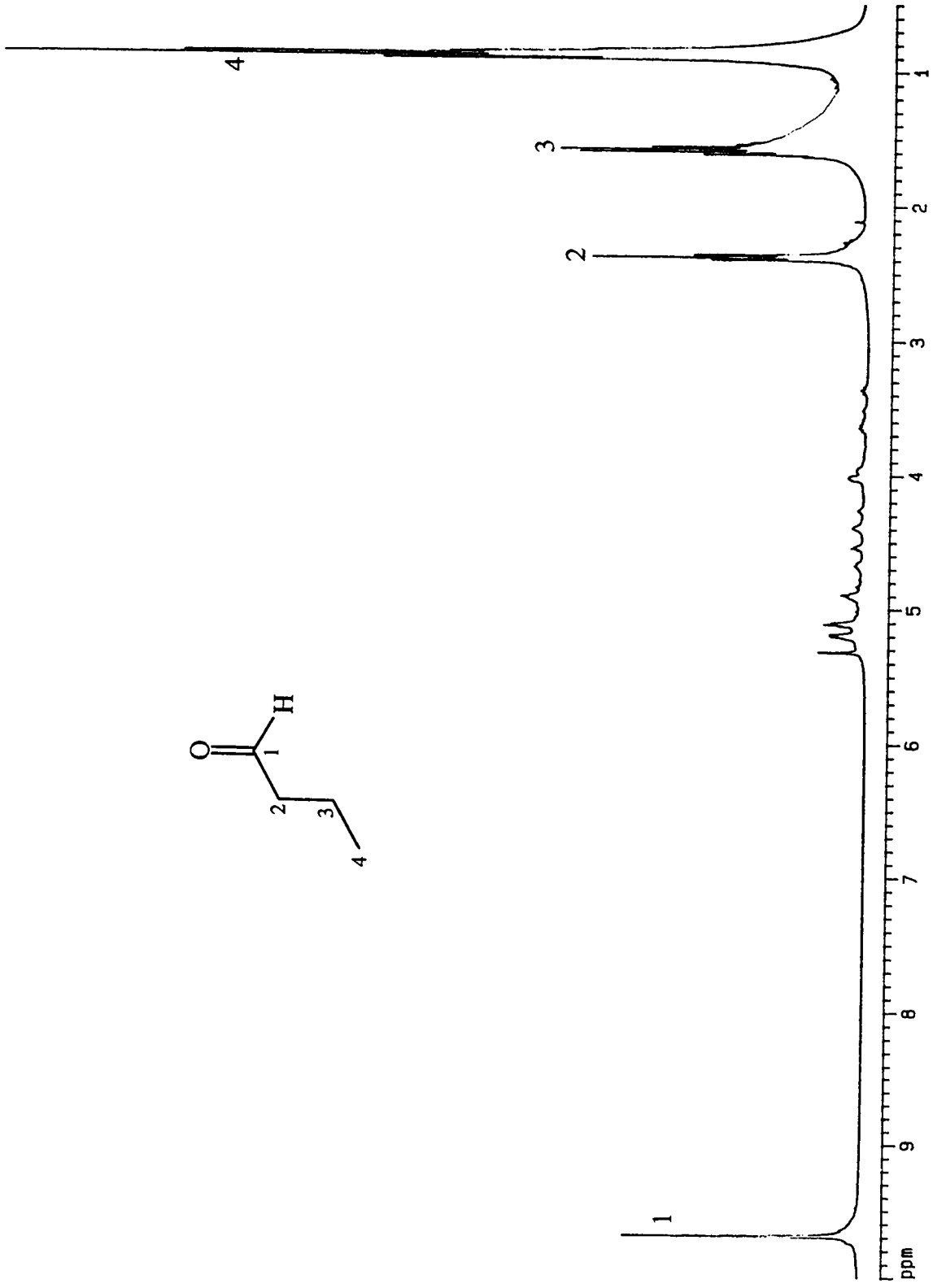


Figure 2-31. Proton NMR Spectrum of BTA at -20°C in CD_2Cl_2

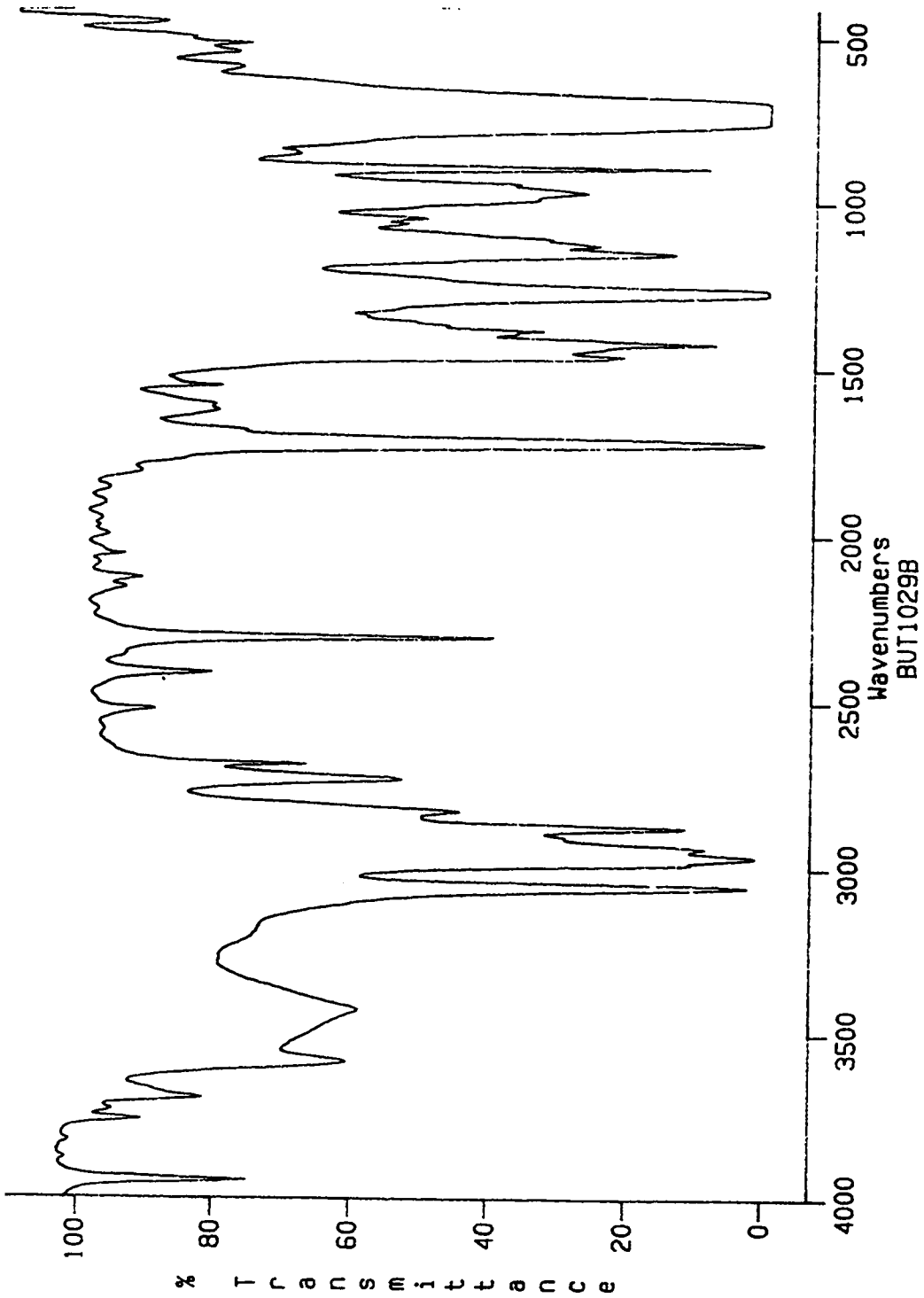


Figure 2-32. IR Spectrum of BTA at -17°C in CH_2Cl_2

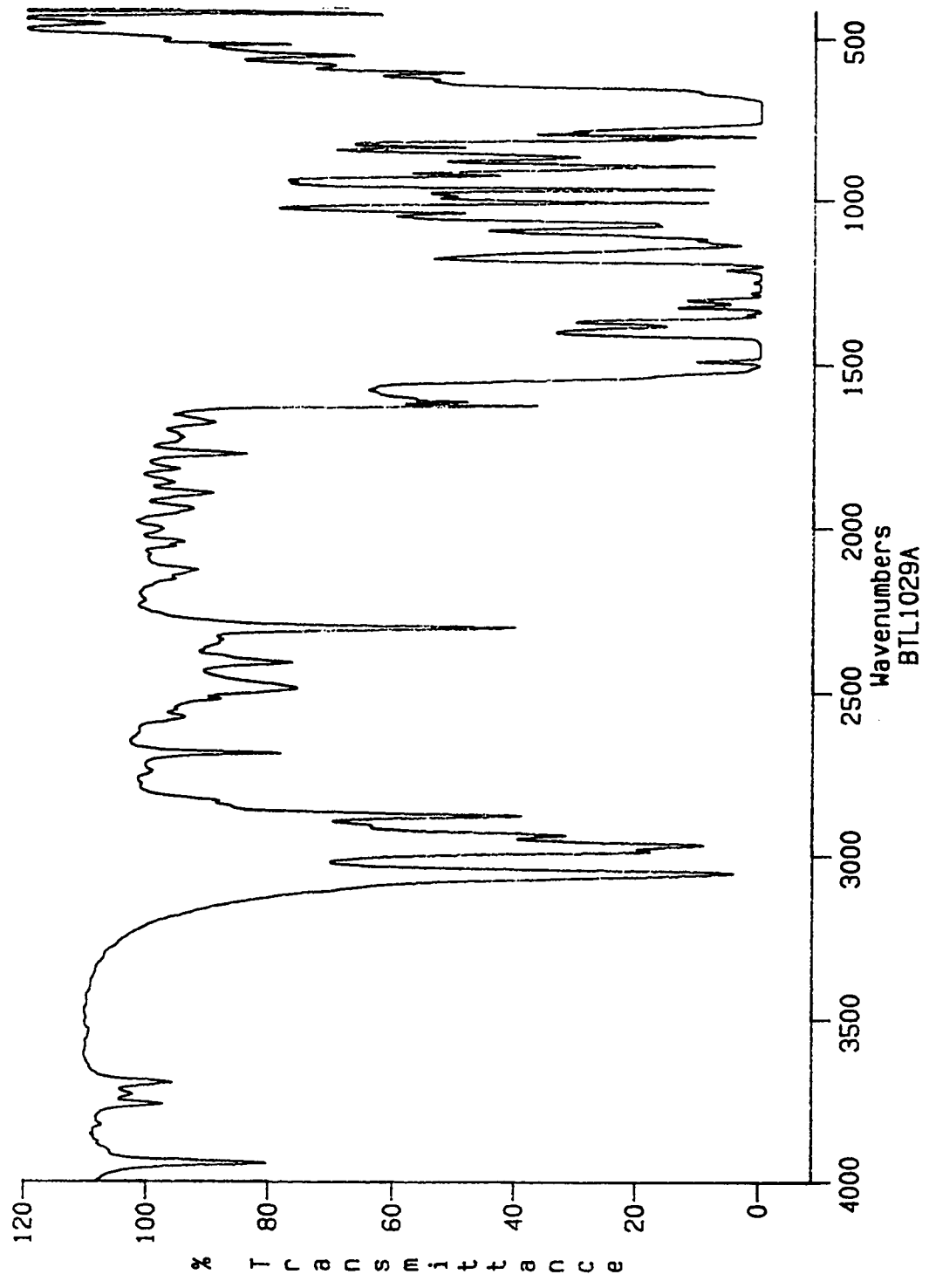


Figure 2-33. IR Spectrum of BTA and BCB at -17°C in CH_2Cl_2

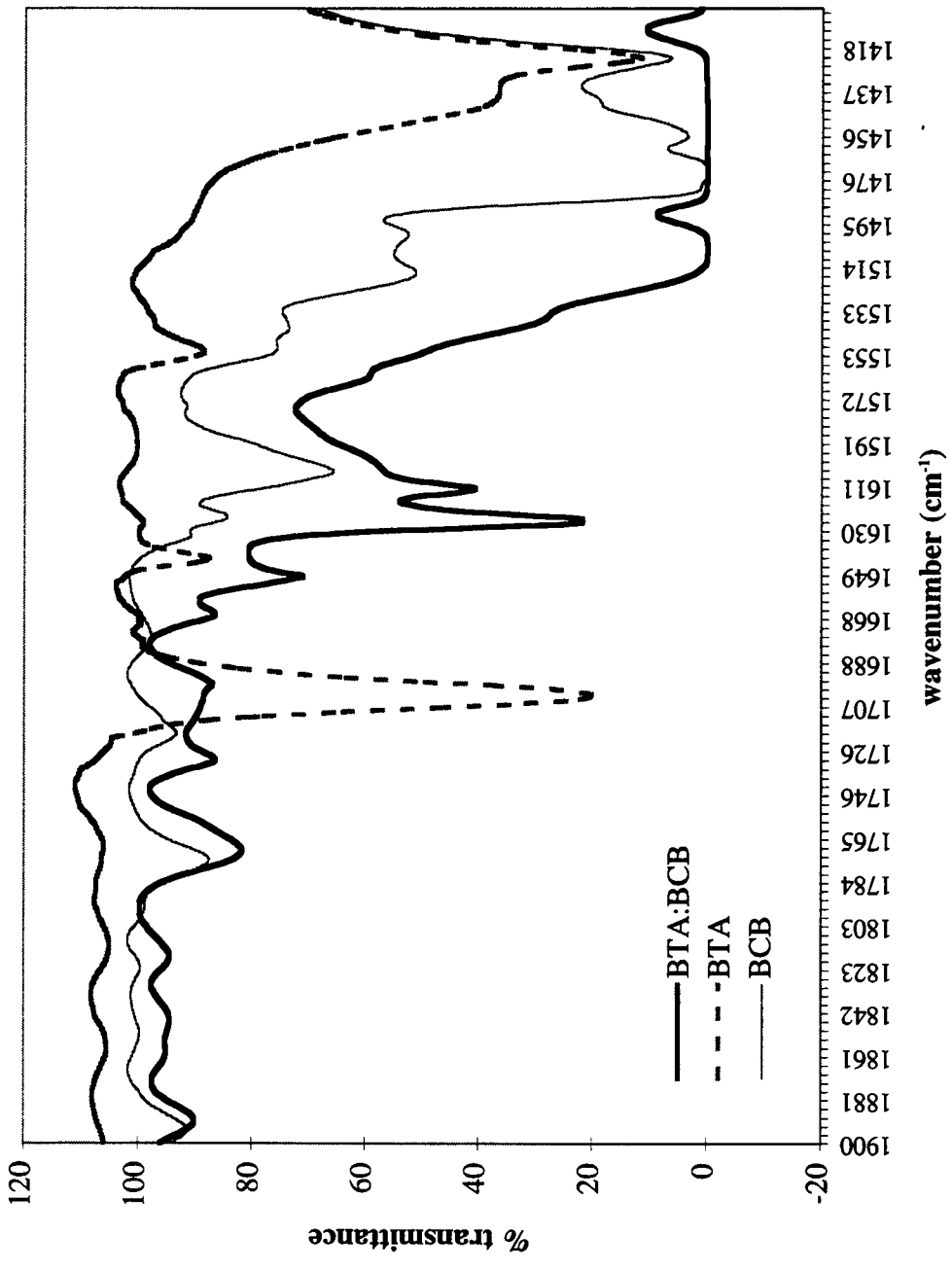


Figure 2-34. Expanded Region of the IR Spectra of BCB, BTA, and BTA:BCB at -17°C in CH_2Cl_2

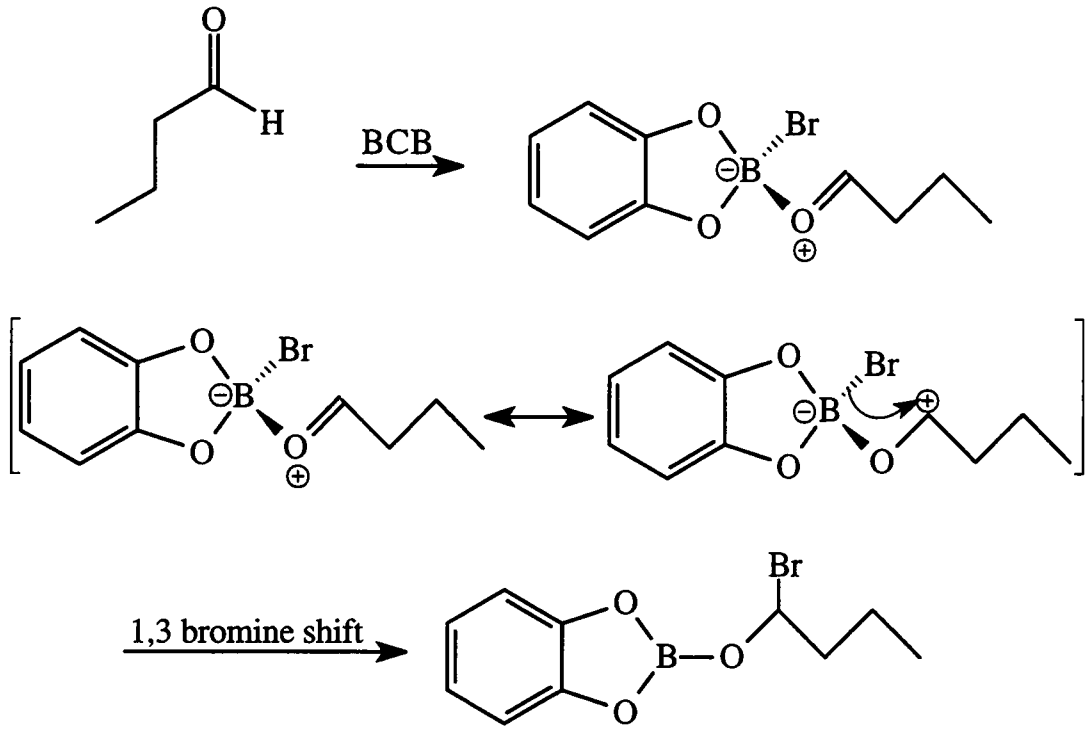


Figure 2-35. Reaction of Butyraldehyde (butanal) and *B*-Bromocatecholborane

Finally, benzaldehyde (BZ) was complexed to BCB. The aldehydic proton presumably shifted upfield significantly as compared to BZ itself, similar to the butyraldehyde case, but the resonance was hidden under the aromatic resonances. The carbon-13 NMR showed that the benzaldehyde's C1 shifted from 192.4 ppm to 79.2 ppm, close to the theoretical value of 77.1 for the 1,3 bromine shift to the benzaldehyde's carbonyl carbon.

Other Lewis Acids' Effect on CA Resonances

In addition to treating a variety of bases with BCB, the Lewis acid was varied to determine if CA's behavior with BCB and CCB was unique. Catecholborane, with a reactive hydride, was the starting material in the synthesis of several Lewis acids similar in structure to the BCB and CCB models (Figure 2-36). Each, in turn, was complexed with *trans*-crotonaldehyde (see Table 2-15 and Table 2-16). Trifluoromethanesulfonic acid (triflic acid; Tf) reacted vigorously when added to catecholborane yielding several side products. Due to the vigorous reaction, the acid was then added slowly to CB which allowed for additional CB borons to react with the uncomplexed and unreacted oxygens. The ^{11}B NMR chemical shifts revealed tetrahedral boron atoms at 9.0, -1.4, and -11.5, which support this structure. An additional ^{11}B resonance of 23.6 showed the trigonal boron species (TfCB) wanted in the reaction of triflic acid and CB. The ^{13}C and ^{1}H NMR spectra taken of the reaction products also indicated that several species had been formed. Due to the number of resonances, chemical shift assignments were difficult.

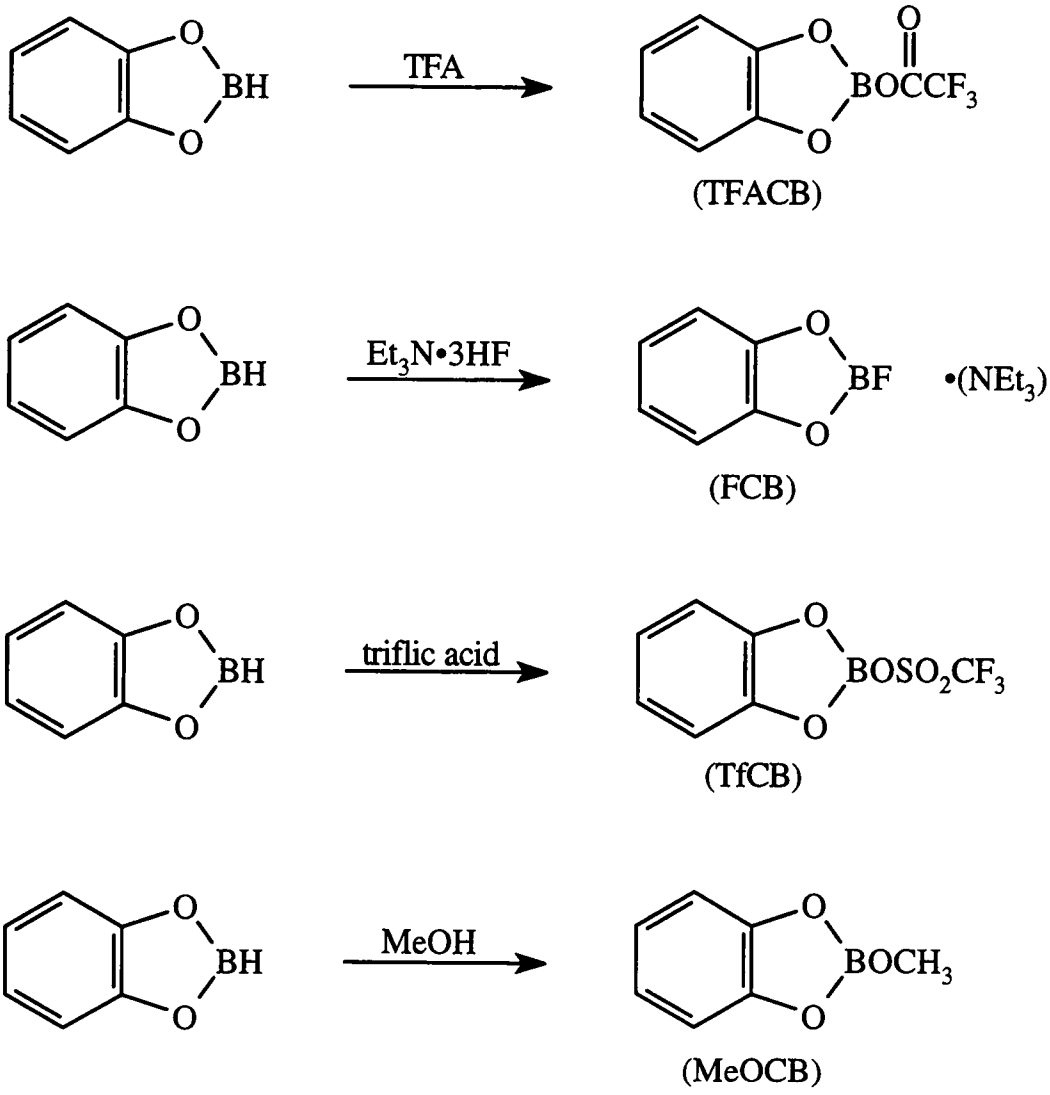


Figure 2-36. Reactions of Catecholborane with Various Acids

Table 2-15. Proton Chemical Shifts of CA with Model Compounds of BCB at -20°C in CD_2Cl_2

Lewis acid	H1 ($\Delta\delta$ ppm)[a]	H2 ($\Delta\delta$ ppm)[a]	H3 ($\Delta\delta$ ppm)[a]	H4 ($\Delta\delta$ ppm)[a]
	9.42	6.05	6.88	1.97
H^+	9.59 (+0.17)	7.07 (+1.02)	8.61 (+1.73)	2.67 (+0.70)
MeOCB	9.44 (+0.02)	6.13 (+0.08)	6.91 (+0.03)	2.00 (+0.03)
TfCB [b]	9.25 (-0.17)	6.84 (+0.79)	8.23 (+1.35)	2.42 (+0.45)
TFACB	9.39 (-0.03)	6.31 (+0.26)	6.97 (+0.09)	2.10 (+0.13)
FCB	9.40 (-0.02)	6.08 (+0.03)	6.91 (+0.03)	1.96 (-0.01)

[a] $\Delta\delta = \delta_{complexed} - \delta_{uncomplexed}$. [b] Presumably CA is complexed to the excess triflic acid and not the TfCB.

Table 2-16. Carbon-13 Chemical Shifts of CA with Model Compounds of BCB at -20°C in CD_2Cl_2

Lewis acid	C1 ($\Delta\delta$ ppm)[a]	C2 ($\Delta\delta$ ppm)[a]	C3 ($\Delta\delta$ ppm)[a]	C4 ($\Delta\delta$ ppm)[a]
none [b]	194.0	134.5	154.9	18.6
none [c]	193.4	134.8	153.9	18.5
H^+	206.1 (+12.1)	130.4 (-4.1)	193.2 (+38.3)	23.6 (+5.0)
MeOCB	195.7 (+1.7)	134.1 (-0.4)	156.9 (+2.0)	19.0 (+0.4)
TfCB [d]	204.7 (+10.7)	130.3 (-4.2)	185.7 (+30.8)	22.9 (+4.3)
TFACB	198.6 (+4.6)	137.2 (+2.7)	162.7 (+7.8)	19.7 (+1.1)
FCB	195.2 (+1.2)	134.0 (-0.5)	156.5 (+1.6)	18.8 (+0.2)

[a] $\Delta\delta = \delta_{complexed} - \delta_{uncomplexed}$. [b] this work. [c] reference 13. [d] Presumably CA is complexed to the excess triflic acid and not the TfCB.

When CA was added to the resulting product of triflic acid and CB (TfCB), large downfield shifts were observed in its ^{1}H and ^{13}C NMR spectra (see Table 2-15 and Table 2-16). Since some excess triflic acid was presumably present, the CA may be complexed to the proton (H^{+}) furnished by the triflic acid. The boron-11 NMR spectrum of the TfCB:CA mixture also suggested that no complex had formed between CA and the new Lewis acid.

Trifluoroacetic acid (TFA) also reacted vigorously when added to catecholborane to produce *B*-trifluoroacetocatecholborane (TFACB) (see Figure 2-36). Unlike the TfCB case, the reddish-orange TFACB solid showed only one species in the proton, carbon-13, and boron-11 NMR spectra. Slight downfield shifts of the CA's protons and carbons were detected when CA was added to the TFACB (see Table 2-15 and Table 2-16). These results are not suprising because TFACB, with its boron bonded to 3 electronegative oxygen atoms which can back-donate electrons, is much less Lewis acidic than BCB.

B-Methoxycatecholborane (MeOCB) was synthesized by adding methanol to catecholborane (see Figure 2-36). MeOCB, a transparent white solid, was clearly identified by its ^{11}B, ^{13}C, and ^{1}H NMR spectra (Table 2-17). The resulting complex of CA with MeOCB produced very small downfield shifts in the CA proton resonances as compared to CA itself (Table 2-10). Like the TfCB and TFACB, MeOCB is less Lewis acidic than BCB because of electron back-donation of the 3 oxygens to the boron's empty 2p orbital. Thus, MeOCB is a poorer electron pair acceptor than BCB.

Table 2-17. NMR Chemical Shifts of *B*-Methoxycatecholborane

	^1H			
	CH_3	OH	^{13}C	^{11}B
MeOH	3.33	4.66	49.78	–
MeOCB	3.88 [a]	-- [b]	51.30 [a]	25.1 [a]

[a] A trivial amount of dimethoxy product $(MeO)_2CB$ appeared at 3.52 ppm (^1H), 51.3 ppm (^{13}C), and 20.4 (^{11}B). [b] No hydroxyl proton was detected, as expected.

B-Flourocatecholborane (FCB) cannot be synthesized by the traditional synthesis of *B*-halocatecholboranes by adding BF_3 to catechol. An alternate synthesis was developed in which triethylamine-trihydrogenflouride ($Et_3N•3HF$; an anhydrous HF provider) was slowly added to catecholborane (see Figure 2-36). The vigorous reaction was very exothermic and copious amounts of gas were released. The resulting white solid showed complicated ^{11}B and ^{13}C NMR spectra and a ^1H spectrum with only aromatic and Et_3N resonances. The most abundant boron-11 resonance appeared at 0.7 ppm which indicated that FCB had been synthesized and was complexed with the excess triethyl amine present. Since the triethyl amine was present, when CA was added to FCB, there were no shifts in the proton or carbon resonances from those of uncomplexed CA (see Table 2-15 and Table 2-16).

C. Conclusion

When *(E)*-2-butenal was complexed with *B*-bromo- and *B*-chlorocatecholborane in CD_2Cl_2 at -78°C, the proton and carbon NMR spectra showed, unexpectedly, the presence of two species, both of whose resonances were upfield compared to CA suggesting pi-complexes with CA in *s-cis* and *s-trans* conformations. The hypothesis was confirmed with COSY, HETCOR, NOESY, and ROESY 2D NMR experiments. The *s-cis* and *s-trans* conformations of the aldehyde exist in equal amounts which interconvert (EXSY 2D NMR). Infrared spectroscopy validated the existence of the carbonyl group. Reaction of the complex with cyclopentadiene afforded the Diels-Alder endo and exo adducts cleanly. Quenching the complex with water generated catechol, boric acid, *(E)*-2-butenal, and 3-bromobutanal, as expected.

Other Lewis acids synthesized with the catecholborane backbone and conjugated carbonyl and nitrile bases other than CA do not pi-complex like CA and BCB or CA and CCB do. Mesityl oxide showed a chemical shift for H2 implicative with a ring current effect on the H2 proton and several bases reacted with HBr to afford the saturated bromoketone or aldehyde. Butanal and benzaldehyde reacted with BCB to afford the boronate by a 1,3 bromine shift.

D. EXPERIMENTAL

General

^{1}H, ^{11}B and ^{13}C NMR (1D and 2D) spectra were recorded on a Brüker AMX-400 instrument. $CDCl_3$ and CD_2Cl_2 were used as solvents. FT-IR spectra were recorded on a Biorad Spec 3200 FTS-60 and FTS-7 instrument. Gas chromatography was carried out on Varian Model 3700 and Hewlett-Packard (HP) 5890 instruments, and GC/MS on a HP 98785A instrument.

All yields reported, except where noted, were calculated from peak areas generated on a Hewlett-Packard 5790 gas chromatograph fitted with a mass spectrometer detector or a Hewlett-Packard 5790 gas chromatograph.

Solid reagents that were oxygen or moisture sensitive and the CD_2Cl_2 were transferred in an AtMos glove bag under an argon or nitrogen atmosphere. Liquid reagents that were oxygen or moisture sensitive were transferred via doubled-ended needle under positive argon pressure. All syringes and needles were oven dried and purged with argon prior to use. Glassware was oven dried and then flame dried while being flushed with argon (mercury bubbler exit) before each reaction.

NMR of (*E*)-2-Butenal (trans-crotonaldehyde) and *B*-Bromocatecholborane Complex

A 5 mm NMR tube was septum-sealed, flame-dried and flushed with argon. *B*-halocatecholborane (0.12 g, 0.60 mmols) was transferred, under argon, in a glove bag. CD_2Cl_2 (400 μL) was injected into the NMR tube which was shaken

to ensure the solid was completely dissolved. The tube was cooled to -78 °C (acetone/CO_2) and (*E*)-2-Butenal (CA, 45 μL, 0.60 mmol) was injected into the tube. The NMR spectra were taken at 253 K (-20 °C) to 173 (-100°C) on a Brüker 400 MHz NMR with a variable temperature (VT) unit. The CCB, MO, MC, MDA, and butanal complexes with BCB were synthesized in a similar manner. The CA, MO, and butanal were distilled by standard methods prior to use.

IR of (*E*)-2-Butenal (trans-crotonaldehyde) and *B*-Bromocatecholborane Complex.

A 5 mm NMR tube was septum-sealed, flame-dried and flushed with argon. *B*-Bromocatecholborane (0.24 g, 1.2 mmols) was transferred, under argon, via a glove bag. CH_2Cl_2 (1000 μL) was injected into the NMR tube which was shaken to ensure the solid was completely dissolved. The tube was cooled to -78 °C (acetone/CO_2) and (*E*)-2-Butenal (90 μL, 1.2 mmols) was injected into the tube. The complex solution was transferred to a previous cooled, factory sealed and roughly insulated (Al/Si cotton and Styrofoam) IR cell via a Teflon canula under positive argon pressure (see Figure 2-22). The IR cell was wrapped with copper tubing that was connected to a constant temperature unit with a glycol/water mixture cooling solution (-20°C). The inner compartment of the IR was flushed with nitrogen. The spectrum was obtained. This method was repeated for BCB in CH_2Cl_2, CA in CH_2Cl_2, BTA in CH_2Cl_2 and neat CH_2Cl_2.

Synthesis of 2-Formyl-3-methylbicyclo[2.2.1]hept-5-ene (BCB Catalyzed D-A Reaction of (*E*)-2-Butenal (trans-crotonaldehyde) and Cyclopentadiene.

B-Bromocatecholborane (1.00 gm; 5.00 mmols) was transferred, under argon, to a flame-dried 100-mL, round-bottomed flask equipped with a septum-sealed side arm and a magnetic stir bar. After the flask was sealed with a septum, it was charged with freshly distilled methylene chloride (20 mL). The reaction flask was lowered into a cooling bath at 0°C (ice/water), -22°C (ice/NaI), or -78°C (CO_2/acetone) and the flask temperature was allowed to equilibrate. (*E*)-2-Butenal (0.37 mL; 5.0 mmols) was added to the flask. After the mixture was stirred for 5 min, cyclopentadiene (1.0 mL; 7.0 mmols) was added. After 3 hours of stirring, 10 mL of cold water was added to quench the reaction mixture. The reaction mixture was extracted with methylene chloride (3 x 15 mL). The combined organic phase was dried over anhydrous $MgSO_4$ (5 g) and gravity filtered. The mixture was concentrated *in vacuo*, and decane (0.20 g; 1.4 mmols) was added as an internal standard for GC analysis or CD_2Cl_2 was added for NMR analysis. ^{1}H NMR: endo CHO, 9.38; exo CHO, 9.80; endo Me, 0.94; exo Me, 1.19.

The cyclopentadiene was prepared by cracking the dicyclopentadiene dimer prior to the reaction.

Synthesis of *B*-Fluorocatecholborane.

In a 25-mL, round-bottomed flask equipped with a septum-sealed side arm and a magnetic stir bar was placed 0.88 g catecholborane (7.3 mmols). The flask was sealed with a septum. While the CB stirred, triethylamine trihydrofluoride

(400 μL; 7.34 mmol) was added slowly over 5-10 minutes via a dried 500-μL syringe. After 3 hours at room temperature, the white solid was transferred to a 5 mm NMR tube in a glove bag for further analysis. ^{1}H NMR (CD_2Cl_2, -20°C): 6.7-7.4 (m, aromatic); 3.09, 1.20 (q,t triethylamine CH_2, CH_3). ^{13}C NMR (CD_2Cl_2, -20°C): 147.4, 145.6, 123.2, 122.8, 112.7, 112.0 (aromatic); 46.8, 8.5 (triethylamine CH_2, CH_3) . ^{11}B NMR (CD_2Cl_2, -20°C): 23.5 (broad s), 1.7 (sharp s), 0.6 (sharp s).

Synthesis of *B*-Trifluoroacetocatecholborane.

In a 25-mL, round-bottomed flask equipped with a septum-sealed side arm and a magnetic stir bar was placed 1.32 g catecholborane (11.0 mmols). The flask was sealed with a septum. While the CB stirred, TFA (0.85 mL; 11.0 mmols) was added via a dried 1.00 mL syringe. After 24 hours at room temperature, the orange-reddish solid was transferred to a 5 mm NMR tube in a glove bag for further analysis. ^{1}H NMR (CD_2Cl_2, -20°C): 6.8-7.8 (m, aromatic); 11.3 (s, $CF_3CO_2\underline{H}$). ^{13}C NMR (CD_2Cl_2, -20°C): 160.8 (q, CF_3); 147.4, 145.6, 123.2, 122.8, 112.7, 112.0 (aromatic); 110.2 ($CF_3\underline{C}O_2B$) . ^{11}B NMR (CD_2Cl_2, -20°C): 23.5 (broad s).

Synthesis of *B*-Methoxycatecholborane.

In a 25-mL, round-bottomed flask equipped with a septum-sealed side arm and a magnetic stir bar was placed 1.29 g catecholborane (10.8 mmols). The flask was sealed with a septum. While the CB stirred, methanol (435 μL; 10.8 mmols) was added via a dried 500-μL syringe. After 3 hours at room temperature, the transparent white solid was transferred to a 5 mm NMR tube in a glove bag for

further analysis. ^{1}H NMR (CD_2Cl_2, -20°C): 6.7-7.4 (m, aromatic), 3.88 (s), 3.52 (s, ($C\underline{H}_3O)_2CB$). ^{13}C NMR (CD_2Cl_2, -20°C): 147.4, 145.6, 123.2, 122.8, 112.7, 112.0 (aromatic); 53.7 (s), 51.3 (s, ($\underline{C}H_3O)_2CB$). ^{11}B NMR (CD_2Cl_2, -20°C): 20.4 (broad s), 25.1 (sharp s, $(CH_3O)_2CB$).

Synthesis of *B*-Trifluoromethansulfonocatecholborane.

In a 25-mL, round-bottomed flask equipped with a septum-sealed side arm and a magnetic stir bar was placed 1.04 g catecholborane (8.67 mmols). The flask was sealed with a septum. While the CB stirred, triflic acid (0.76 mL; 8.59 mmol) was added via a dried 1.00-mL syringe. After 3 hours at room temperature, the compound was transferred to a 5 mm NMR tube in a glove bag for further analysis. ^{1}H NMR (CD_2Cl_2, -20°C): 7.0-7.4 (m, aromatic); 10.13 (s), 8.55 (d), 7.45 (d), 4.22 (s), 2.90 (d). ^{13}C NMR (CD_2Cl_2, -20°C): 147.4, 145.6, 123.2, 122.8, 112.7, 112.0 (aromatic); 187.6, 173.1, 132.4, 119.9, 116.7, 39.4, 19.2. ^{11}B NMR (CD_2Cl_2, -20°C): 23.6 (broad s), 9.0 (sharp s), -1.4 (sharp s).

E. Materials

Solvents

Dichloromethane (methylene chloride), Fisher Chemical Company

Diethyl ether, Mallinkrodt Chemical Company

Hexanes, Fisher Chemical Company

Methanol (dry, HPLC grade), Fisher Chemical Company

Toluene, Fisher Chemical Company

Acetone, Fisher Chemical Company

NMR solvents

Chloroform-d, Aldrich Chemical Company

Dichloromethane-d_2 (methylene chloride-d_2), Aldrich Chemical Company

Gases

Argon (prepurified), National Welders and MG Industries

Nitrogen (prepurified), National Welders and MG Industries

Reagents

(E)-2-Butenal (*trans*-crotonaldehyde), Aldrich Chemical Company

Acrylonitrile, Aldrich Chemical Company

Aluminum chloride, Aldrich Chemical Company

B-Bromocatecholborane, Aldrich Chemical Company

B-Chlorocatecholborane, Aldrich Chemical Company

Benzaldehyde, Aldrich Chemical Company

Boric acid, Aldrich Chemical Company

Boron tribromide (99+%), Aldrich Chemical Company

Boron trifluoride etherate, Aldrich Chemical Company

Butyraldehyde (butanal), Aldrich Chemical Company

Catecholborane, Aldrich Chemical Company

Dicyclopentadiene, Aldrich Chemical Company

Magnesium sulfate, Aldrich Chemical Company

Mesityl oxide, Aldrich Chemical Company

Methanol (HPLC grade), Aldrich Chemical Company

Methyl acrylate, Aldrich Chemical Company

Methyl crotonate, Aldrich Chemical Company

Methyl 3,3-dimethylacrylate, Aldrich Chemical Company

Sodium iodide, Aldrich Chemical Company

Triethylamine trifluoride, Aldrich Chemical Company

Trifluoromethanesulfonic acid (triflic acid), Aldrich Chemical Company

Trifluoroacetic acid, Aldrich Chemical Company

List of References

1. Landolf, M. *C. R. Hebd. Seances Acad. Sci.* **1878**, *86*, 671.

2. a. Shambayati, S.; Schreiber, S.L. In *Comprehensive Organic Synthesis, Vol. 1, Lewis Acid Carbonyl Complexation, Part 10*; Schreiber, S.L., Ed.; Pergamon Press: Oxford, 1991; pp 283-324. b. Shambayati, S.; Crowe, W.E.; Schreiber, S.L. *Angew. Chem., Int. Ed. Engl.* **1990**, *29*, 256.

3. a. Lowry, T.H.; Richardson, K.S. *Mechanism and Theory in Organic Chemistry, 3rd ed.*; Harper & Row: New York, 1987. b. March, J. *Advanced Organic Chemistry, 3rd ed.*; John Wiley and Sons: New York, 1985.

4. Eaton, P.E.; Yates, P. *J. Am. Chem. Soc.* **1960**, *82*, 4436.

5. a. Hawkins, J.M.; Loren, S.; Nambu, M. *J. Am. Chem. Soc.* **1994**, *116*, 1657. b. Denmark, S.E.; Almstead, N.G. *J. Am. Chem. Soc.* **1993**, *115*, 3133. c. Dorigo, A.E.; Morokuma, K. *J. Am. Chem. Soc.* **1989**, *111*, 6524. d. Loncharich, R.J.; Schwartz, T.R.; Houk, K.N. *J. Am. Chem. Soc.* **1987**, *109*, 14. e. Blackburn, C.; Childs, R.F.; Cremer, D.; Gauss, J. *J. Am. Chem. Soc.* **1985**, *107*, 2442. f. Müllen, K.; Kotzamani, E.; Schmickler, H.; Frei, B. *Tet. Lett.* **1984**, 25, 5623. g. Blom, C.E.; Grassi, G.; Bauder, A. *J. Am. Chem. Soc.* **1984**, *106*, 7427. h. Levy, G.C.; Cargioli, J.D.; Racela, W. **1970**, *92*, 6238. i. Deno, N.C.; Wisotsky, M.J. *J. Am. Chem. Soc.* **1963**, *85*, 1737. j. Edward, J.T.; Chang, H.S.; Yates, K.; Stewart, R. *Can. J. Chem.* **1960**, *38*, 1518. k. Campbell, H.J.; Edward, J.T. *Can. J. Chem.* **1960**, *38*, 2109. l. Yates, K.; Stewart, R. *J. Am. Chem. Soc.* **1958**, *80*, 6355.

6. Fratiello, A.; Onak, T.P.; Schuster, R.E. *J. Am. Chem. Soc.* **1968**, *90*, 1194.

7. a. Rabinovitz, M.; Grinvald, A. *J. Am. Chem. Soc.* **1972**, *94*, 2724. b. Myhre, P.C.; Fisher, C.D.; Nielsen, T.; Schubert, W.M. *J. Am. Chem. Soc.* **1965**, *87*, 29.

8. Laszlo, P.; Teston, M. *J. Am. Chem. Soc.* **1990**, *112*, 8750.

9. Childs, R.F.; Mulholland, D.L.; Nixon, A. *Can. J. Chem.* **1982**, *60*, 801.

10. Silverstein, R.M.; Bassler, G.C.; Morrill, T.C. *Spectrometric Identification of Organic Compounds, 5th ed.*; John Wiley and Sons: New York, 1991.

11. Boyd, D.R.; Evans, T.A.; Jennings, W.B.; Malone, J.F.; O'Sullivan, W.O.; Smith, A. *Chem Commun.* **1996**, 2269.

12. Hankes, G.E.; Herwig, K.; Roberts, J.D. *J. Org. Chem.*, **1974**, *39*, 1017.

13. Childs, R.F.; Manendram, M.; Blackburn, C.; Antoniadis, G. *Can J. Chem.* **1988**, *66*, 1355.

14. Neuhaus, D.; Williamson, M.P. *The Nuclear Overhauser Effect in Structural and Conformational Analysis*; VCH: New York, 1989. b. Braun, S.; Kalinowski, H.-O.; Berger, S. *100 and More Basic NMR Experiments*; VCH: New York, 1996. c. Bothner-By, A.A.; Stephens, R.L.; Lee, J.M.; Warren, C.D.; Jeanloz, R.W. *J. Am. Chem. Soc.* **1984**, *106*, 811. d. Bax, A.; Davis, D.G. *J. Magn. Reson.* **1985**, *63*, 207. e. Bax, A.; Davis, D.G. *J. Magn. Reson.* **1985**, *65*, 355.

15. Maruoka, K.; Imoto, H.; Yamamoto, H. *J. Am. Chem. Soc.* **1994**, *116*, 12115.

16. a. Abraham, R.J.; Coppell, S.M.; Ramage, R. *Org. Mag. Res.* **1974**, *6*, 658. b. Gringore, O.; Haslouin, J.; Rouessac, F. *Bull. Chem. Soc. Fr.* **1976**, *9-10*, 1524.

17. a. Friedrich, E.C.; Runkle, K.G. *J. Chem. Ed.* **1984**, *61*, 830. b. Friedrich, E.C.; Runkle, K.G. *J. Chem. Ed.* **1986**, *63*, 127.

APPENDIX

Supplementary NMR Spectra

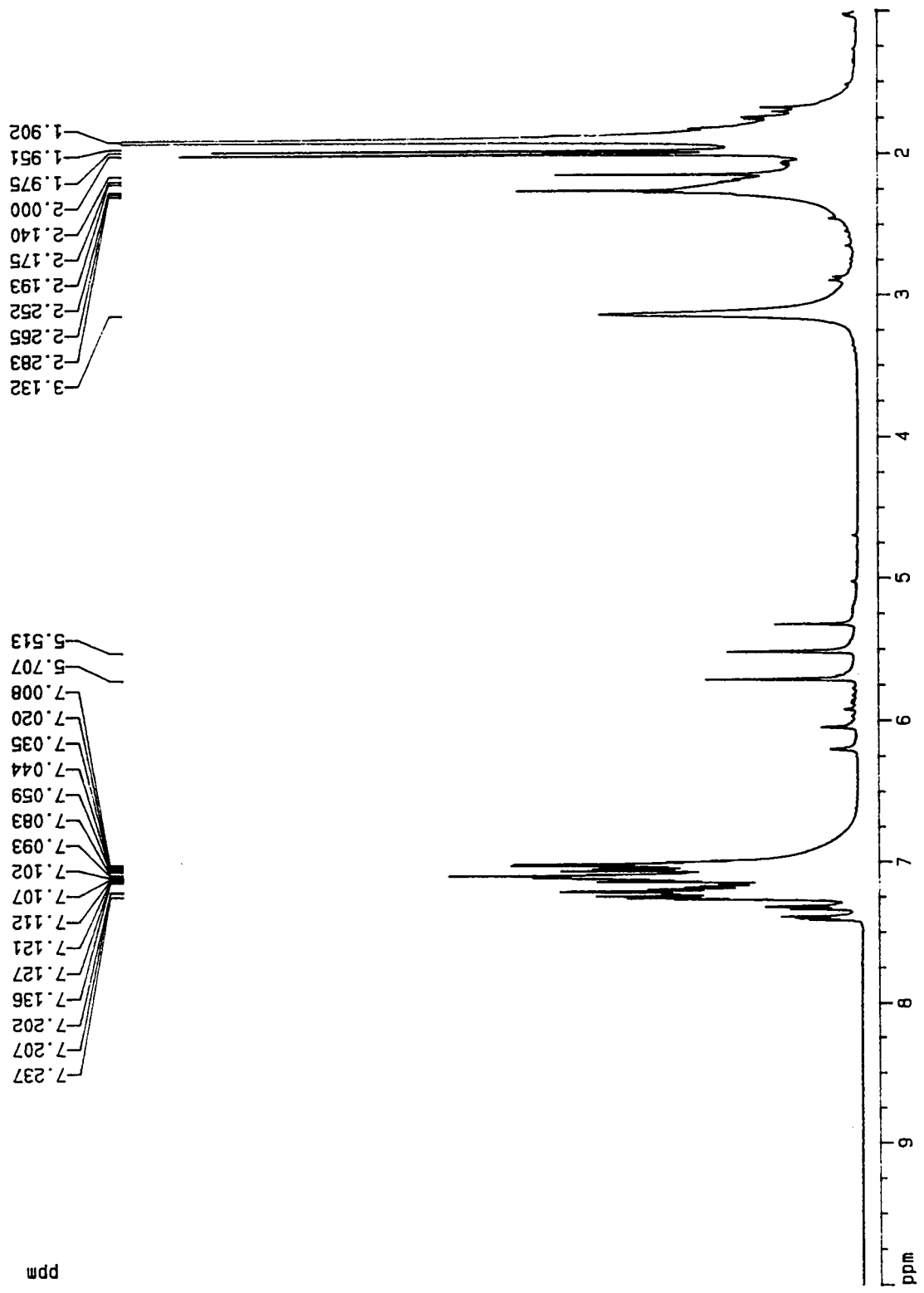


Figure A-1. Proton NMR Spectrum of MSO and BCB at -20°C in CD_2Cl_2

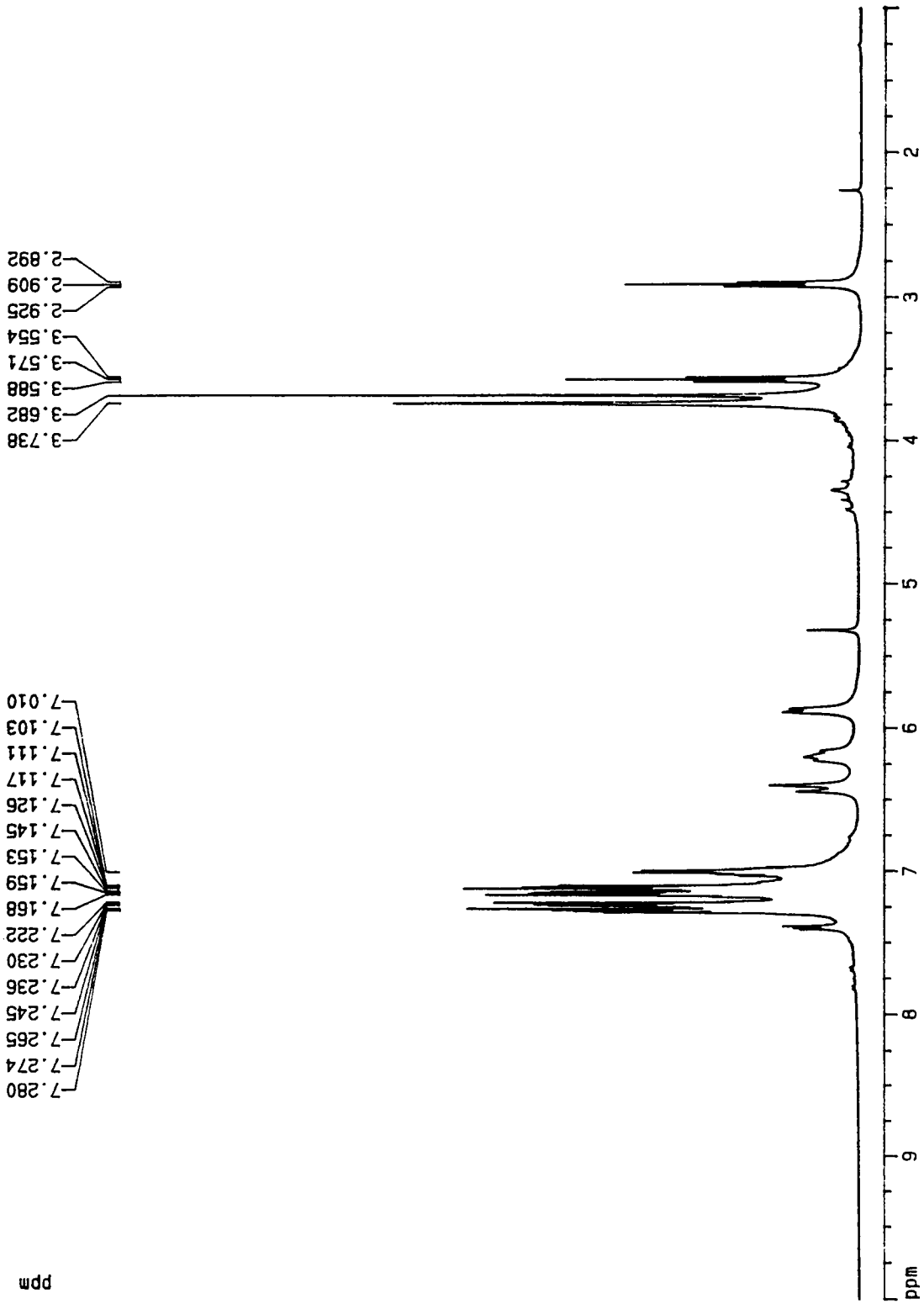


Figure A-2. Proton NMR Spectrum of MA and BCB at -20°C in CD_2Cl_2

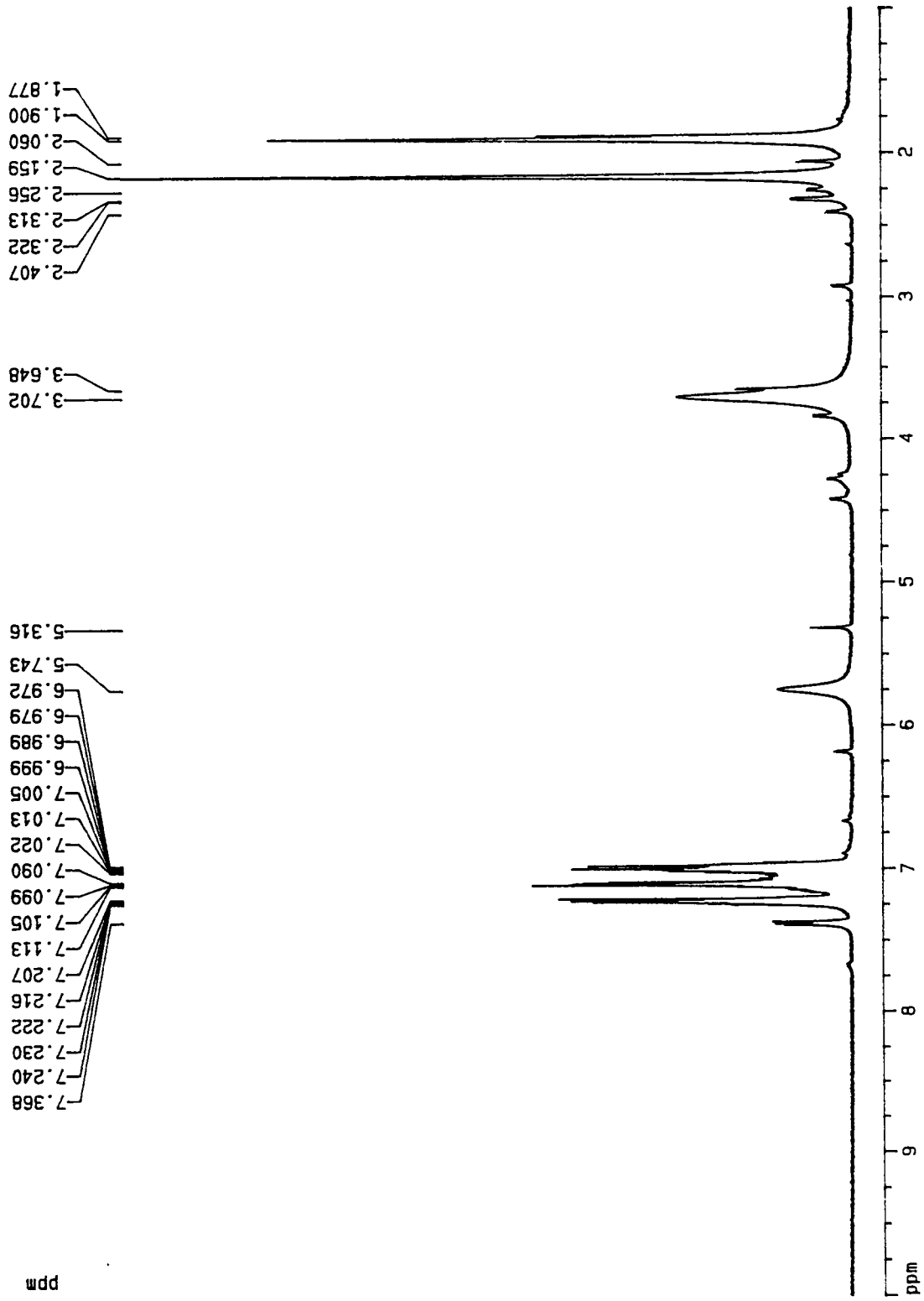


Figure A-3. Proton NMR Spectrum of MDA and BCB at -20°C in CD_2Cl_2

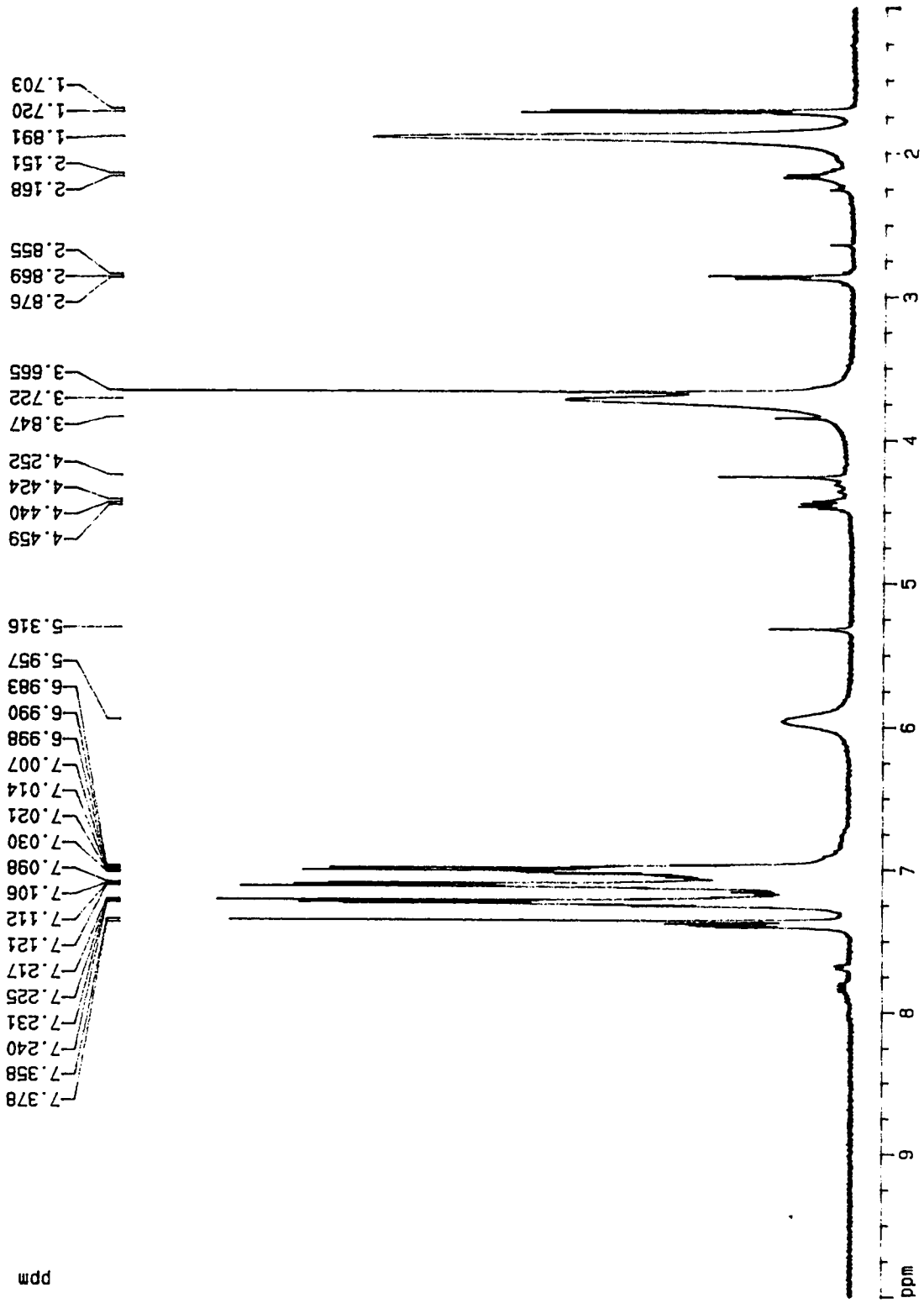


Figure A-4. Proton NMR Spectrum of MC and BCB at -20°C in CD_2Cl_2

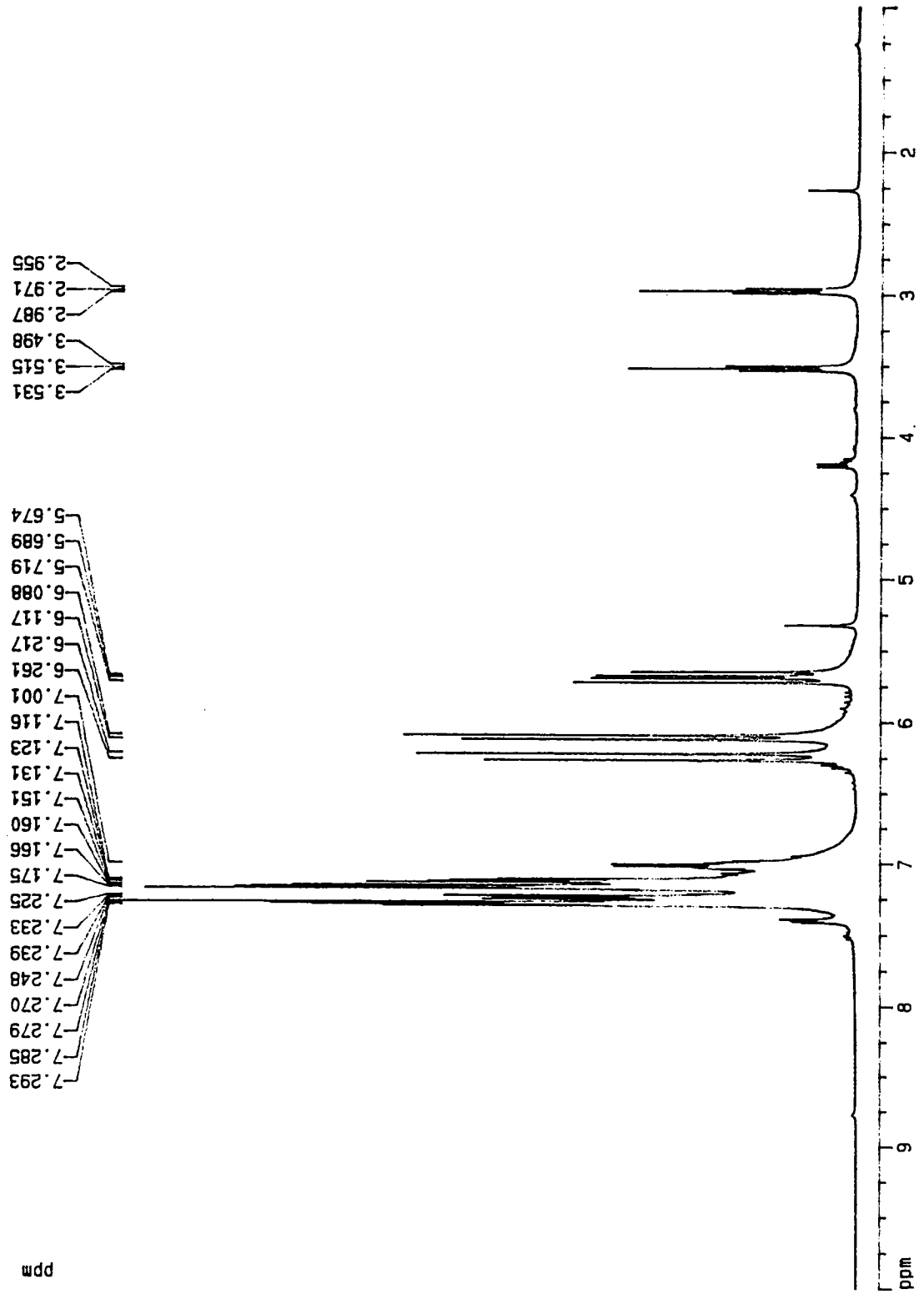


Figure A-5. Proton NMR Spectrum of AN and BCB at -20°C in CD_2Cl_2

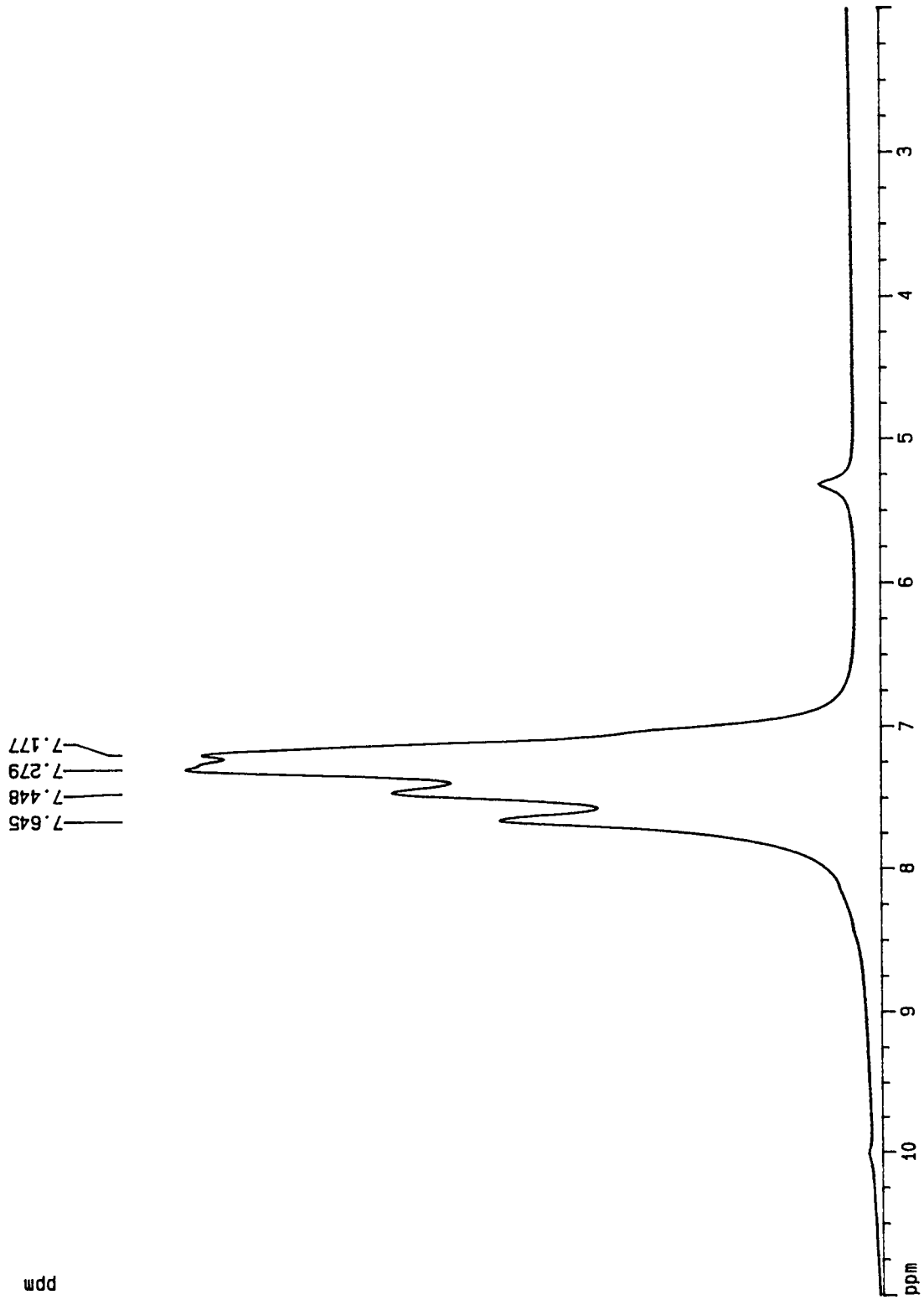


Figure A-6. Proton NMR Spectrum of BZ and BCB at -20°C in CD_2Cl_2

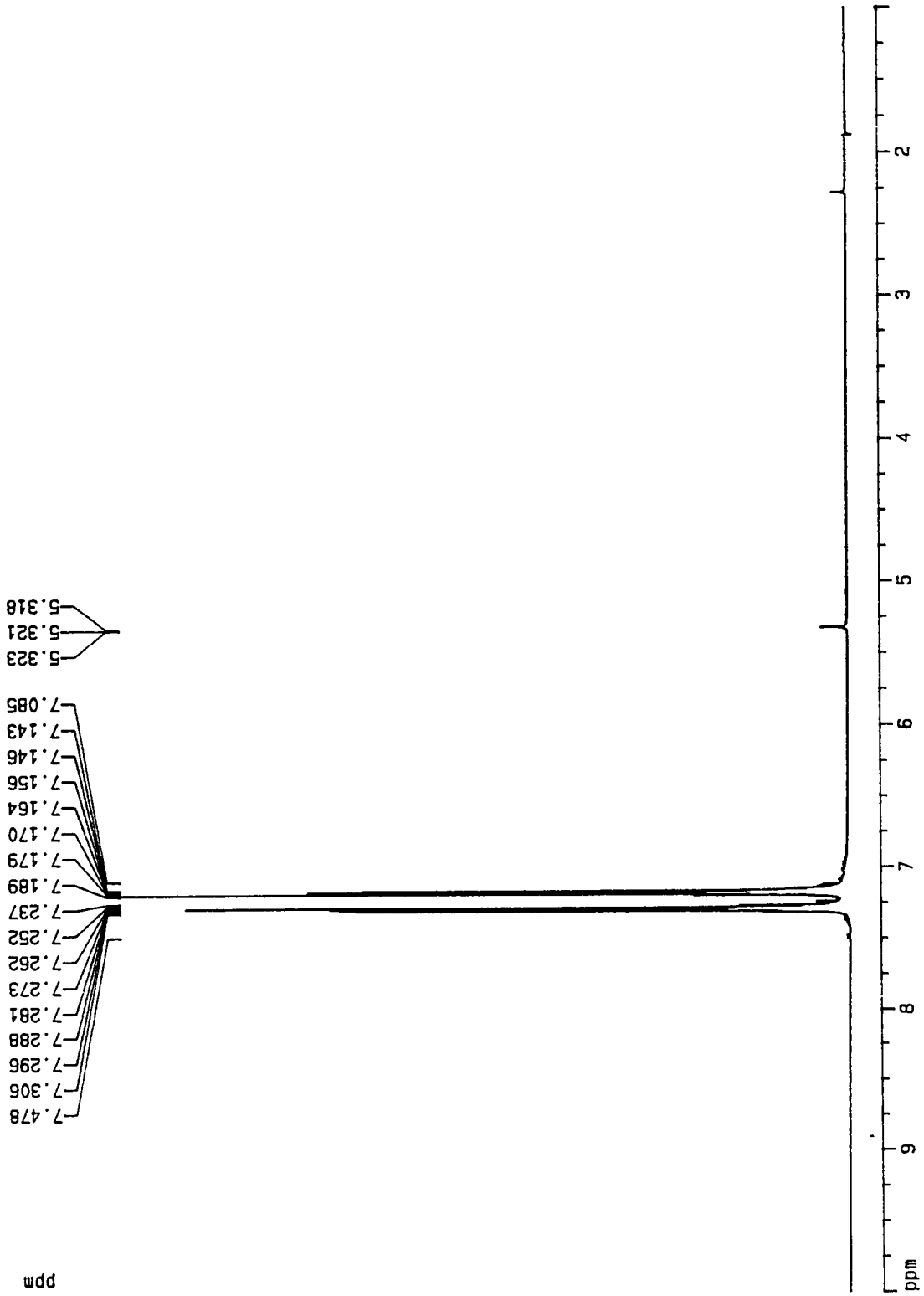


Figure A-7. Proton NMR Spectrum of CB at -20°C in CD_2Cl_2

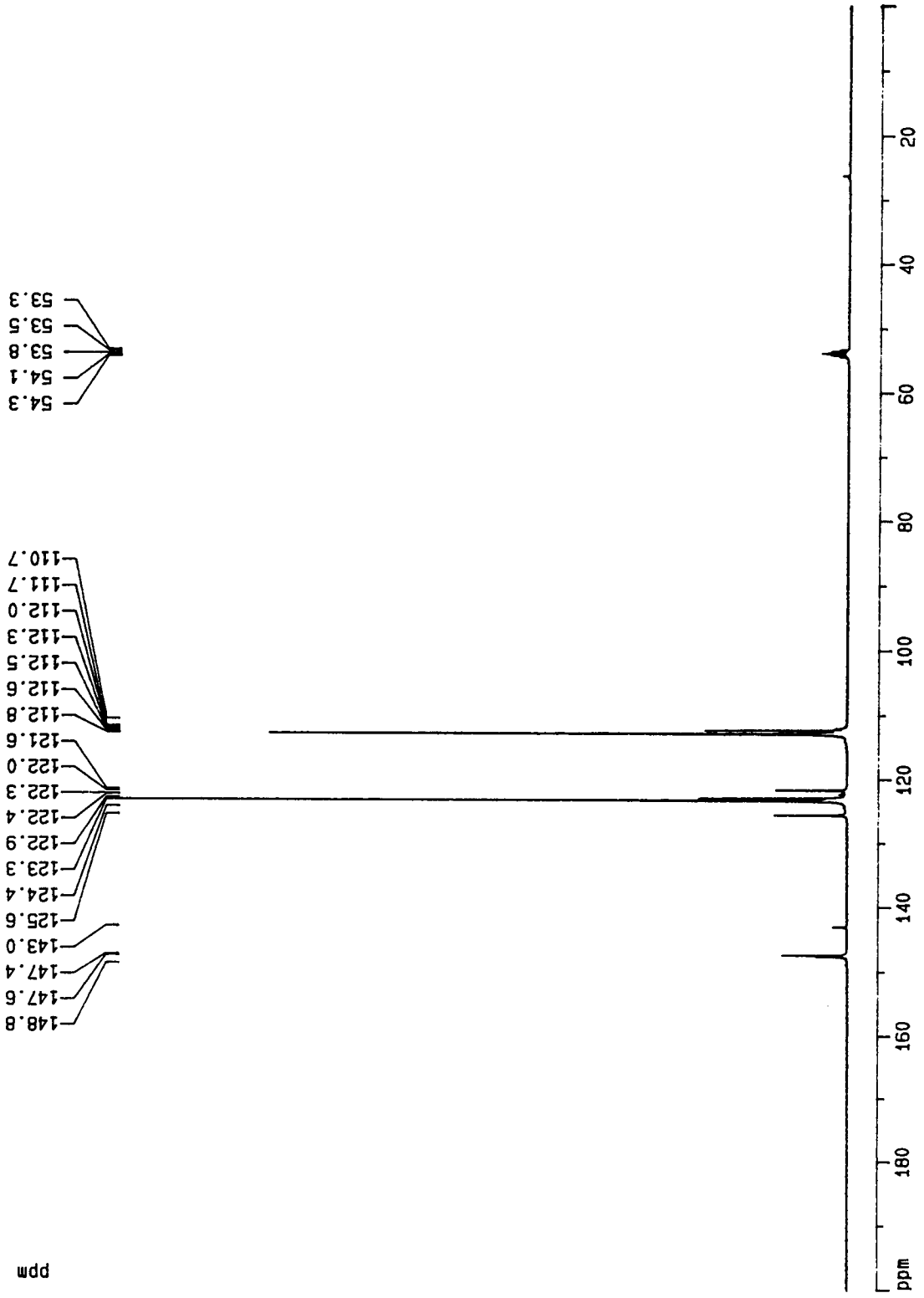


Figure A-8. Carbon-13 NMR Spectrum of CB at -20°C in CD_2Cl_2

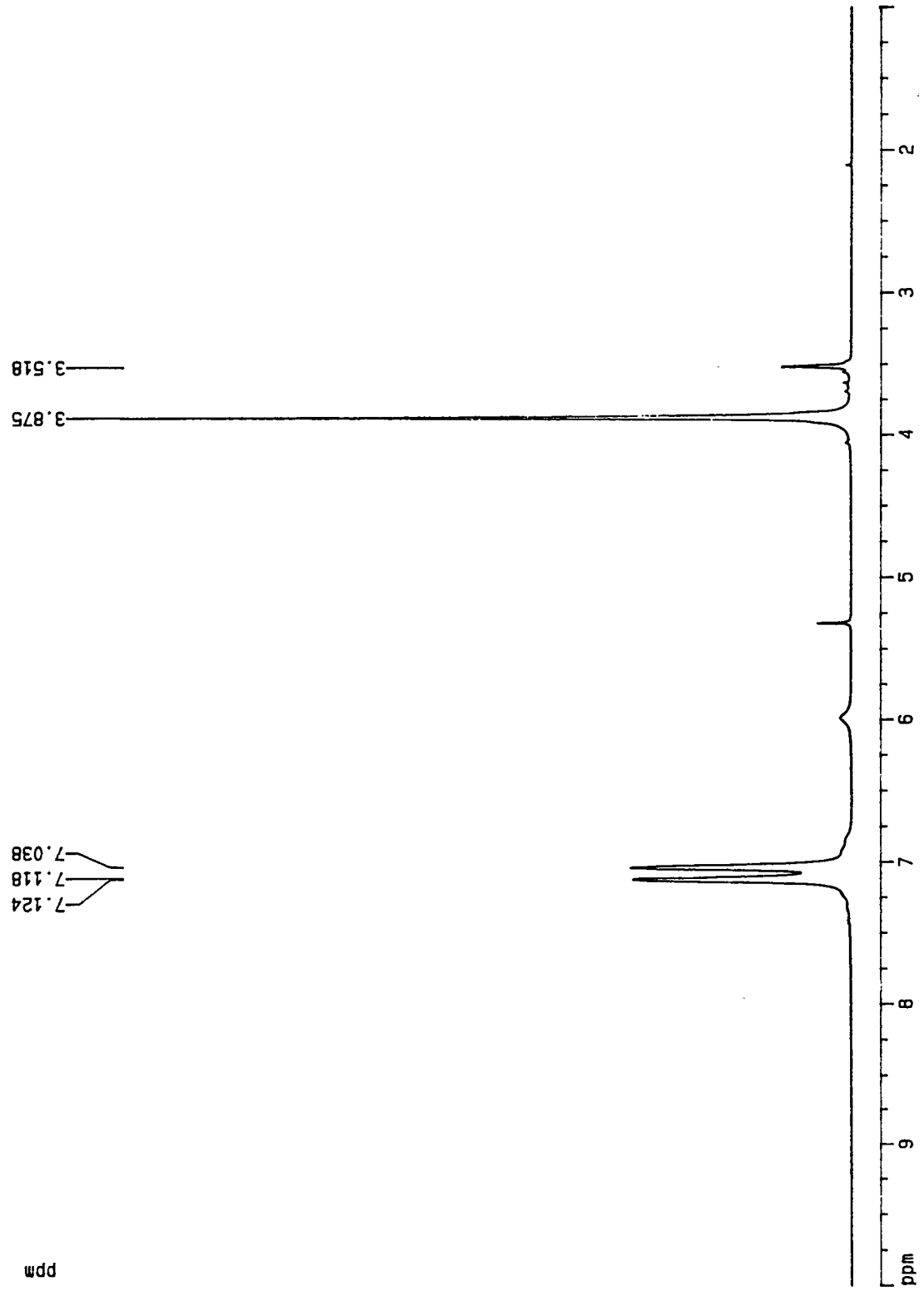


Figure A-9. Proton NMR Spectrum of MeOCB at -20°C in CD_2Cl_2

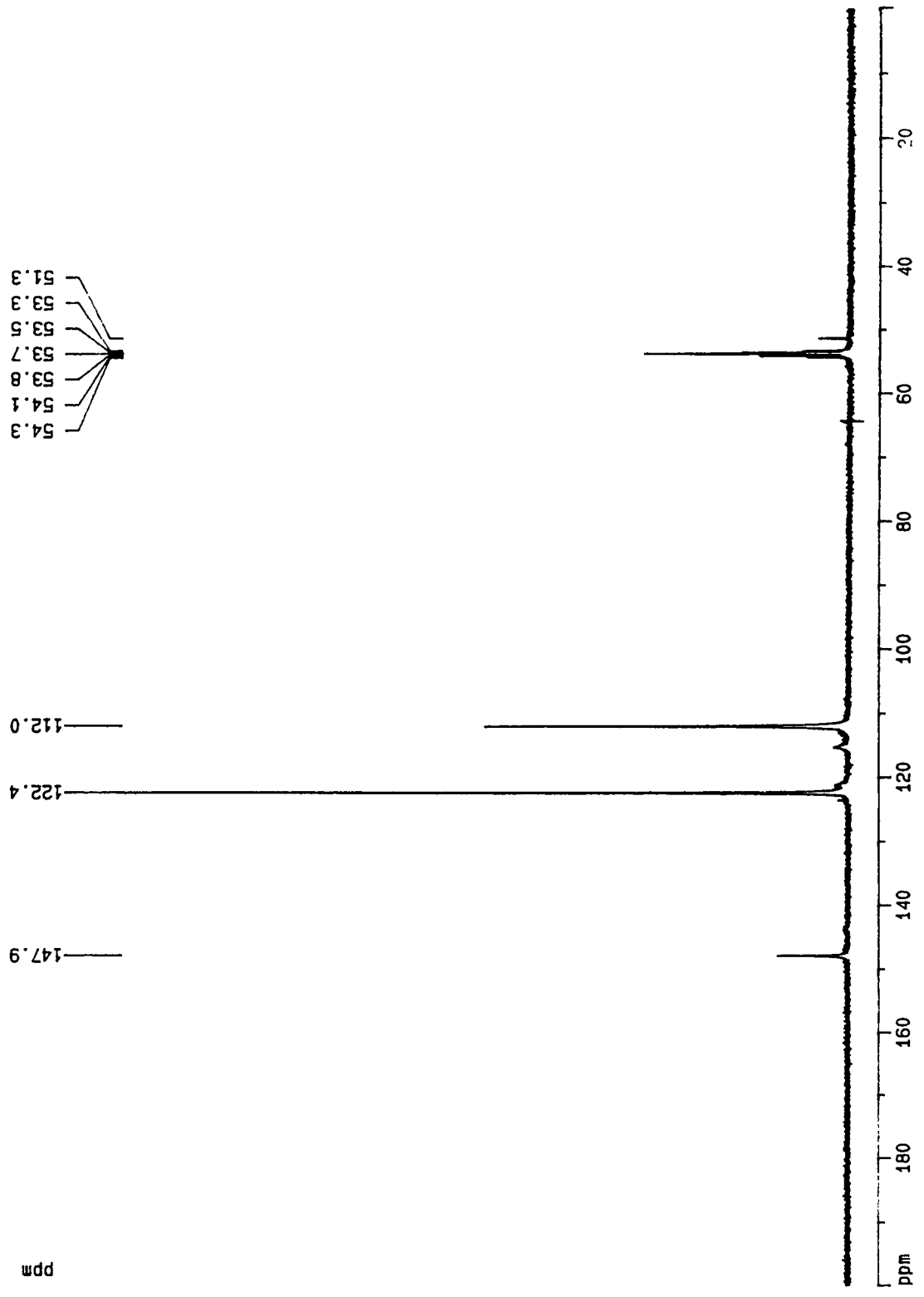


Figure A-10. Carbon-13 NMR Spectrum of MeOCB at -20°C in CD_2Cl_2

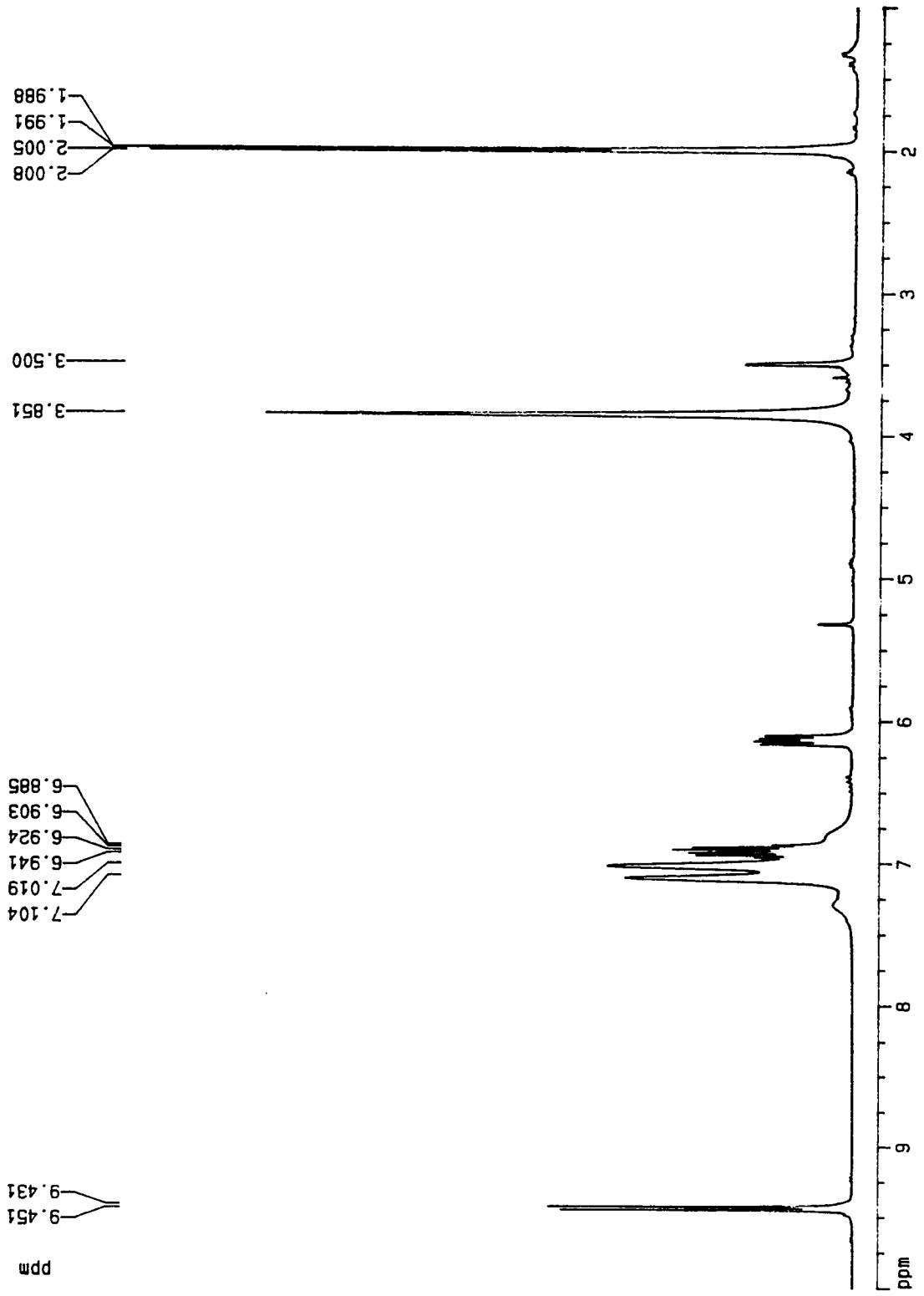


Figure A-11. Proton NMR Spectrum of MeOCB and CA at -20°C in CD_2Cl_2

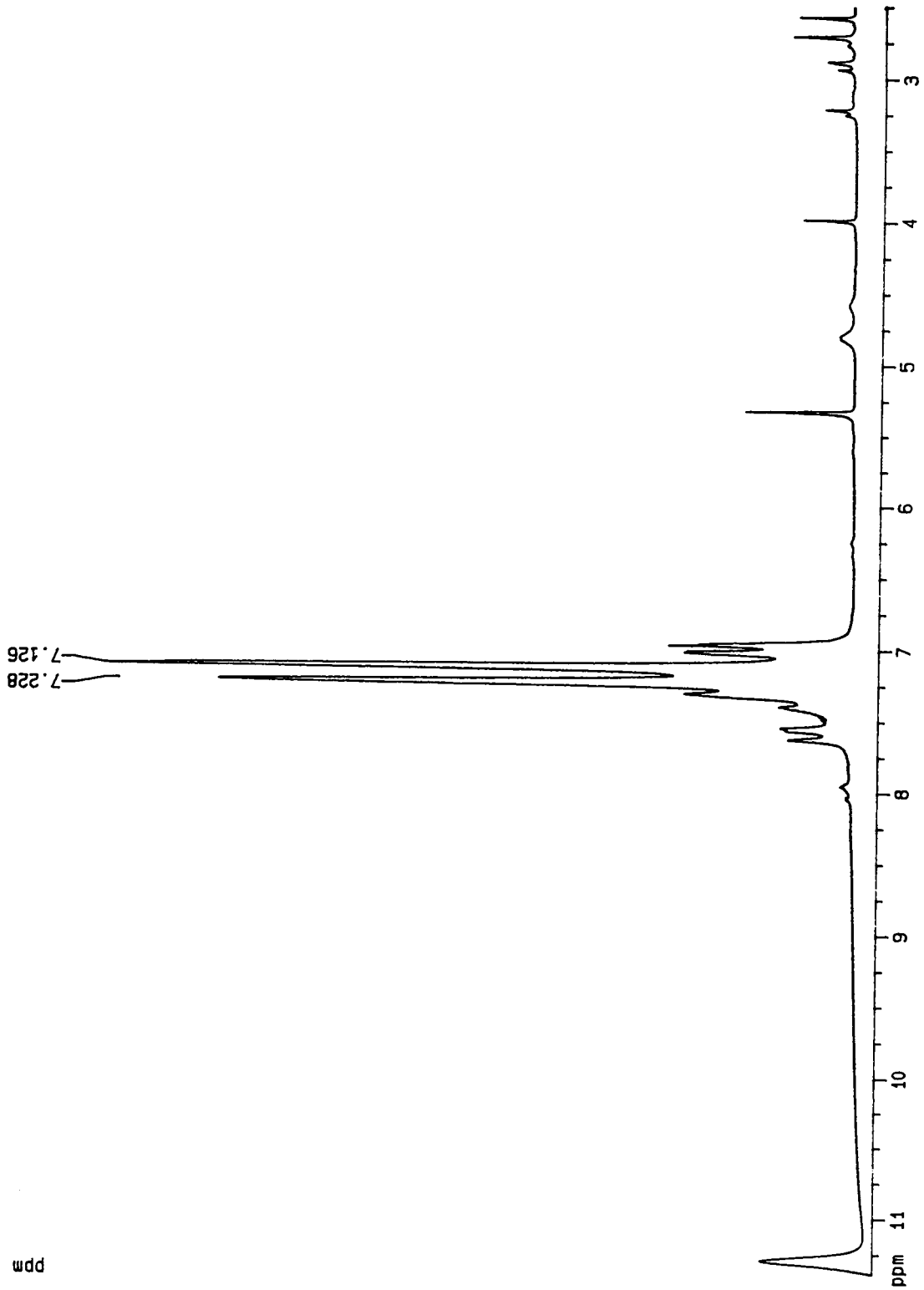


Figure A-12. Proton NMR Spectrum of TFACB at -20°C in CD_2Cl_2

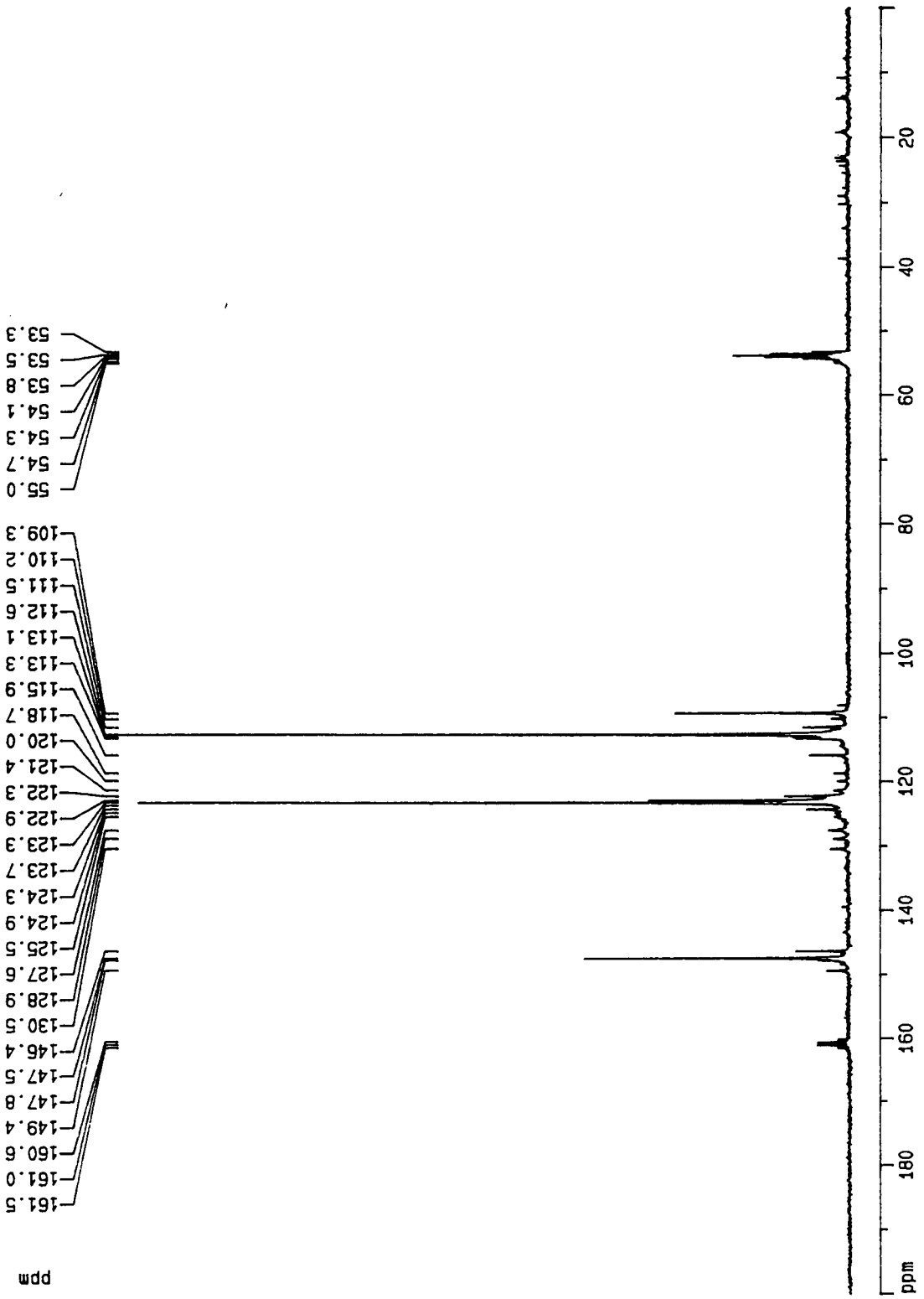


Figure A-13. Carbon-13 NMR Spectrum of TFACB at -20°C in CD_2Cl_2

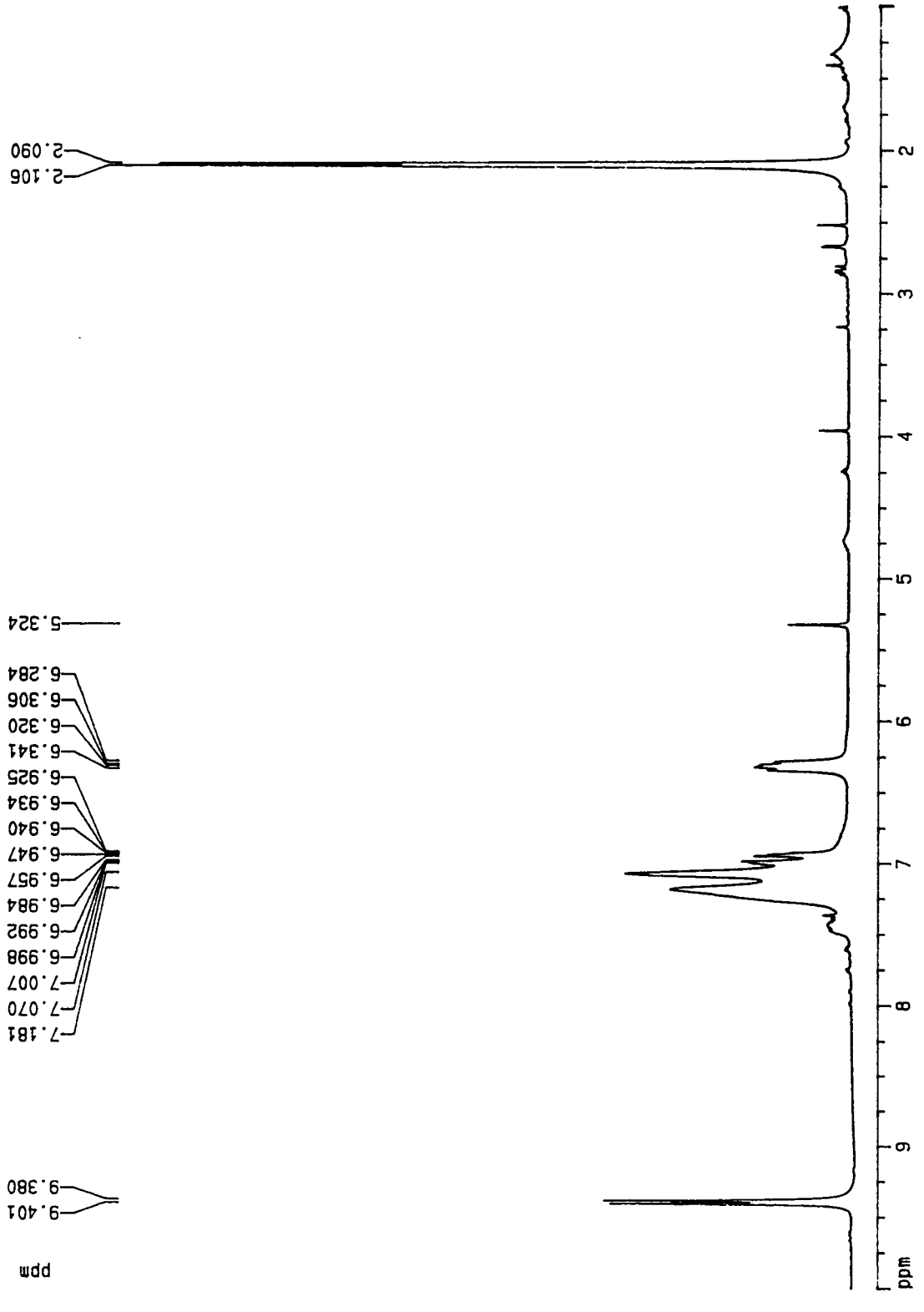


Figure A-14. Proton NMR Spectrum of TFACB and CA at -20°C in CD_2Cl_2

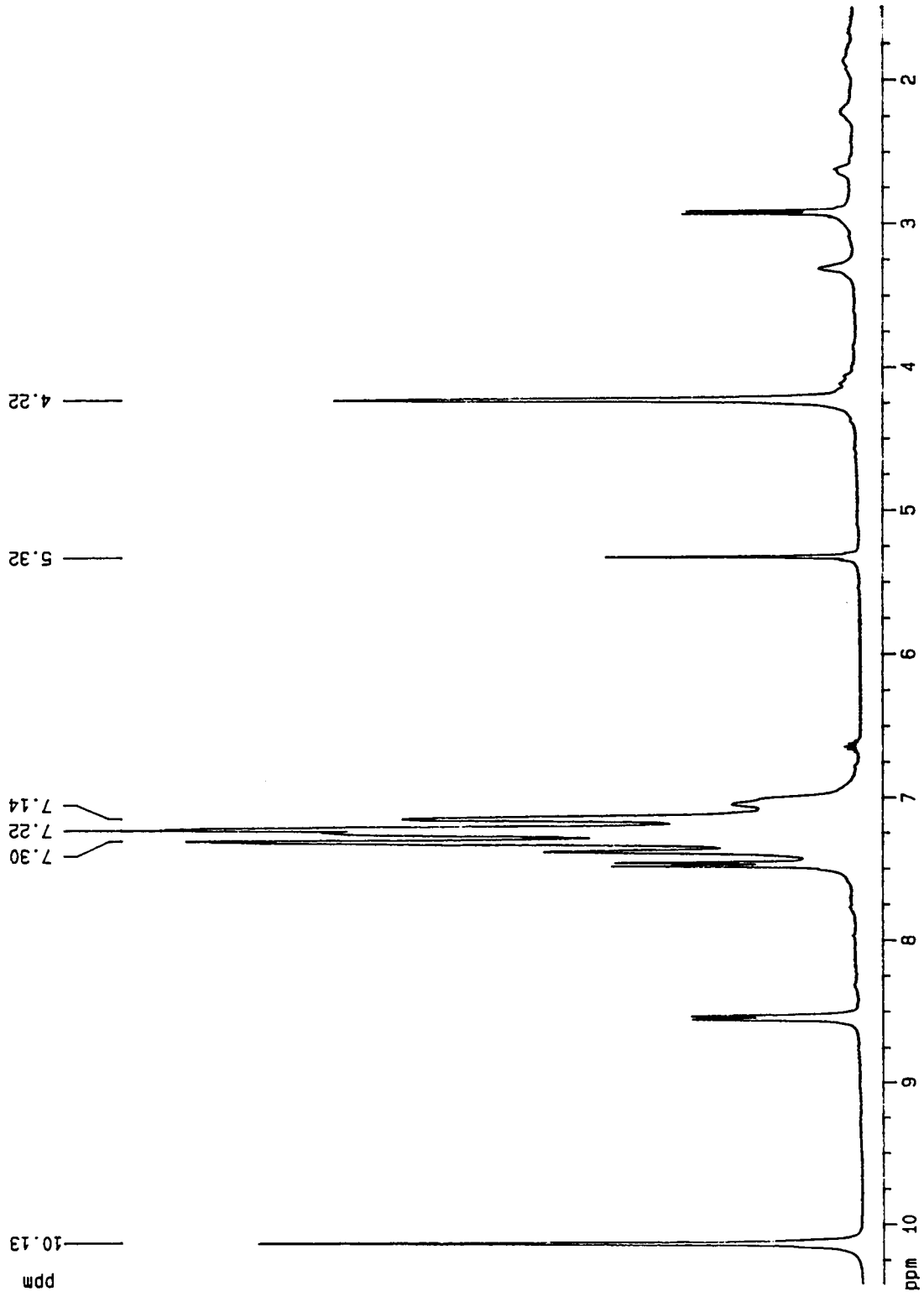


Figure A-15. Proton NMR Spectrum of TfCB at -20°C in CD_2Cl_2

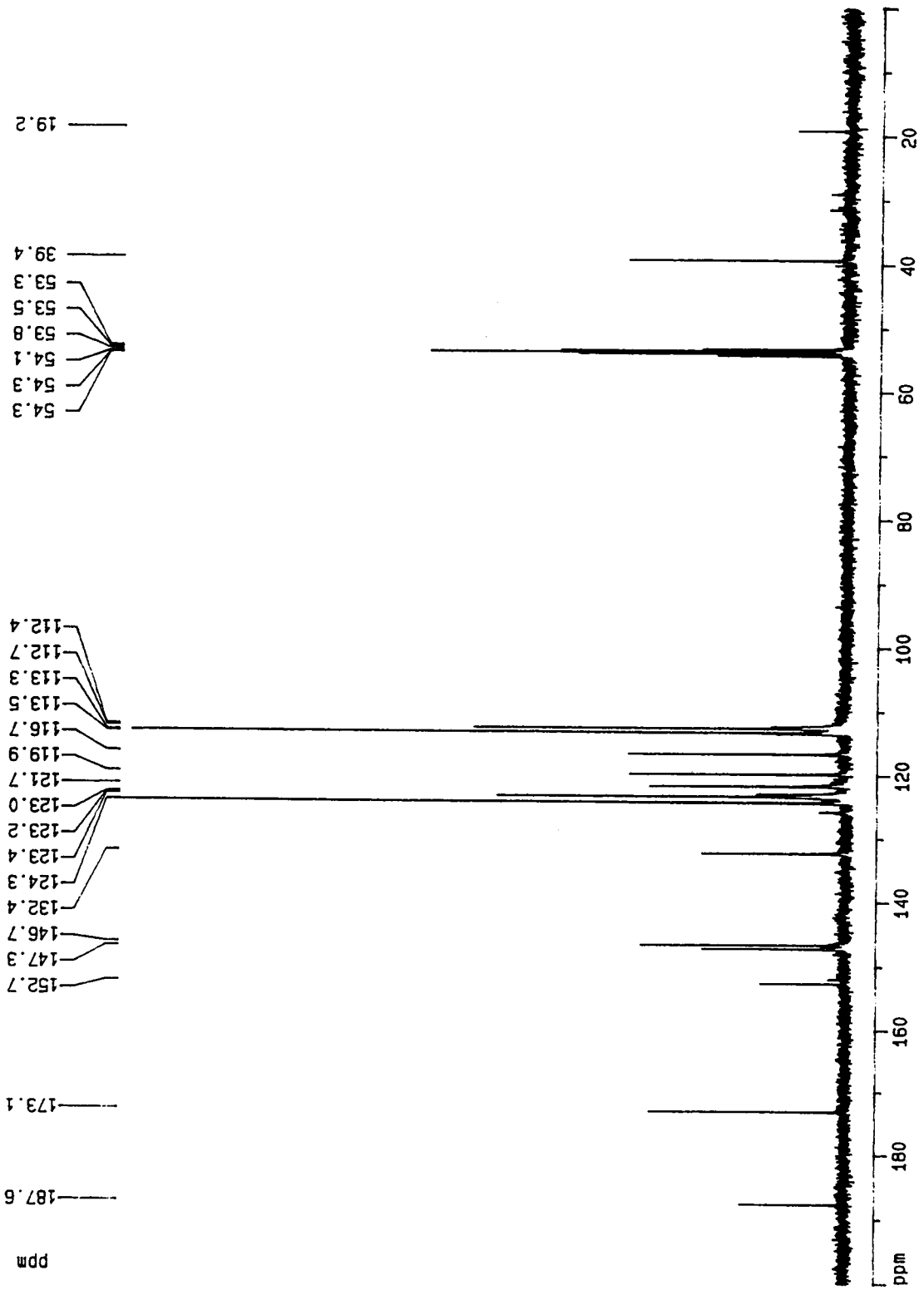


Figure A-16. Carbon-13 NMR Spectrum of TfCB at -20°C in CD_2Cl_2

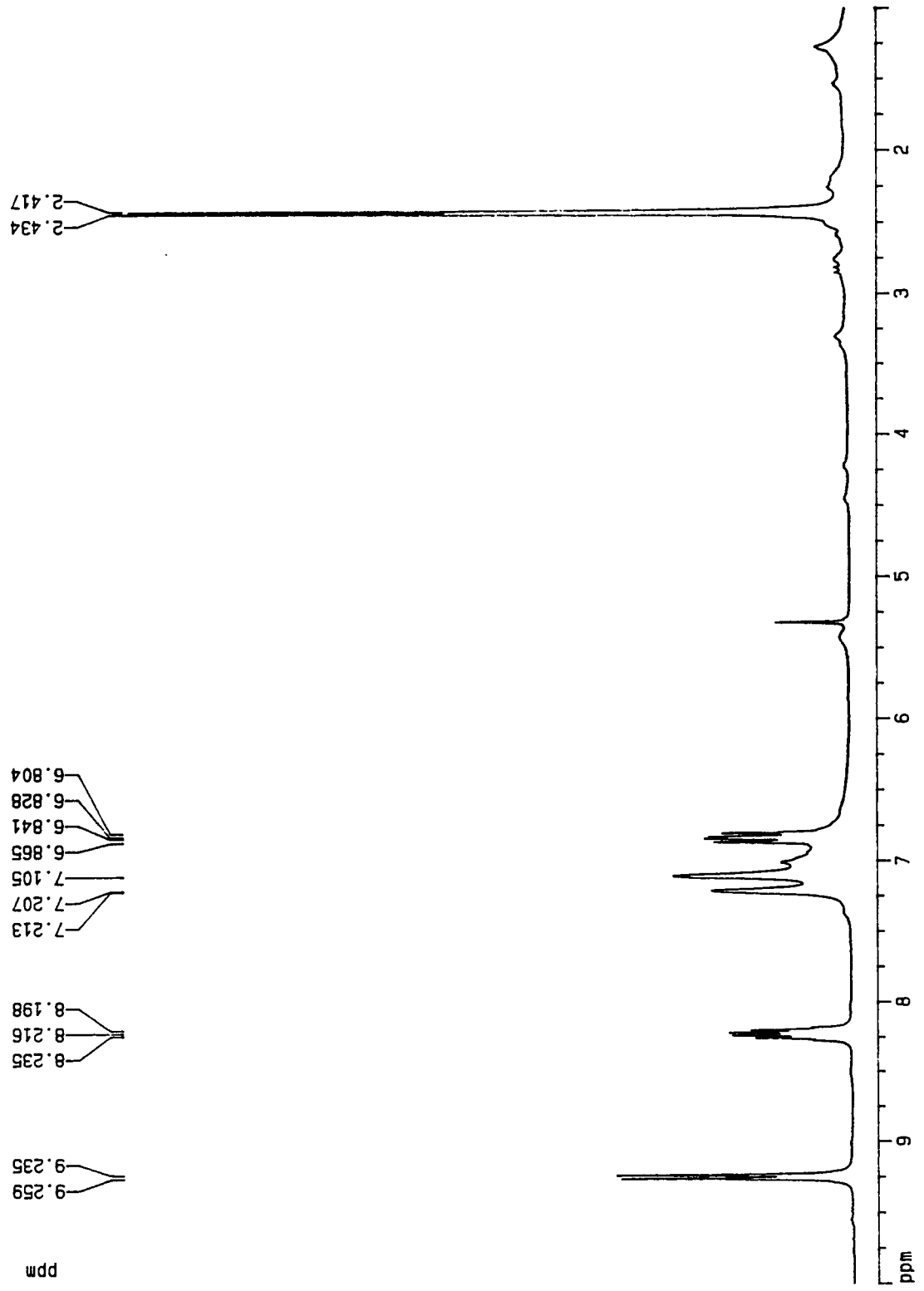


Figure A-17. Proton NMR Spectrum of TfCB and CA at -20°C in CD_2Cl_2

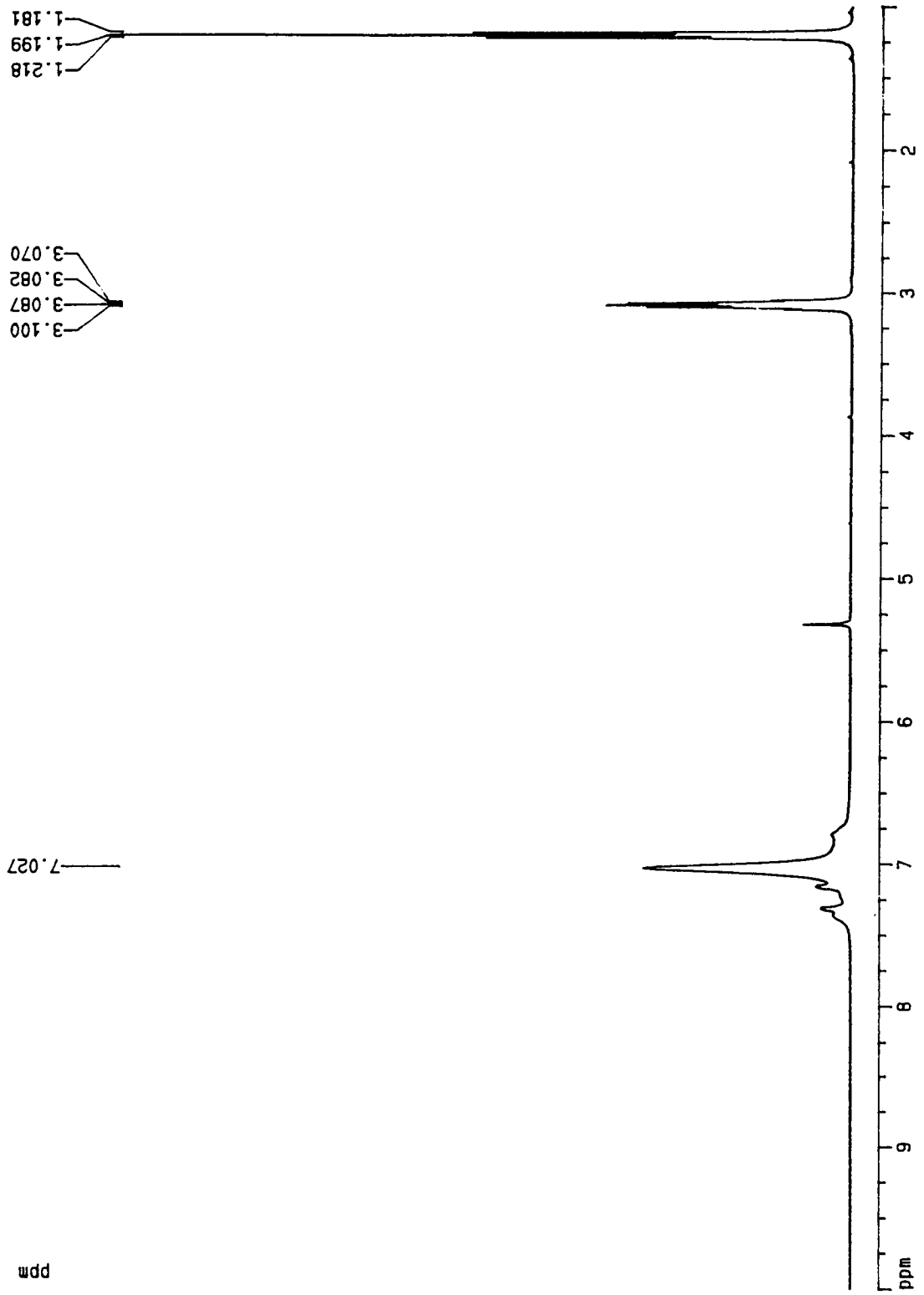


Figure A-18. Proton NMR Spectrum of FCB at -20°C in CD_2Cl_2

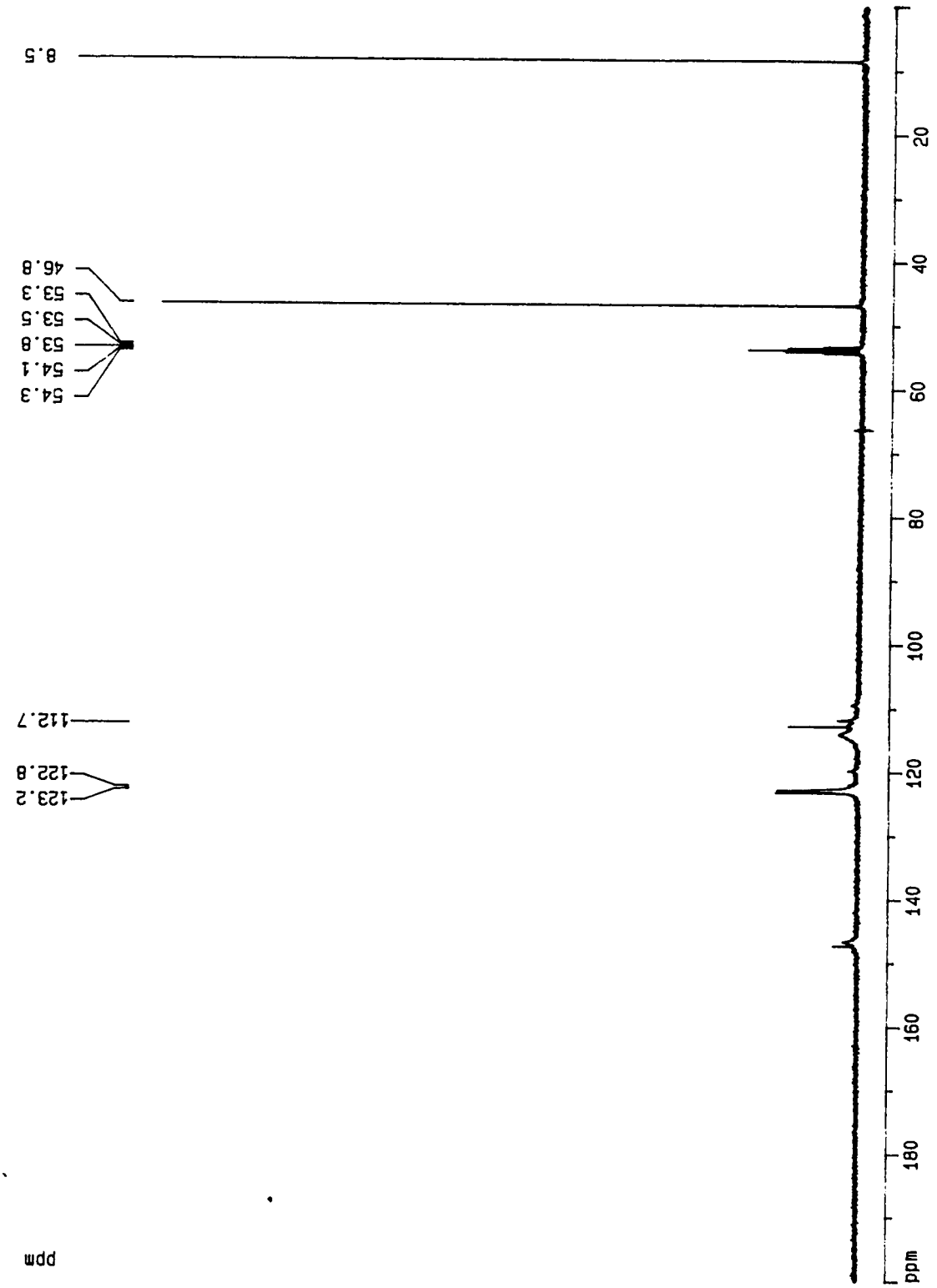


Figure A-19. Carbon-13 NMR Spectrum of FCB at -20°C in CD_2Cl_2

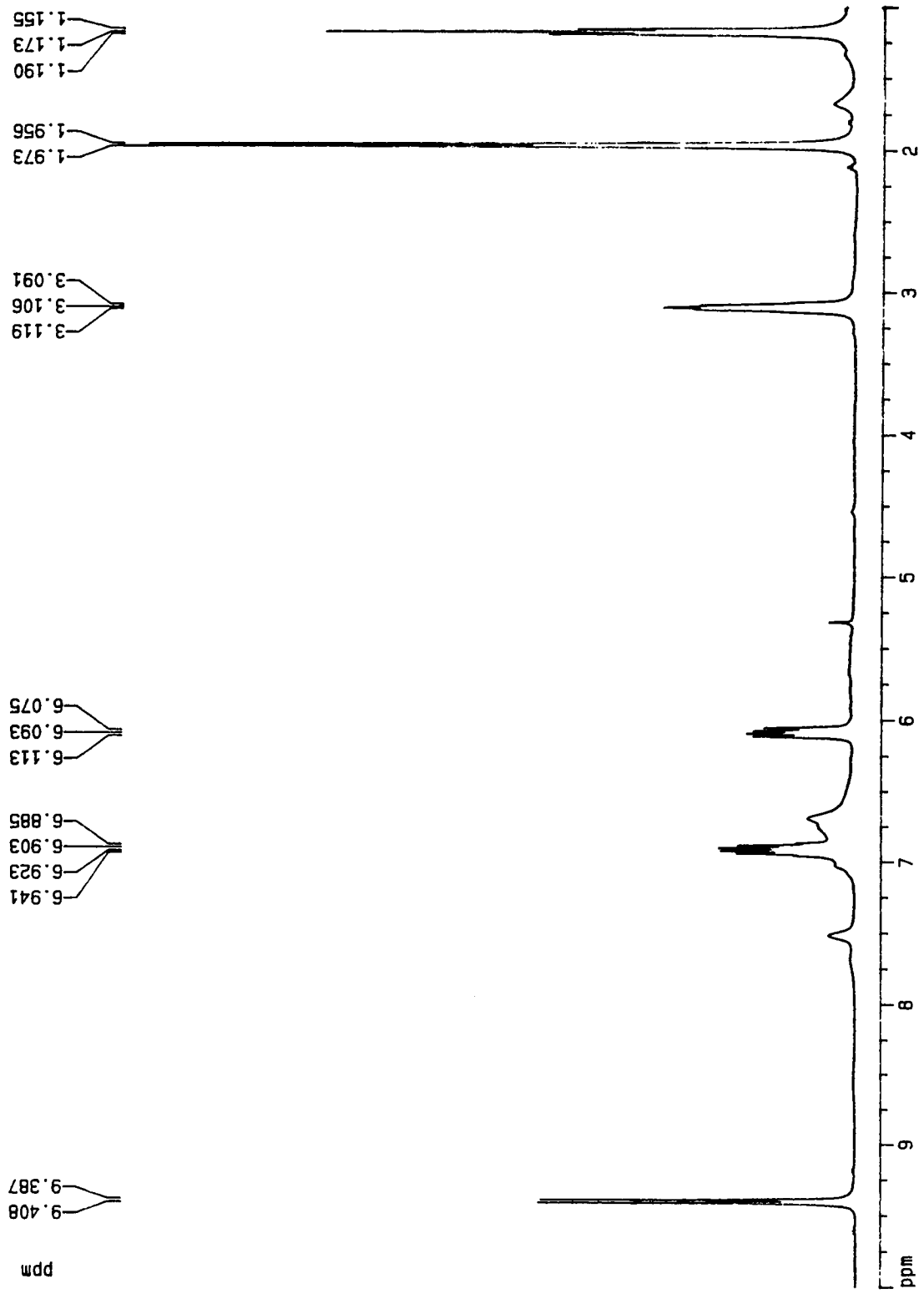


Figure A-20. Proton NMR Spectrum of FCB and CA at -20°C in CD_2Cl_2

VITA

Michael Boyd McGinnis was born in Baltimore, Maryland on March 3, 1970. He attended schools in the public system of Hampstead, Maryland, the Carroll County Public School System, where he graduated from North Carroll High School in June 1988. He entered Elizabethtown College in Elizabethtown, Pennsylvania during August 1988 where he graduate with a Bachelor of Science in Chemistry in May 1992. In August of 1992, he entered The University of Tennessee, Knoxville under the direction of Drs. Richard M. Pagni and George W. Kabalka. He has accepted an instructor position at the University of Tennessee, Department of Chemistry.